ENERGY TRENDS IN IRRIGATION: A METHOD FOR ESTIMATING LOCAL AND LARGE-SCALE ENERGY USE IN AGRICULTURE

By

Benjamin Michael McCarthy

A THESIS

Submitted to
Michigan State University
in partial fulfillment of the requirements
for the degree of

Geological Sciences — Master of Science

2021

ABSTRACT

ENERGY TRENDS IN IRRIGATION: A METHOD FOR ESTIMATING LOCAL AND LARGE-SCALE ENERGY USE IN AGRICULTURE

By

Benjamin Michael McCarthy

Agricultural Intensification has presented various opportunities for study in the field of water use, crop trends and energy consumption. In the United States alone, 70% of water consumed is used for the agricultural sector. Whether sourced from surface bodies or groundwater, the energy required to irrigate fields has changed over the last three decades. The advent of efficient irrigation systems has created new avenues for farmers to grow crops, through new planting practices, increased water extractions and varied on-farm practices. In this thesis, I evaluate the impact of shifting technologies on the FEW nexus, with emphasis on energy consumption from irrigation.

In Chapter 1, I developed an energy model for Kansas, one of the states with the highest data availability for farm practices. I used a combination of state and federal datasets to estimate the impact of shifting irrigation technologies on energy consumption. The results of this study are then investigated by energy source and a life cycle assessment model is applied to understand the role of shifting energy sources on the agricultural system. For Chapter 2, I expanded my energy model to encompass the continental United States. I estimate county level aggregates of direct energy consumed for irrigation. The results are then leveraged by agricultural region, and the crop types are evaluated spatially. Understanding how energy consumption in the agricultural sector is distributed both spatially and temporally can become a key asset when determining how to improve water practices, which regions need further study, and develop spatial relationships.

For Chloe, who’s constant support, love and encouragement kept me motivated through this program. Thank you, my love.

ACKNOWLEDGMENTS

During my time at the MSU Department of Earth and Environmental Science, I met a lot of brilliant people. The work presented in this thesis could not have been possible without their help. I appreciate the support I received from friends, family, and colleagues. The finalization of this thesis came at a difficult personal and global time, the part that everyone played in encouraging me to finalize this work is tremendous. I could not have done this without the support of all of you.

I would like to especially thank my advisors, Dr. David Hyndman, Dr. Anthony Kendall, and Dr. Annick Anctil for their continued support and mentorship throughout this endeavor. Your support and guidance helped defined key aspects of this research. All of you have provided me with moments of clarity, helpful nudges, and encouragement throughout this process. The patience and assurances that were given to me by them enabled me to continue during a global pandemic, begin a new career and expand my horizons in northern Michigan. I would like to thank Dr. Erin Haacker, who sat with me in the beginning stages of my writing process and helped me identify key structural pillars to this research. Her constant guidance and mentorship helped me through various writer's blocks.

To the Hydrolab friends, thank you for being a neighborly source of advice with difficult problems. Thank you for your support through a difficult graduate school journey, I will miss our lunch stops and late-night AGU poster sessions. The comradery and support in that lab is unsurmountable, and I hope that one day I'm lucky enough to work with a group as great as this lab.

Finally, I would like to thank my friends and family. My parents, Silvia and David, for

providing me with the necessary tools to succeed during my studies, for their support and encouragement throughout my studies. Thank you to my siblings, Priscilla, Chris, Patricio, and Felipe for all the optimistic encouragement. I would like to thank my soon-to-be wife Chloe for everything she's done to help me see this work to the end. There were times where I struggled emotionally and mentally. Your help helpful light guided me through those times. You have been there for me in moments of difficulty and moments of joy through this journey. I will be eternally grateful to all who helped me see this through to the end. Thank you!

TABLE OF CONTENTS

LIST OF TABLES viii

LIST OF FIGURES ix

KEY TO ABBREVIATIONS xi

CHAPTER 1: TRENDS IN WATER USE, ENERGY CONSUMPTION, AND CARBON EMISSIONS FROM IRRIGATION: ROLE OF SHIFTING TECHNOLOGIES AND ENERGY SOURCES 1
1. Abstract 1
2. Introduction: 2
3. Study Region: 5
4. Materials and Methods: 6
4.1 Data Sources: 6
4.2 Estimating Pumping Rates: 9
4.3 Pressure Requirements: 11
4.4 Energy and Carbon Calculations: 12
4.5 Direct Energy Consumption: 12
4.6 Direct Carbon Emissions from Groundwater Depletion: 15
4.7 Carbon and Energy Footprint Calculation: 16
4.8 Scenario Analysis: 17
4.9 Life Cycle Greenhouse Gas Emissions and Cumulative Energy Demand: 18
4.9.1 Type of Energy Carrier Used for Pumping 19
4.9.2 Pump and Power Unit Efficiencies 21
4.9.3 Electricity 22
4.9.4 Diesel 22
4.9.5 Natural Gas 23
4.9.6 Liquefied Petroleum Gas 24
4.9.7 Gasoline 25
5. Results: 25
5.1 Irrigation Technology and Energy Sources: 25
5.2 Energy Footprint and Water Consumption: 27
5.3 Carbon Footprint: 30
5.4 Energy Sources: 31
6. Discussion: 33
6.1 Changing Systems: 33
6.2 Implications & Future Work: 35
7. Acknowledgments 36
APPENDIX 37

CHAPTER 2: CONUS ENERGY MODEL 56
1. Abstract 56
2. Introduction 57

3. Materials and Methods 60
3.1 Study Region: 60
3.2 Data Sources: 61
3.3 Farms and Irrigated acreage: 62
3.4 Irrigation Requirements: 64
3.5 Water Use and Source: 66
3.6 Direct Energy Estimates by County: 66
3.7 Kansas Validation: 68
4. Results & Discussion 69
4.1 Kansas Validation Results: 69
4.2 Direct Energy Use: 72
4.3 Water Sources: 74
4.4 Energy Use by Farm Resource Region and Major Crop: 75
4.5 Limitations and Future Work: 80
5. Conclusions 80
6. Acknowledgments 81
APPENDIX 83
REFERENCES 92

LIST OF TABLES

Table 1.1 Pumping Estimate Linear Statistics. 10

Table 1.2 Irrigation Pressurization Requirements. 11

Table A1.1 Percent Distribution of Systems..... 55

LIST OF FIGURES

Figure 1.1 Changes in irrigation technology and energy source from 1994 to 2016..... 27

Figure 1.2 Energy Footprint and Water Use..... 28

Figure 1.3 Energy Results on Scenarios 30

Figure 1.4 Total Carbon Footprint and Groundwater percent contribution..... 32

Figure A1.1 Pump Rate Linear Regressions..... 38

Figure A1.2 Forward Fill Method Example. 39

Figure A1.3 Distribution Of Irrigation Wells By Energy Source..... 40

Figure A1.4 Comparison Between Observed and Extrapolated Energy Sources..... 41

Figure A1.5 Energy Source Comparisons (WIMAS vs FRIS)..... 42

Figure A1.6 Energy Source from 1994 to 2016 for HPA..... 43

Figure A1.7 Electric Grid Definitions 44

Figure A1.8 Electricity Generation Over Time 45

Figure A1.9 GWP & LCA of Electricity Production..... 46

Figure A1.10 Ratio of Gas to Diesel Prices..... 47

Figure A1.11 GWP of Natural Gas from Irrigation..... 48

Figure A1.12 CED of Natural Gas from Irrigation..... 49

Figure A1.13 Bicarbonate Kiriging Results..... 50

Figure A1.14 Proposed Pumping Buffer. 51

Figure A1.15 Scenarios on Carbon Footprint..... 52

Figure A1.16 Energy Footprint on Various Scenarios..... 53

Figure A1.17 GHG on Various Scenarios 54

Figure 2.1 Map of Continental United States Counties. 59
Figure 2.2 Farm Resource Regions. 61
Figure 2.3 MiRAD Estimated Acreage vs USGS reported acreage by county. 64
Figure 2.4 Selected Counties for Validation. 68
Figure 2.5 Percent difference in energy consumption WIMAS vs CONUS. 70
Figure 2.6 Linear relationship between WIMAS vs CONUS results. 72
Figure 2.7 County-level Energy Results. 74
Figure 2.8 Water source distribution throughout CONUS. 75
Figure 2.9 Distribution of Crops and Total Lift along Farm Resource Regions. 79
Figure A2.1 AWC in Top Meter of Soil 84
Figure A2.2 Estimated Irrigation Days from 1991 to 2020 85
Figure A2.3 Estimated Irrigation Days for 2015 86
Figure A2.4 Maturity Date Regression Models 87
Figure A2.5 Maturity Date Regression Validation 88
Figure A2.6 County-level Surface Water Use 89
Figure A2.7 County-level Groundwater Use 90
Figure A2.8 Kansas Validation Results 91

KEY TO ABBREVIATIONS

LEPA	Low-Energy Precision Application
GHG	Greenhouse Gas
LCA	Life Cycle Assessment
HPA	High Plains Aquifer
WIMAS	Water Information and Analysis System
CONUS	Continental United States
USDA	United States Department of Agriculture
FRIS	Farm Ranch & Irrigation Survey
NASS	National Agricultural Statistics Service
USGS	United States Geological Survey
FIPS	Federal Information Processing Standards
AWC	Available Water Capacity
INFEWS	Innovations at the Nexus of Food, Energy and Water Systems

CHAPTER 1:
TRENDS IN WATER USE, ENERGY CONSUMPTION, AND CARBON EMISSIONS FROM IRRIGATION: ROLE OF SHIFTING TECHNOLOGIES AND ENERGY SOURCES

1. Abstract

Novel low-pressure irrigation technologies have been widely adopted by farmers, allowing both reduced water and less energy use. However, little is known about how the transition from legacy technologies affected water and energy use at the aquifer scale. Here, we examine the widespread adoption of Low Energy Precision Application (LEPA) and related technologies across the Kansas High Plains Aquifer. We combine direct energy consumption and carbon emissions estimates with Life Cycle Assessment to calculate the energy and greenhouse gas (GHG) footprints of irrigation. We integrate detailed water use, irrigation type, and pump energy source data with aquifer water level and groundwater chemistry information to produce annual estimates of energy use and carbon emissions from 1994-2016. The rapid adoption of LEPA technologies did not slow pumping, but it reduced energy use by 19.2% and GHG emissions by 15.2%. Nevertheless, water level declines have offset energy efficiency gains due to LEPA adoption. Deeper water tables quadrupled the proportion of GHG emissions resulting from direct carbon emissions, offsetting the decarbonization of the regional electrical grid. We show that low-pressure irrigation technology adoption, absent policies that incentivize or mandate reduced water use, ultimately increases the energy and carbon footprints of irrigated agriculture.

2. Introduction:

Groundwater is the source of over 30% of worldwide water withdrawals, and extractions are increasing in many locations due to agricultural intensification (Nejadhashemi et al., 2012; Smidt et al., 2019). Technological innovations during the 1940s and 50s accelerated the amount of groundwater pumped for irrigation (Dennehy et al., 2002). In particular, the development of center pivot irrigation systems allowed for the expansion of irrigated area into topography that was previously unsuited for gravity-fed flood or other surface irrigation types (Ashworth, 2006). Rapid adoption of these then-new technologies allowed irrigation water extraction greatly in excess of aquifer recharge, leading to declines in groundwater storage around the world (Konikow & Kendy, 2005). In the United States, the two most intensively exploited aquifers (High Plains and California's Central Valley Aquifers) today account for approximately half of the total U.S. groundwater pumping (Scanlon et al., 2012), and are global hotspots for groundwater depletion (Rodell et al., 2018). Declines in saturated thickness of aquifers such the High Plains Aquifer (HPA) over the decades have led to greater drawdown of water tables during pumping, reduced well yields, and negative economic consequences (Foster et al., 2015, 2017).

The advent of more energy and water conservative irrigation systems helped lower the cost of pumping even as water levels declined in the HPA and elsewhere. Low-pressure systems such as the Low Energy Precision Application (LEPA) and related drop nozzle spray systems were introduced in the HPA in the late 1980s (Kenny & Juracek, 2013). These new technologies require less water than legacy systems due to reduced evaporative losses, lower flow rates, and reduced pressurization requirements. Given the favorable economics of adoption, these systems became the most common technology in areas with deep groundwater levels (Kenny & Juracek,

2013; Pfeiffer & Lin, 2014; Velasco-Muñoz et al., 2018). Although adopting water- and energy-saving irrigation technology may provide a mechanism to reduce groundwater depletion, it can enhance groundwater storage declines by enabling irrigation in areas with little saturated thickness or reduced well yields (Daher et al., 2019). Low-pressure irrigation systems have also been associated with increased consumptive water use, as farmers may choose to grow crops with larger water demand or irrigate more acres with their existing water rights (Pfeiffer, 2010; Pfeiffer & Lin, 2014; Sears et al., 2018). Previous literature in the region that focused on irrigation trends has mainly evaluated changes in water use and crop yield, with little attention to embodied energy use and shifting energy sources (Handa et al., 2019; Pfeiffer, 2010).

Irrigation systems use a tremendous amount of energy (Martin et al., 2011), which results in substantial greenhouse gas (GHG) emissions depending on the energy source (McGill et al., 2018; Rothausen & Conway, 2011). These systems use energy directly to pump water to the surface and pressurize the system, and indirectly via inefficiencies within the prime mover (i.e. diesel engine or electric motor). One groundwater management district in Kansas estimated that 1679 GWh of direct energy was used to pump ~2.5 km^3 of water (*Revised Management Program Southwest Kansas Groundwater Management*, 2020). While the direct use of energy for farmers is measurable and impactful, it is also important to account for "hidden" energy use of irrigation. Life Cycle Assessments (LCA) can quantify the embodied energy and GHG emissions due to irrigation (Pfister et al., 2016). Greenhouse gases are emitted directly from the depletion of bicarbonate rich groundwater storage (Wood & Hyndman, 2017) and indirectly due to the embodied energy used for these pumps. These otherwise-hidden components accumulate along the pathway from the extraction of raw materials, processing, transport, and refinement of fuels, energy generation at the plant, and transport or transmission of energy to the individual farm.

Global energy demand is expected to increase dramatically in the next 30 years (EIA, 2020b) and farmers will face increasing pressure to reduce their energy costs to remain profitable. While farmers respond to these pressures to cut costs and increase crop yields, government regulation and policies are needed to better monitor water consumption and help mitigate future water level declines. Therefore, we need to examine the factors that affect water use, irrigation, and technology practices. Previous work on embodied energy for irrigation has generally emphasized inter-state magnitude differences with limited focus on local- to state-scale results, or it has focused on specific crop types. Published research estimated embodied energy using cost-to-energy and food transfer equivalent conversions, finding significant value from LCA methods and agreeing that there is a gap in the embodied energy and GHG emissions of irrigation water consumption (Salmoral & Yan, 2018a; Vora et al., 2017a). Another study used the water balance of a region to estimate national irrigation energy demand and found that less water would be used if irrigation technology were modernized, yielding a surprising increase in carbon emissions (Daccache et al., 2014). Such studies, however, have used estimated water consumption and broad assumptions about the energy sources of pumping wells; they also did not account for the significant CO_2 contributions from direct depletion of groundwater (Wood & Hyndman, 2017).

Using national or global data in an LCA study can limit the applicability of results on local to regional scales. Studies of impacts at these scales should use data that are specific to the region of interest, where parameters and information are readily available. Global trends can facilitate awareness, but for policymakers to make informed decisions about management of local water resources, local analyses are needed (Ireland & Clausen, 2019). With better understanding of local trends, we can facilitate agricultural improvements and enhance efficiency

of irrigation technologies. For example, a study of irrigation in the panhandle of Oklahoma found that total depth to groundwater and sub-standard pump maintenance affected emissions and energy use (Handa et al., 2019). Energy use per cubic meter of water pumped was 1.84 kWh on average over the 17-year study period, with over 20% of that energy directly linked to pump maintenance issues. Research dealing with center pivot energy use in the Upper Midwest also showed that 13% of excess consumption can be attributed to increased pumping lift requirements and improper maintenance (DeBoer et al., 1983). Both studies attribute energy increases to deeper groundwater levels and pump valve deficiencies, however, neither study quantified the dynamic changes of energy sources and irrigation trends of the study area, allowing them to remain static.

Here, we leverage a suite of unique data sources from the state of Kansas, USA to quantify the energy and GHG footprints of irrigation during a time of rapid LEPA adoption and shifting energy sources. We calculate the direct energy consumption from over 30,000 pumping wells across the Kansas portion of the HPA using annual reported irrigation technology and water consumption data alongside maps of interpolated annual water level change observations (Haacker et al., 2016). We then apply life-cycle embodied energy and GHG emission analysis using co-located records of pumping energy source and electrical grid mix data. Using aquifer geochemical composition data, we also compute emissions of CO_2 due to aquifer depletion. To our knowledge, this is the first study to quantify the role of LEPA adoption in the reduction of the energy and GHG footprints of irrigation.

3. Study Region:

The HPA provides water to approximately 28% of irrigated land in the US (Pervez & Brown, 2010). The Kansas High Plains region has detailed data on water consumption and the energy

source used for irrigation. For this study, we aggregate and analyze these data from 1994 until 2016. Kansas is also an ideal location for this research due to its extensive water and energy consumption for crop production. The state had the second largest cropland area in the United States as of 2018, with main crops being corn, wheat, and soybeans all of which require high water inputs (18 to 48 inches per growing season) (Holman & Foster, 2017; Kenny & Juracek, 2013; McClaskey & Colyer, 2018). During our study period, corn continued to be the crop with most allotted acreage, and in a state that depends on groundwater use, this means large water consumption. The Kansas portion of the HPA is mainly composed of unconsolidated sediments, with a large saturated thickness in the central portion of the aquifer (Butler et al., 2020; Gutentag et al., 1984). High hydraulic conductivities and large saturated thicknesses in this region have provided high well yields over long periods. However, extractions that greatly exceed recharge rates have depleted ~450 km^3 of aquifer storage in the HPA since pre-development (Famiglietti, 2014; Famiglietti & Rodell, 2013; Haacker et al., 2016)

4. Materials and Methods:

4.1 Data Sources:

Survey data from the Kansas WIMAS (Wilson et al., 2005) database were compiled on a yearly basis from 1994 to 2016. WIMAS provides farmer-reported values of metered water use, pumping rate, acres irrigated, irrigation system type, water source, and pump energy source, among other fields. Surface elevations were extracted from the Continental United States (CONUS) Digical Elevation Model (DEM) (*National Elevation Dataset - NAVD88 Meters - 1/3rd-Arc-Second (Approx. 10m)*, 2012), and saturated thicknesses and water table elevations are based on rasters interpolated from USGS data (Haacker et al., 2016). Bicarbonate (HCO_3^-) concentration data from the National Water Information System (NWIS) (*National Water*

Information System Data Available on the World Wide Web (USGS Water Data for the Nation), 2016) were used to interpolate bicarbonate concentrations across the Kansas HPA. The Farm and Ranch Irrigation Surveys from 1994-2003 (*Farm and Ranch Irrigation Survey*, n.d.) were used to develop Kansas energy source estimates in years prior to this information becoming available in WIMAS. The WIMAS points of diversion (PDIVs, locations where water is diverted for irrigation use) were mapped in ArcGIS based on their reported latitude and longitude. Non-irrigation pumping data (residential and industrial wells) were excluded from the analysis.

The PDIVs were geographically associated with map estimates of water level, saturated thickness (Haacker et al., 2016), specific yield (McGuire et al., 2012), and hydraulic conductivity (Cederstrand & Becker, 1998).We quantified direct energy for pumping using WIMAS data on irrigation systems and water use. Direct energy estimates were then scaled using efficiencies based on known energy sources mapped to the selected wells and matched with Farm and Ranch Irrigation Survey data (*Farm and Ranch Irrigation Survey*, n.d.).

Each location where water is pumped in Kansas needs to be approved by the DWR and apply for a Water Right (New Applications and Permits, n.d.). The information contained in the water rights attributes include: location, water supply, and water rights priority information. Here, the water rights information was used to pull the specific water rights we needed regarding farm type. The following subset of the water rights information was used, columns 'wr_id', 'longitude', 'latitude', 'source_of_supply', 'priority_date'. This information was used to verify the specific wells that are needed for the study. A series of data cleaning techniques were employed before the data was used in the analysis: removal of leading whitespace, indexing the water attributes based on their water right ID (‘wr_id’), removing blank values in the data, and converting the cell values to float numeric type.

This analysis used the columns describing ‘Latitude’ and ‘Longitude’ from the water rights file for each well. The georeferenced dataset was plotted using the WGS 1984 spatial reference (*WORLD GEODETIC SYSTEM 1984 (WGS 84)*, n.d.). Key details with water rights attributes were converted into an XY event layer using the arcpy python package (*ArcGIS Pro Python Reference*, n.d.). The column of interest that was drawn into the event table was the ‘wr_id’ value. Using the new event layer, we clipped the WIMAS dataset to the region of interest. In this case, a polygon of the High Plains Aquifer was used to determine the points (Qi, 2010). The result was a series of well locations that were within the study region.

The water rights attributes were used to extract yearly data for each farm. Water rights were needed to obtain active well information and to intersect with the region of interest. The yearly files contain the information we need: 'FPDIV_KEY', 'LONGITUDE', 'LATITUDE', 'SYSTEM', 'DPTH_WATER', 'DPTH_WELL', 'SOURCE', 'HOURS_PUMP', 'PUMP_RATE', 'AF_USED', 'ACRES_IRR', 'WUA_YEAR'. Using the ‘wr_id’ column, we merged the water rights attributes and the yearly survey data with the new clipped boundary. We ran a yearly loop for data from 1994 to 2016.

The yearly files provided information regarding irrigation system, water use, water source, and pump rate. For the final estimate, we also required aquifer property information, such as hydraulic conductivity, specific yield, surface elevation, water table elevation, and saturated thickness (Cederstrand & Becker, 1998; Haacker et al., 2016; McGuire et al., 2012; *National Elevation Dataset - NAVD88 Meters - 1/3rd-Arc-Second (Approx. 10m)*, 2012). These values were extracted for each well in the study region using a series of ArcGIS “Extract raster to points” tool iterations.

During the irrigation season, the pumping from wells in an unconfined aquifer will form cones of depression, the depths of which depend on hydraulic conductivity and specific yield information. We pulled hydraulic conductivity and specific yield estimates into the yearly files using a raster created for the High Plains Aquifer (Cederstrand & Becker, 1998; McGuire et al., 2012) was extracted by points into yearly files.

The WIMAS database maintains records of water table depth. For water table elevation we used rasters for the High Plains Aquifer that were previously derived by interpolating annual water level data across the aquifer (Haacker et al., 2016). The water table rasters were used in the study to calculate the component in the direct energy analysis and for the water level change in the carbon emission from groundwater depletion. To estimate depth to water, we subtracted the water table elevation raster from the USGS continental United States Digital Elevation Model (*National Elevation Dataset - NAVD88 Meters - 1/3rd-Arc-Second (Approx. 10m)*, 2012).

Following data cleanup, we noticed that farmers apparently only report the irrigation system type in years when they changed system type. Other than years in which a farm changed irrigation system type, the cell value for irrigation system type is blank. In years in which no irrigation system type was reported but that reported water use and pump rate data, we assumed the system type was the same as most recently reported until a new system was declared. To implement this, we used a pivoting technique coupled with the python ffill() function to fill in the missing values. This forward fill method is described in Fig A2.

4.2 Estimating Pumping Rates:

In the pumping data set, there are some sections that contain total water used, pump rate, and days pumped. However, some rows are missing one or more of these items. As with the irrigation system, we found that some wells did not report the pump rate for some years, thus we

needed to estimate the values (Table 1.1**)**. We used a linear regression per system of reported daily pump rate (y-axis) vs. annual water used (x-axis) to estimate missing pump rate data for each irrigation system (Figure A1.1 & Table 1). After plotting, we used linear regression to develop our pump rate equations. With moderate confidence (Table 1), we were able to estimate the pump rate for wells that had irrigation system type and water use information.

Table 1.1 Pumping Estimate Linear Statistics. Pump rate estimates made using regression lines.

Irrigation System Name	System Number	n	% Missing	slope	intercept	P value	r value	Std err
Unused	0	435538	NA	NA	NA	NA	NA	NA
Flood	1	61329	30.1	0.0063	2181.4	<<0.05	0.523	5.15E-05
Trickle-Drip	2	2223	47.5	0.0090	1675.6	5.38E-143	0.662	0.000305
Center Pivot (CP)	3	86164	35.3	0.0051	2687.4	<<0.05	0.448	4.35E-05
Center Pivot LEPA	4	242754	43.0	0.0058	2122.1	<<0.05	0.489	2.79E-05
Non- CP Sprinkler	5	5859	31.4	0.0091	1258.6	<<0.05	0.610	0.000198
CP and flood	6	30233	39.4	0.0060	2064.0	<<0.05	0.585	6.20E-05
Subsurface drip	7	873	48.9	0.0090	1362.8	2.05E-62	0.697	0.000452
Other	8	809	29.5	0.0103	1208.1	2.39E-114	0.798	0.000343
CP w/ Mobile drip	9	20	10	0.0060	960.71	0.003554	0.649	0.001753

4.3 Pressure Requirements:

We estimated pressure head (meters) for pressurized systems. Due to data limitations, we assumed 10 psi in pipe and friction losses for all systems (G. O. Brown, 2002a; Kranz et al., 2008). Pressure requirements and losses were summed and converted into meters using standard temperature and water density assumptions.

Table 1.2 Irrigation Pressurization Requirements. Pressurization energy for each irrigation system type. We first assigned a value for each system type, then we converted this to meters of head.

Irrigation System Type	System Number	Pressurization Requirement (psi)	Pressurization losses (psi)*	Total head (m)
Flood	1	~6(*Furrow Irrigation*, 2011; Hanson & Putnam, 2004)	10	11.25
Trickle-Drip	2	~15(Service, n.d.)	10	17.58
Center Pivot	3	~30 (Kranz et al., 2007a, 2008)	10	28.12
Center Pivot LEPA	4	~8(Curtis & Tyson, 1988; Kranz et al., 2007a)	10	12.65
Sprinkler other than CP	5	~8	10	12.65
Center pivot and flood	6	~10 (Hanson & Putnam, 2004; Henggeler & Vories, 2009)	10	14.06
Subsurface drip	7	~30 (Rogers et al., 2018)	10	9.14
Other	8	~5	10	10.55
Center pivot w/ Mobile drip	9	~15 (Kranz et al., 2007a)	10	17.58

***** Assumption for pressurization losses along the length of the piping in irrigation systems due to pipe friction derived from Brown (G. O. Brown, 2002b).

4.4 Energy and Carbon Calculations:

In this analysis, we examine two related aspects of energy consumption and carbon emissions: direct and embodied. The sum of the direct and embodied components are included in the total footprints of energy consumption and equivalent carbon emissions. Direct energy consumption describes the amount of energy required at the pump to lift water and pressurize it within the irrigation system, multiplied by the efficiency of the pump. Here we also include a novel calculation of direct carbon emissions, i.e., CO_2 emitted to the atmosphere due to degassing of bicarbonate-rich groundwater at the site of water extraction (Wood & Hyndman, 2017).

The embodied energy required to supply this direct energy depends on the pump energy source, the energy requirements of fossil fuel supplies (effort to extract, refine, and transport the fuels), and the electrical grid energy source mixture. Embodied carbon emissions respond to fluctuating carbon residuals of the fossil fuel supply, as well as the shift toward an increasingly renewable-powered electrical grid. Carbon footprint is the sum of the total life-cycle GHG emissions associated with the irrigation energy footprint and the direct carbon emissions resulting from groundwater depletion. We define water use efficiency as the amount of water pumped per unit of energy (m^3/MJ), without accounting for evaporative losses or application rate; the inverse of this value is the energy intensity of irrigation (MJ/m^3).

4.5 Direct Energy Consumption:

Direct energy consumption (E_D, PJ/yr) at each well can be computed as the work required to lift and pressurize the mass of water pumped annually, multiplied by the efficiency of each pump:

$$E_D = \rho g V L_T \times \epsilon_P \quad \text{Equation 1}$$

where:

ρ is the density of water, assumed to be 1000 kg/m^3 since USGS and Kansas Geological Survey data as most areas have total dissolved solids < 500 mg/L (Gutentag et al., 1984; Whittemore et al., 2000),

g is the gravitational constant, 9.8016 m/s^2,

V is the annual volume of water pumped (m^3/yr) based on WIMAS data (Wilson et al., 2005)

ϵ_P is the efficiency of the pump and prime-mover (-). We use the typical pump efficiency of 77% based on New (1988) and prime mover efficiency assumed by estimated energy source described in section 3.9, and

L_T is the total effective lift (m), given by:

$$L_T = L_{WT} + L_{CD} + L_{WD} + L_{PR} \quad \text{Equation 2}$$

where:

L_{WT}(m) is the lift from the water table to the ground surface at the start of the pumping season (this is set to 0 for surface water irrigation sources),

L_{CD}(m) is the additional lift due to the cone of depression that forms just outside the well screen during the pumping season,

L_{WD} (m) is the additional lift due to drawdown within the well as a result of frictional losses in and within the immediate vicinity of the well,

L_{PR} (m) is the effective lift due to pressurization and of water and pipe losses necessary for each irrigation system type.

We briefly describe the calculation of each term in Equation 2 here, and provide detailed descriptions of the components below. Each component of Equation 2 was calculated annually for each PDIV, which is dependent on aquifer characteristics, irrigation technology, and water table depth. Depth to water at the beginning of the pumping season (L_{WT}) was computed annually as the difference between the DEM elevation and the annual water table elevation at each PDIV (Haacker et al., 2016). We assume that, at the start of each year's pumping, the water table is essentially flat at the scale of an individual field, and that the in-season cone of depression around each well relaxes prior to each subsequent year's pumping. With a typical pumping season of ~90 days (Hecox et al., 2002) this is a reasonable assumption. Without this assumption, detailed evaluation of cones of depression would be extremely complex and computationally intensive. Roughly 35% of the entries in the WIMAS database did not specify the average pumping rate; those values were estimated annually using system-specific linear regressions against water consumption. The last component of the total dynamic head equation is drawdown, which was estimated for each well using the Cooper-Jacobs method (Kranz et al., 2007a, 2008). The pump rate (Q), was available directly from survey data or estimated (Fig A1.2). Hydraulic conductivity was multiplied by Saturated Thickness to obtain Transmissivity estimates (Cederstrand & Becker, 1998; Haacker et al., 2016). Specific yield estimates from a USGS map were used (McGuire et al., 2012).

$$L_{cd\&wd} = \frac{Q}{4\pi T}\left[-0.5772 - \ln\left(\frac{r^2 S}{4Tt}\right)\right] \qquad \text{Equation 3}$$

Where:

$L_{cd\&wd}$ is the lift, both from *cd* (cone of depression) and *wd* (additional drawdown from well efficiency.

Q is the pump rate, as recorded in WIMAS or estimated for gaps,

T is the Transmissivity, which we calculated using hydraulic conductivity values from the USGS and multiplying by the saturated thickness (USGS),

S is the specific yield, r is the well radius, t is the time pumped. Assuming a well efficiency of 50%, we multiplied $L_{cd\&wd}$ by 1.5 to account for well drag.

4.6 Direct Carbon Emissions from Groundwater Depletion:

(*National Water Information System Data Available on the World Wide Web (USGS Water Data for the Nation)*, 2016)Depletion from groundwater also produces significant CO_2 emissions (Wood & Hyndman, 2017). The CO_2 contribution can be estimated by using information about the volume of water depleted and the bicarbonate concentrations (HCO_3^-) in the aquifer. For this analysis, we computed direct CO_2 emissions over the entire aquifer, rather than at each PDIV as with the direct energy requirements. We interpolated a surface of bicarbonate concentrations based on point data from NWIS (National Water Information System Data Available on the World Wide Web (USGS Water Data for the Nation), 2016), including HCO_3^- concentrations from the Kansas Quaternary deposits and Ogallala Formation (Gutentag et al., 1984). From Wood & Hyndman (2017), we used the HCO_3^- ratio of 0.357 mg CO_2 released

for every 1 mg of HCO_3^- depleted, as described in detail in S3.6. Direct emissions of CO_2 due to groundwater depletion (C_D) are:

$$C_D = V_{dep} \times GW_{CO_2} \quad \text{Equation 4}$$

where:

V_{dep} is the volumetric groundwater depleted in the region of interest (km^3), equivalent to the volume pumped (i.e. V from Equation 1) minus the net annual recharge.

GW_{CO_2} is the equivalent CO_2 concentration in groundwater.

We estimated annual drawdown using successive yearly water table elevation rasters, geographically clipped to a 1 km radius circular buffer around each active pumping well (Figure A1.9). The annual drawdown was then multiplied by the 1 km buffered area and estimated values of specific yield (McGuire et al., 2012) to obtain estimates of groundwater depletion, V_{dep}. We interpolated monitoring well bicarbonate concentrations (*National Water Information System Data Available on the World Wide Web (USGS Water Data for the Nation)*, 2016) using kriging across the buffered portion of the HPA. We then converted the bicarbonate concentrations into equivalent CO_2 released using the mass balance approach for HCO_3^- ratio described in Wood & Hyndman (2017). Equivalent CO_2 released per km^3 depleted (GW_{CO_2}) was estimated from the product of the CO_2 released and the rate of groundwater depletion.

4.7 Carbon and Energy Footprint Calculation:

We calculated the energy and carbon footprint with the direct energy used for pumping using LCA methods. Irrigation technologies and the energy sources for pumping are not uniform across the study region (Figure 1). Pumping and energy use data for Kansas was available within the WIMAS database for 2005-2016. Years prior to 2005 were interpolated using the Farm and Ranch Irrigation Surveys (*Farm and Ranch Irrigation Survey*, n.d.) from 1994, 1998 and 2003,

matched to our wells. With both datasets, we estimated energy type used for each FPDIV_KEY (our unique well identifier) in the region of study from 1994-2016.

For each energy type, we computed carbon footprint per unit of direct pumping energy used, as kg of carbon dioxide-equivalent per PJ (CO_2-eq/PJ). This factor included GHG emissions associated with the pump/prime mover and all upstream activities associated with providing the energy carrier (e.g., electricity, diesel) at each well. In a similar manner, we computed the energy footprint associated with each unit of direct energy used at a well by accounting for all energy expenditures and losses from the well back to the point of extraction of the original energy resources (e.g., oil or natural gas well). Using the equivalent GHG emission factors and energy footprint factors along with estimates of total direct energy used at each FPDIV_KEY, we then computed the total GHG emissions (i.e., carbon footprint) and total energy used (i.e., energy footprint) by year for groundwater irrigation in the Kansas High Plains, accounting for irrigation technology and energy source changes over the analysis period. The annual carbon and energy footprints for electricity used in Kansas were calculated considering changes in electricity production and grid losses.

4.8 Scenario Analysis:

To quantify the influence of widespread adoption of lower pressure technology on the energy and carbon footprints of irrigation, we computed the carbon and energy footprints of three counterfactuals: one scenario assumed LEPA technology transitions had not occurred across Kansas, the other assumed that energy source transitions had not occurred, and the last scenario assumed both irrigation technology and energy source transitions had not occurred. For the energy source scenarios, we assumed that the energy sources for all wells in our study area did not change from the estimated 1994 values. This allowed us to analyze the impact of shifting

energy sources on the energy and carbon footprint of irrigation. In the scenarios that held irrigation technology constant, all FPDIV_KEYs where LEPA systems were newly installed or older irrigation systems were converted to LEPA were treated instead as conventional higher pressure center pivots. Constructing this scenario required only that the pressurization value L_{PR} for the LEPA systems (8 psi) was replaced by that for conventional center pivots (30 psi). Note that wells with estimated pumping rates for both LEPA and conventional center pivots had similar pumping rate regressions (Table 1.1), so estimated pumping rates remained the same for both scenarios. We assume that there were no feedbacks between irrigation technology, energy source, or pumping volumes. For clarity, our baseline analysis, including observed shifts in both irrigation technology and energy sources is termed "Actual w/ LEPA" to contrast with our counterfactual scenario: "Scenario w/o LEPA."

4.9 Life Cycle Greenhouse Gas Emissions and Cumulative Energy Demand:

Using geographically referenced data from WIMAS, we determined the type of energy used at each FPDIV_KEY to pump water from the Kansas portion of the HPA. For each energy type, we estimated pump efficiency and power unit efficiency. As reported in section 1.9, we also estimated the annual amount of direct energy used to lift and pressurize water at each FPDIV_KEY based on WIMAS data (e.g., annual water pumped, depth to water, and irrigation technology used). Combining the direct energy use estimates with pump and power unit efficiencies yielded the total energy used for pumping at each FPDIV_KEY by energy type. For each energy type, we computed the total life-cycle emission of greenhouse gases (GHG) per unit of direct pumping energy used, as kg of carbon dioxide-equivalent per MJ (CO_2-eq/MJ). This factor included GHG emissions associated with the power unit (e.g., diesel engine) and all upstream activities associated with providing the energy carrier (e.g., diesel fuel) at the

FPDIV_KEY location. In a similar manner, we computed the Cumulative Energy Demand (CED) associated with each unit of energy used at a FPDIV_KEY by accounting for all energy expenditures and losses from the FPDIV_KEY back to the point of extraction of the original energy resources (e.g., oil or natural gas well). Using the GHG emission factors and CED factors in combination with estimates of total energy used at each FPDIV_KEY, we then computed an estimate of the total GHG emissions ("carbon footprint") and total energy used (i.e., CED) by year for groundwater irrigation in the Kansas portion of the HPA, accounting for irrigation and energy technology changes over the analysis period.

The following sections provide additional detail on the procedures used for each step of the process described above

4.9.1 Type of Energy Carrier Used for Pumping

We received WIMAS geographically referenced data defining the type of energy used for water pumping in the Kansas portion of the HPA for 2005-2016 from Brownie Wilson of the Kansas Geological Survey. The energy types included in the data are electricity, gasoline, propane, oil, natural gas, diesel, and wind. The number of wells included in this data set ranged from 660 in 2005 to 1234 in 2016, which is a subset of the wells represented in the WIMAS dataset. The energy type data exhibited a clear regional pattern that corresponds to the relative cost and availability of the different energy types in different locations in the study region (see Figure 1, left column).

The "spatial join" ArcGIS geoprocessing tool was used to assign an energy type to all irrigation wells (FPDIV_KEY) for which this information is not available, but water use data are provided in WIMAS within the Kansas portion of the High Plains Aquifer (HPA). Energy type was assigned according to the energy type used at the nearest FPDIV_KEY for which the energy type

feature was defined (i.e., a “nearest neighbor” approach). The spatial distribution of FPDIV_KEY by energy type is shown in the right column of Figure A1.3. The extrapolation maintained the observed proportions of energy types well (Figure A1.4).

Energy type data were not available from the WIMAS dataset for years prior to 2005. Therefore, the energy type assigned to each FPDIV_KEY for the period from 1994 to 2004 was based on data from the Farm and Ranch Irrigation Surveys (FRIS) of 1994, 1998 and 2003 (NASS-USDA 1994) (*Farm and Ranch Irrigation Survey*, n.d.). Tables 17 (1994, 1998) or 20 (2003) of the FRIS reports by state the number of pumps powered by electricity, natural gas, LP gas/propane/butane, diesel fuel, and gasoline/gasohol. Based on the assumption that once in-place, the energy type of a pump was unlikely to change, we began with the WIMAS-based assignment of energy type by FPDIV_KEY in 2005 and working backward, maintained the same energy type assignment in 2004. We assigned an energy type to those few FPDIV_KEYs included in WIMAS for the year 2004 that were not included for 2005 according to the proportions necessary to match the energy type distribution reported in the FRIS data for 2004. The energy type that was assigned to a specific FPDIV_KEY was chosen by random draw.

To make sure our energy source estimates were in line with those reported by the WIMAS database, we use Farm and Ranch Irrigation Surveys from 2008 and 2013. Results showed that energy source estimates compared to WIMAS survey data from 2008 and 2013 were a close match (Fig A1.5). We then used the spatial join to interpolate between Farm and Ranch Irrigation years to compare our linear regression to known energy source estimates form WIMAS shown on Figure A1.6. The strong correlation shown allowed us to justify using Farm and Ranch Irrigation Survey data for the missing energy source years from 1994 to 2004.

4.9.2 Pump and Power Unit Efficiencies

Irrigation pumps are usually powered with an electric motor or a diesel, gasoline, or LP gas engine. Such power units operate at their highest efficiency when loaded near the unit's maximum continuous horsepower rating, and efficiency is reduced if the power unit is overloaded or underloaded (Martin et al., 2011). Electric motors are highly efficient and are easily maintained. New(New, 1988) states that electric motors up to 10 horsepower usually have efficiencies from 75 to 85 percent, while motors of 100 horsepower or larger usually attain efficiencies of 90 to 92 percent. Based on an average irrigation pump size of 78 - 129 horsepower in Kansas (Smajstrla & Zazueta, 2003), we assume an electric motor efficiency of 90%. Large stationary diesel engines can achieve efficiencies of 45 to 50 percent. Schneider and New(A. D. Schneider & L. L. New, 1986) reported diesel engine efficiency from 26.0 to 34.8 percent in tests in the Texas High Plains. Fraizer (Fraizer, 2004) reported a typical engine efficiency of 30 percent for irrigation engines. We thus use a diesel engine efficiency of 30%. Schneider and New (A. D. Schneider & L. L. New, 1986) reported average natural gas-powered engine efficiency of 20.5 percent in tests in the Texas High Plains. Frazier (Fraizer, 2004) reports a typical performance efficiency of about 26 percent for irrigation engines. New (New, 1988) states that a typical natural gas-powered irrigation engine efficiency of 24 percent and a range of 24 to 27 percent. We use a natural gas engine efficiency of 25%. Frazier(Fraizer, 2004) states that 26% efficiency should be expected for LP gas engines under Oklahoma conditions. We use an LP gas engine efficiency of 25%. Schneider and New (A. D. Schneider & L. L. New, 1986) reported average gasoline-powered industrial engine efficiency of 22.3 percent. Frazier (Fraizer, 2004) reported gasoline engine efficiency up to 27%. New (New, 1988) described gasoline-

powered irrigation engine efficiency ranging from 20% to 26%. We use a gasoline engine efficiency of 23%.

4.9.3 Electricity

The carbon footprint and the embodied energy for Kansas was calculated using the modified Process 1MJ Electricity, at eGrid, SPNO from the US-EI 2.2 SimaPro database (*LTS. DATASMART LCI Package n.d.*, n.d.). The eGrid represents the regional electricity production as well as import and export. For the 1990-2016 period, this region corresponds roughly to Kansas since there was no electricity import and between 3-13% of the annual electricity generation that was exported (*Kansas Electricity Profile 2018. Table 10. Supply and Disposition of Electricity*, 2018). The annual electricity generation and grid loss report from the U.S. Kansas Electricity Report was used to calculate the life cycle impact of electricity generation and transmission over time (*Kansas Electricity Profile 2018. Table 10. Supply and Disposition of Electricity*, 2018).

4.9.4 Diesel

Diesel fuels are sold to the residential, commercial, industrial and transportation sectors for use both as heating oil and fuel. Cost for diesel saw a decrease compared to gas (Figure A1.8) around 2005. The total, life-cycle GHG emission from "well-to-pump" of diesel fuel was taken from the GREET model("Greenhouse Gases, Regulated Emissions, and Energy Use in Transportation (GREET) GREET.Net Computer Model," 2017a) as 18.38 g CO_2-equivalents/MJ. Emission of GHG (CO_2, CH_4, and N_2O) due to combustion of diesel (Distillate Fuel Oil No. 2) was taken from Table A-3 of *Direct Emissions from Stationary Combustion Sources* (EPA, 2008). Emissions of CH_4 and N_2O were converted to CO_2-eq using IPCC Fifth Assessment Report (AR5) GWP conversion factors (Stocker et al., 2013). The total, life-cycle GHG emission from

extraction through combustion ("well-to-irrigation") was 88.7 g CO_2-eq/MJ. The CED was computed from the value in Table 4.3 of Aguilera et al. (Aguilera et al., 2017) of the value of energy used for "resource extraction, raw resource transport, refining, processing and distribution of refined products to farm". The CED was 1.26 MJ/MJ (LHV basis, including fuel energy value).

4.9.5 Natural Gas

The life-cycle GHG emission of natural gas from "well-to-delivery" was based on data from the DOE National Energy Technology Laboratory (NETL) report *Life Cycle Analysis of Natural Gas Extraction and Power Generation* (Skone et al., 2016). Natural gas emissions are driven by the source and technology of gas production, both of which change over time. The NETL data accounts for technology profiles in 12 onshore regions and for the supply mix within each region. The Western Kansas region of study is included in the Central Technology Region of natural gas production (Fig 2-1 of Skone) (Skone et al., 2016). Table 3-1 of Skone (Skone et al., 2016) provides a mix of natural gas sources in the Central Technology Region (i.e., percentage derived from coal bed methane, onshore conventional, oil wells, shale, tight gas). Data describing the change in natural gas source from 1993-2016 was provided by T. Skone of NETL based on data from *Annual Energy Outlook 2014* (EPA, 2014). The upstream cradle-to-gate emissions to air of CO_2, CH_4, and N_2O for each natural gas source are provided in Table C-5 of Skone.(Skone et al., 2016) Combining the well-to-delivery GHG emissions associated with each natural gas source and the change in source mix over time and the IPCC Fifth Assessment Report (AR5) GWP conversion factors (Stocker et al., 2013) yielded a yearly value of life-cycle GHG emissions per MJ of gas delivered (Figure A1.7). Emissions due to combustion of natural gas were taken from Table A-3 of *Direct Emissions from Stationary Combustion Sources* (EPA,

2008). Combining the well-to-delivery GWP with combustion emissions gave the total, life-cycle GHG emissions on a well-to-irrigation basis.

Cumulative Energy Demand (CED) data for natural gas in the Central Technology Region were provided by James A. Littlefield of NETL. The CED data are on a well-to-delivery basis and correspond to the data reported in *Life Cycle Analysis of Natural Gas Extraction and Power Generation* (Skone et al., 2016). The CED data include natural gas that is emitted via venting and flaring, as well as the consumptive losses of natural gas for heat, power generation across the natural gas supply chain and resources for transmission pipeline electricity. The CED data were calculated using data from Appendix C of Skone (Skone et al., 2016) and NETL's *Grid Mix Explorer* (Skone et al., 2015). The CED per MJ of natural gas combusted over time is shown in Figure A1.7.

4.9.6 Liquefied Petroleum Gas

LPG or Liquefied petroleum gas is the term commonly used to refer to a family of light hydrocarbons, the most prominent of which are propane and butane, and is commonly called "propane". The total, life-cycle GHG emissions due to combustion of LPG from "well-to-pump" was taken from the GREET ("Greenhouse Gases, Regulated Emissions, and Energy Use in Transportation (GREET) GREET.Net Computer Model," 2017b) as 14.17 g CO_2-eq/MJ. Emission of GHG (CO_2, CH_4, and N_2O) was taken from Table A-3 of *Direct Emissions from Stationary Combustion Sources* (EPA, 2008). Emissions of CH_4 and N_2O were converted to CO_2-eq using IPCC Fifth Assessment Report (AR5) GWP conversion factors (Stocker et al., 2013). The total, life-cycle GHG emission from extraction through combustion ("well-to-irrigation") was 72.4 g CO_2-eq/MJ. The values of CED of LPG from natural gas and crude oil

were taken from the GREET model ("Greenhouse Gases, Regulated Emissions, and Energy Use in Transportation (GREET) GREET.Net Computer Model," 2017b) to be 1121 and 1214 kJ/MJ, respectively. These values were combined using the weighting of 75% from natural gas processing and 25% from petroleum refining according to data from Anne Keller of Midstream Energy Group (Keller, 2012),to give 1.14 MJ/MJ.

4.9.7 Gasoline

The total, life-cycle GHG emission from "well-to-pump" of gasoline was taken from the GREET model ("Greenhouse Gases, Regulated Emissions, and Energy Use in Transportation (GREET) GREET.Net Computer Model," 2017b) as 24.27 g CO_2-equivalents/MJ. Emission of GHG (CO_2, CH_4, and N_2O) due to the combustion of gasoline was taken from Table A-3 of *Direct Emissions from Stationary Combustion Sources* (EPA, 2008). Emissions of CH_4 and N_2O were converted to CO_2-eq using IPCC Fifth Assessment Report (AR5) GWP conversion factors.(Stocker et al., 2013) The total, life-cycle GHG emission from extraction through combustion ("well-to-irrigation") was 91.0 g CO_2-eq/MJ. The CED was computed from the value in Table 4.3 of Aguilera et al. (Aguilera et al., 2017) of the value of energy used for "resource extraction, raw resource transport, refining, processing and distribution of refined products to farm". The CED was 1.30 MJ/MJ (LHV basis, including fuel energy value).

5. Results:

5.1 Irrigation Technology and Energy Sources:

Three irrigation types made up the bulk of 38,014 PDIVs across the Kansas HPA: flood/furrow, conventional center pivots, and LEPA center pivots (Figure 1). At the start of the dataset in 1994, most irrigation systems were flood or furrow systems (36%, hereafter "flood")

and conventional higher pressure center pivot systems (49%, hereafter "center pivot"). Flood systems were relatively abundant within floodplains, while center pivots dominated the upland areas of the aquifer. The transition away from these legacy irrigation technologies to LEPA systems began accelerating in 1996, increasing from 6.9% in 1994 to 52% in 2001, reaching 81% by 2016 (Table S3). The adoption of LEPA systems came mostly as conversion of flood or center pivot systems into LEPA, plus installations of LEPA onto newly irrigated lands. By 2016, 95% of former center pivot and 69% of former flood irrigation PDIVs had transitioned to using LEPA systems (Figure 1). Basic sprinkler and other systems (other non-center pivot systems) also declined in abundance from 9% in 1994 to 6% by 2016, although drip systems increased from just 0.2% in 1994 to 1.6% in 2016.

Irrigation pump energy sources also shifted substantially over the last two decades. In 1994, the three main irrigation energy sources in Kansas were natural gas (64%), electricity (19%), and diesel (9.9%). From 2000 to 2005, diesel use increased to 30%, coincident with a decrease in use of natural gas and electricity. Around this time, there was a reduction in the cost of diesel compared to that of natural gas, making it a more viable energy source (Fig A1.7). After 2005, diesel use gradually decreased to levels similar to those from 1994 (11% in 2016). Broadly, electric pump usage also increased, particularly along the edges of the aquifer (Figures 1d-e). Regions with significant transitions from flood to LEPA irrigation commonly switched to using electricity for their pumps, as aquifer saturated thickness decreased. Use of electricity grew from 19% in the early 90s to 39% by 2016. Electricity production also shifted from coal, nuclear, and natural gas in the 1990s towards more renewable sources (Figure A1.5). Wind started to become an important source for electricity production in 2005, rising from 5% to over 20% of generation by 2016 (Figure A1.5).

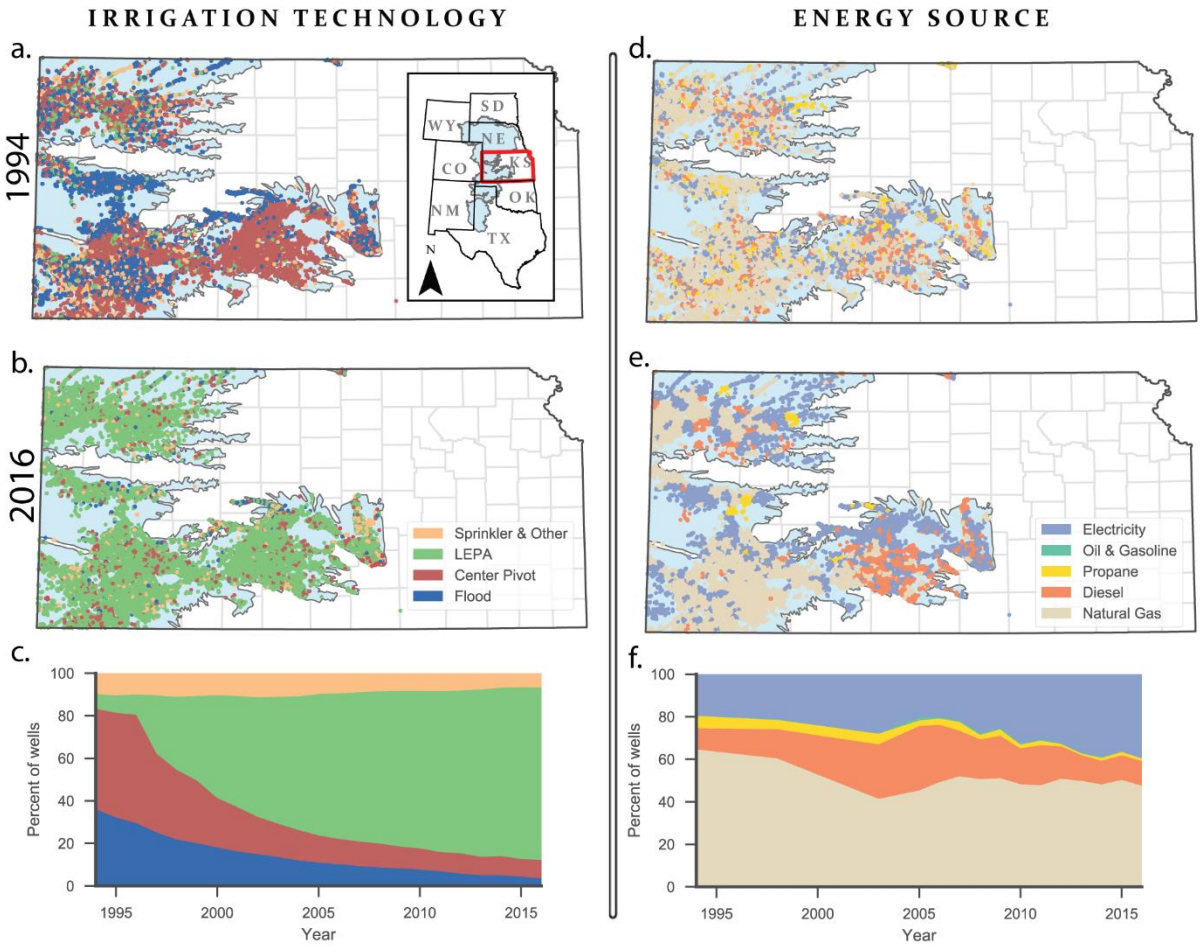

Figure 1.1 Changes in irrigation technology and energy source from 1994 to 2016. This is from the Kansas WIMAS database of over 35,000 wells in the High Plains region of western Kansas. (a-c) From 1994 to 2016 for irrigation technology, Low Energy Precision Application (LEPA) center pivot systems were rapidly adopted while flood irrigation and conventional center pivot systems declined in prevalence. (d-f) Electricity gradually increased as an energy source for pumping while natural gas, still the main energy source, slightly decreased by 2016.

5.2 Energy Footprint and Water Consumption:

Energy footprint values were calculated as a combination of direct energy consumption and embodied energy consumption based on energy source estimates (Figure 2). Energy and water consumption both had cycles of rise and fall through the decades. Water consumption has followed this pattern, with total annual water pumped averaging 3.89 km^3/year, varying from 4.84 km^3/year to 3.03 km^3/year. This trend is paralleled by the energy footprint of irrigation in

Kansas, which averaged 15.0 PJ/year, varying from 18.2 PJ to 12.2 PJ between 1994 and 2016. This is roughly the annual energy produced by a small nuclear power plant in the United States.(EIA, 2020a) The energy footprint trended downward slightly (0.849 PJ/decade), though non-significantly at the 90% level (p = 0.13). The two peaks centered at 2002 and 2011 occurred during historical droughts, resulting in an increase of around 30% in energy footprint relative to normal years (Figure 2a). As with energy use, there is a similar approximately 30% increase in water pumped during peak drought years. The patterns of energy footprint and water consumption through time are broadly similar because direct energy consumption for pumping (Equation 1) is linearly related to the pumped volume of water, mediated by irrigation system type (Table S2), aquifer properties, and depth to water. Direct energy use, in turn, controls the pattern of energy footprint of pumping, which includes embodied energy factors that differ by pump energy source.

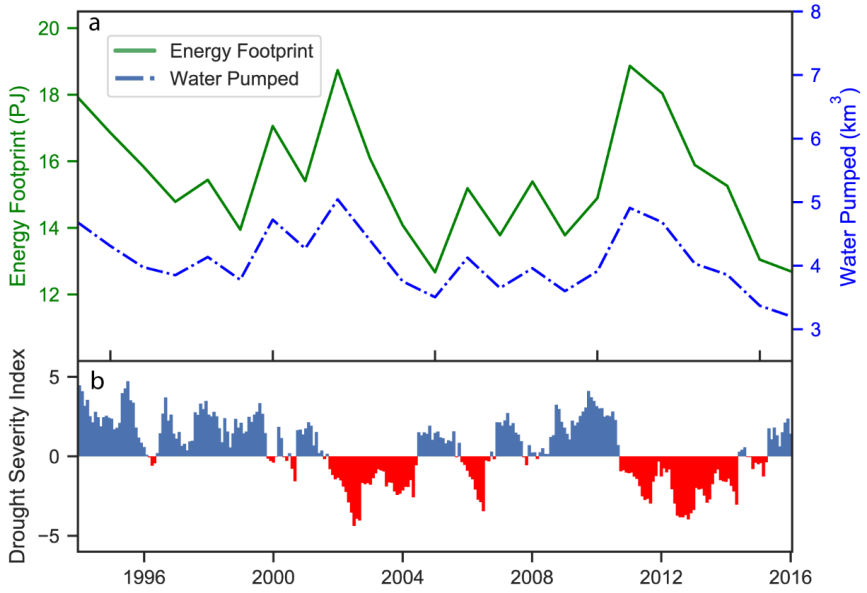

Figure 1.2 Energy Footprint and Water Use. a) Energy footprint (PJ/total annual irrigation) and water use from irrigation from 1994 to 2016 for the HPA portion of Kansas. b) Palmer Drought Severity Index (National Oceanic and Atmospheric Administration, 2020) averaged for the Climate Divisions 1, 4, 7 and 8 of western Kansas, which shows two drought periods from 2002-2004 and 2011-2014.

Transitioning to LEPA irrigation technologies substantially reduced the energy footprint of irrigation across the Kansas HPA (Figure 3). By 2016, the "Scenario w/o LEPA" energy footprint averaged 17.1 PJ/year over the previous 5 years (not shown), compared to "Actual w/ LEPA" that averaged 2.73 PJ/year less. This equates to an energy savings of 18.9%, which grew through time as LEPA adoption became more widespread across the Kansas HPA (Figure 3b). Early in the analysis period, the energy savings of adding LEPA systems was small due to limited adoption, but this grew to around 18.9% by 2005 (Figure 3).

Widespread adoption of LEPA across the Kansas HPA almost entirely offset the increased energy required to pump water from steadily declining water tables. This is illustrated via the region wide-average energy intensity (energy footprint per unit pumped volume), shown in Figure 3c. In the "Actual w/ LEPA" scenario (Figure 3c) the energy intensity of pumping stayed relatively stable between 3.68 and 4.05 MJ/m^3 in most years through 2016. In contrast, for the "Scenario w/o LEPA" energy intensity of pumping increased steadily as depth to water increased, at a rate of 0.315 MJ/m^3/decade ($p < 0.01$). Indeed, over the 23-year study period, mean depth to water increased from 31.3 meters in 1994 to over 41.1 meters in 2016, a linear decline rate of 40.7 cm/year or 4.08 km^3 of water. In both scenarios, there is no notable response in energy intensity of the irrigation systems to drought periods (Figure 2).

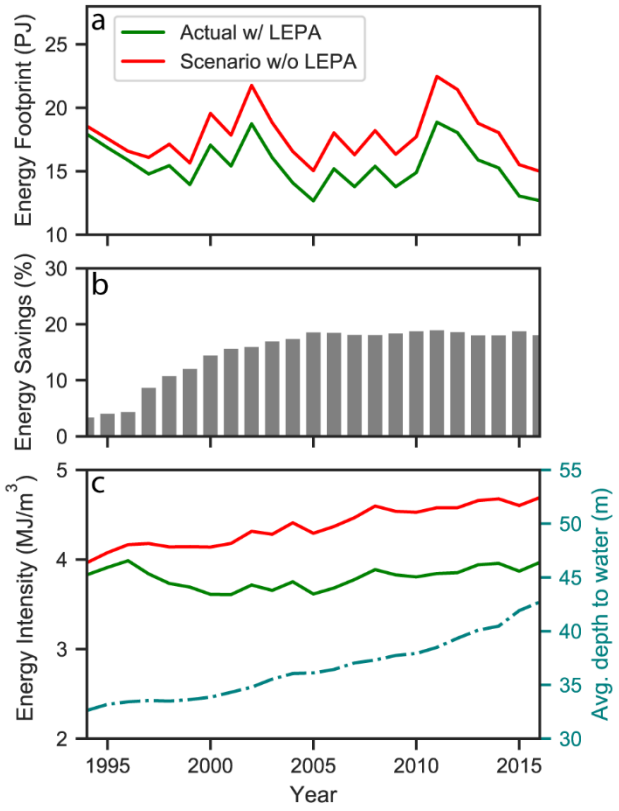

Figure 1.3 Energy Results on Scenarios a) Change in energy footprint of irrigation water pumping (PJ/total annual irrigation) across the Kansas HPA, b) Calculated percent energy saved due to LEPA adoption relative to "Actual w/ LEPA" results, c) Energy intensity for the two scenarios (MJ/m^3 water pumped).

5.3 Carbon Footprint:

The total carbon footprint of irrigation includes both the equivalent carbon emissions from direct and embodied energy consumption, along with carbon released due to groundwater depletion. We found that annual carbon emissions average 1.09 Million Metric Tons per year (MMT/yr.), ranging from 0.85 to 1.44 MMT/yr. (Figure 4). Like the energy footprint, the carbon footprint is driven primarily by direct energy consumption for pumping, with small changes due to the shifting energy sources of pumping, and the changing mix of energy sources in the regional electrical grid. Furthermore, direct groundwater depletion provides a variable

contribution to the total carbon footprint, responding to increased pumping during drought as well as changing rates of water table drawdown regionally.

Continuing declines in groundwater storage have caused the contribution to carbon emissions from groundwater depletion to increase, especially when the rate of depletion is magnified by drought. Since 1994, the contribution from groundwater depletion to the carbon footprint quadrupled from 6.13% to 30.5% (Figure 4), a linear rate of 9.57%/decade ($p < 0.01$). Carbon emissions from energy use alone averaged 0.897 MMT/yr and declined slightly at a rate of 0.0630 MMT/decade ($p = 0.07$). In contrast, carbon emissions from groundwater depletion averaged 0.196 MMT/yr and increased significantly at a linear rate of 0.109 MMT/decade ($p < 0.01$). This increasing role of groundwater depletion in carbon emissions led to a non-significant increase in the overall carbon footprint of pumping 4.70 $x\ 10^{-3}$ MMT/decade, ($p = 0.38$), even though both water and energy consumption have decreased somewhat over the study period. Increasing groundwater depletion emissions have overwhelmed carbon savings due to the LEPA transition, causing carbon intensity (kg CO_2/m^3 water) to increase, though notably less so than in the "Scenario w/o LEPA" (Figure A1.15).

5.4 Energy Sources:

Our analysis included scenarios that held energy source constant from estimated 1994 values. Results from this analysis show relatively little change to energy footprint when energy source is held constant. The "Actual w/ LEPA" scenario had little change in terms of energy footprint when energy sources are held constant (Fig A1.16), with the largest difference being a 1.2% increase in energy footprint in 2016; all other years are less than 1% different than the "Actual w/ LEPA" scenario. When compared to our "Scenario w/o LEPA," the scenario where we hold energy source constant at the 1994 percentages shows a similar trend. Holding energy

source constant did not have a large effect on energy footprint for our study region, with 2016 being the only year exceeding 1% change in magnitude relative to the "Scenario w/o LEPA" results.

In terms of carbon footprint, we begin to see a larger influence of energy sources on GHG emissions. Here, in the "Actual w/ LEPA" scenario, there are two periods where the carbon footprint varies. From 2003 to 2006, there is a 2.2% decrease in carbon footprint for Kansas and from 2013 to 2016, and a 2.1% increase in carbon footprint relative to the "Actual w/ LEPA (Fig A1.16). A similar change occurs when energy source is held constant in the "Scenario w/o LEPA." From 2003-2006, there is a 2.2% decrease in carbon footprint relative to the "Scenario w/o LEPA," and from 2013 until 2016 there is a 2.1% increase in carbon footprint.=

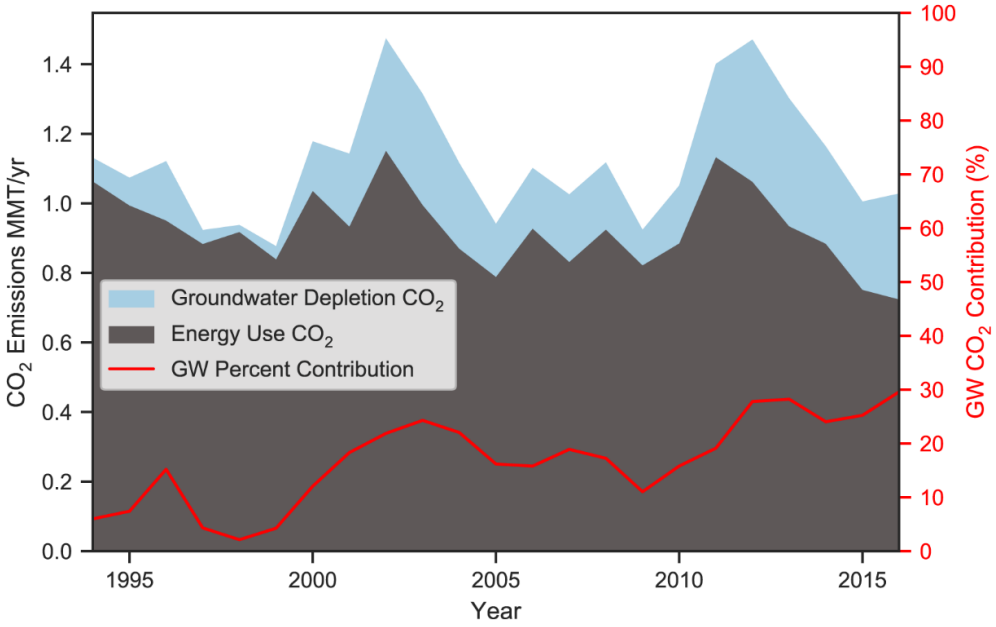

Figure 1.4 Total Carbon Footprint and Groundwater percent contribution. Total carbon footprint from all wells, along with the proportion of CO_2 emissions due to direct groundwater (GW) emissions. Direct (groundwater depletion) and indirect (energy) carbon equivalent emissions are included. The gray area represents cumulative CO_2 equivalent emissions associated with energy consumption for pumping. Light blue shading represents the contribution to CO_2 emissions from groundwater depletion, estimated based on Wood & Hyndman[18]. The percent CO_2 contributions from groundwater depletion are shown in red.

6. Discussion:

6.1 Changing Systems:

Over the last two decades, irrigators in Kansas shifted from legacy systems to water- and energy-conservative Low-Energy Precision Application (LEPA) systems. The shift to LEPA largely occurred from 1996 - 2005 (Figure 1); in that 10-year period 16,580 points of diversion (PDIVs) transitioned to LEPA, and 4,641 new LEPA PDIVs came online. Irrigators shifted pump energy sources from diesel to natural gas in response to decadal commodity price fluctuations, but have steadily transitioned to electrical-powered pumps, particularly in areas of the HPA with lower saturated thicknesses. While the transitions analyzed here are specific to the Kansas HPA, they are driven by changes in technology and energy that are playing out globally in other extensively irrigated areas of the world.

Wholesale LEPA adoption over the entire Kansas HPA has transformed the water, energy, and carbon profile of irrigation. Through scenario analysis, we estimate that LEPA and related systems have reduced the energy footprint and resultant carbon equivalent emissions of irrigation in Kansas by 19.2% and 15.2%, respectively. These savings accumulated quickly as legacy irrigation technologies transitioned to LEPA, and largely levelled off by 2000 (Figure 3b, A1.12b). Despite this widespread technology transition, however, water table depths continued to increase unabated. Others have shown that by adopting water- and energy-conserving technologies, water and energy use may actually accelerate, a phenomenon known variously as Jevons Paradox(Polimeni et al., 2012) or the Rebound Effect.(Li & Zhao, 2018) Nevertheless, widespread LEPA adoption allowed average irrigation energy intensity (MJ/m^3 pumped) to remain constant over the study period. Had the transition to LEPA not occurred, irrigation energy intensity would have increased in concert with depths to water in the HPA (Figure 3c). Going

forward, now that the transition to LEPA has plateaued, offsetting increased energy demands from continued aquifer drawdown will require reducing other terms in Equation 1, including pump efficiency and, most importantly, pumped volume. Our analysis of energy source transition scenarios showed use that while shifting energy sources did not have a large effect on energy footprint, it did affect carbon footprint for 2003-2006 and 2013-2016. Coincidentally, these are periods when energy source transitioned the most. As we mentioned above, the years surrounding 2005 saw a decrease in diesel prices. This shift increased the carbon footprint of irrigation in Kansas, and it is very apparent in our results. From 2013 until 2016, we see an increase in electricity use for the region (Fig 1). The shift to more electricity had a noticeable impact on the carbon footprint of irrigation in Kansas. Our results for direct energy consumption are comparable to work done by Groundwater Management District 3, which estimated 1679 GWh of direct energy being used in their district to pump water in 2017.(*Revised Management Program Southwest Kansas Groundwater Management*, 2020) Our direct energy results for that district estimate that roughly 2,000 GWh were used in in this district in 2016. These results are comparable, and the differences can be attributed to parameter details. While the Groundwater Management District 3 estimate used an average depth to water for the whole district (~91 m), we extracted depth to water from each well. Our energy footprint is similar to those from research conducted in Oklahoma.(Handa et al., 2019) Our irrigation energy intensity averaged 3.8 MJ/m^3, while the previously mentioned study ranges around 6.63 MJ/m^3. The differences between these values can be explained by the greater average depths to groundwater in the Oklahoma study (approximately 62 meters for their 20 study wells in 2018) versus across our Kansas HPA region (42m in 2016). This further emphasizes the need for more sustainable water table management. As a result, appropriate management practices and conservative water

policies are crucial to incentivize adoption of new irrigation technology and water conservation measures.

Our analysis also shows the large impact that droughts (Figure 2b) have on a region's water use, energy footprint, and carbon footprint. During droughts, there is an increase in groundwater extraction (Figure 2a), which drives an increase in energy use, leading to an increase in equivalent carbon emissions both from energy consumption and the direct contributions from groundwater depletion. This was also observed in studies where drought years in central and panhandle portions of Oklahoma experienced greater emissions.(Handa et al., 2019) Increasing water use during drought periods reduces the water table, which is why we see increased energy intensity during drought periods (Fig 3c). During the two main drought periods in our study period, the energy footprint rose by approximately 20% (Figure 2). Carbon footprint during droughts increased from ~20% to 30% in 2002-2003, and from 25% to 40% in 2010-2012 (Figure 4). Because groundwater depletion increases during droughts, the contribution of CO_2 emissions from groundwater is magnified. Droughts clearly have a significant impact on water use, as well as energy and carbon footprint. Low-pressure irrigation technologies can help mitigate energy, water, and carbon costs during droughts, but they need to be accompanied by appropriate water management policies to improve sustainability.

6.2 Implications & Future Work:

We analyzed the effects of irrigation technology changes on water consumption and energy and carbon footprints in the Kansas portion of the High Plains Aquifer. This region has large areas of irrigated agriculture and water extractions are exceeding aquifer recharge. Adoption of LEPA irrigation technologies allowed the extraction of water from increasingly thin aquifers, led to savings in the energy and carbon footprints of irrigation, and limited increases in

irrigation energy intensity. Although, despite adoption of more water-conservative irrigation technologies, water tables continue to decline, and will drive increases in both the energy and carbon intensity of irrigation in the years to come. In particular, deepening water tables have increased carbon emissions directly due to groundwater depletion. In drought years, these effects are magnified as increased water consumption directly drives increases in energy consumption and carbon emissions.

Most studies that explore the role of direct carbon emissions due to groundwater depletion are relatively coarse.(Wood & Hyndman, 2017) Understanding this aspect of the global carbon cycle in more detail will not only help to better understand the carbon and energy footprints of our food, fiber, and fuel agricultural systems, but also better identify changes in carbon emissions due to land use practices worldwide. Furthermore, a more detailed examination of how the water, energy, and carbon footprints of irrigation change across agricultural regions for a range of crops and other agricultural products is warranted. There is also a need for additional research on how changes at the nexus of food, water and energy associated with shifts in irrigation. Finally, it will be important to both quantify how other technologies (such as variable rate irrigation) may help increase energy efficiency going forward, and link adoption of these technologies and practices to policies that incentivize reduced water consumption that ultimately reduces energy use and carbon emissions.

7. Acknowledgments

This Chapter was coauthored by Anthony D. Kendall, Erin M.K. Haacker, Annick Anctil, Yong Wang, Robert Anex, and David W. Hyndman. This work is supported by INFEWS grant 2018-67003-27406 (accession no. 1013707) from the USDA National Institute of Food and Agriculture, “Developing Pathways Toward Sustainable Irrigation across the United States

Using Process-based Systems Models (SIRUS)". Work by E.M.K. Haacker was supported by the National Institute of Food and Agriculture, U.S. Department of Agriculture, under award 2016-68007- 25066, "Sustaining agriculture through adaptive management to preserve the Ogallala Aquifer under a changing climate." Any opinions, findings, and conclusions or recommendations expressed in this publication are those of the authors and do not necessarily reflect the views of the USDA. Reprinted (adapted) with permission from: McCarthy, B., Anex, R., Wang, Y., Kendall, A. D., Anctil, A., Haacker, E. M. K., & Hyndman, D. W. (2020). Trends in Water Use, Energy Consumption, and Carbon Emissions from Irrigation: Role of Shifting Technologies and Energy Sources. Environmental Science and Technology. https://doi.org/10.1021/acs.est.0c02897.

APPENDIX

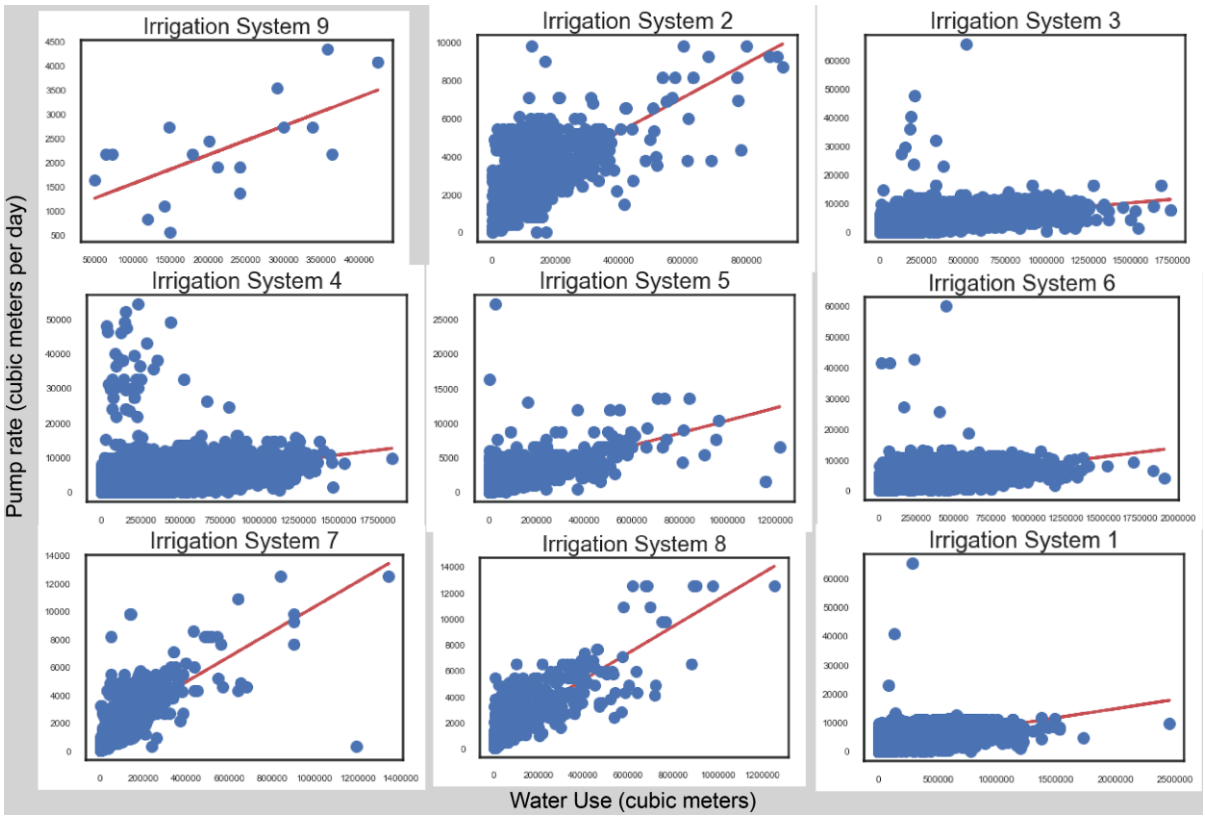

Figure A1.1 Pump Rate Linear Regressions Pump rate estimates made using regression lines with annual water use (m3) in x-axis and pump rate (m3/day) in y-axis. Systems are are follows: 1) Flood 2) Trickle-Drip 3) Center Pivot 4) Center Pivot LEPA 5) Sprinkler other than CP 6) Center pivot and flood 7) Subsurface drip 8) Other 9) Center pivot w/ Mobile drip.

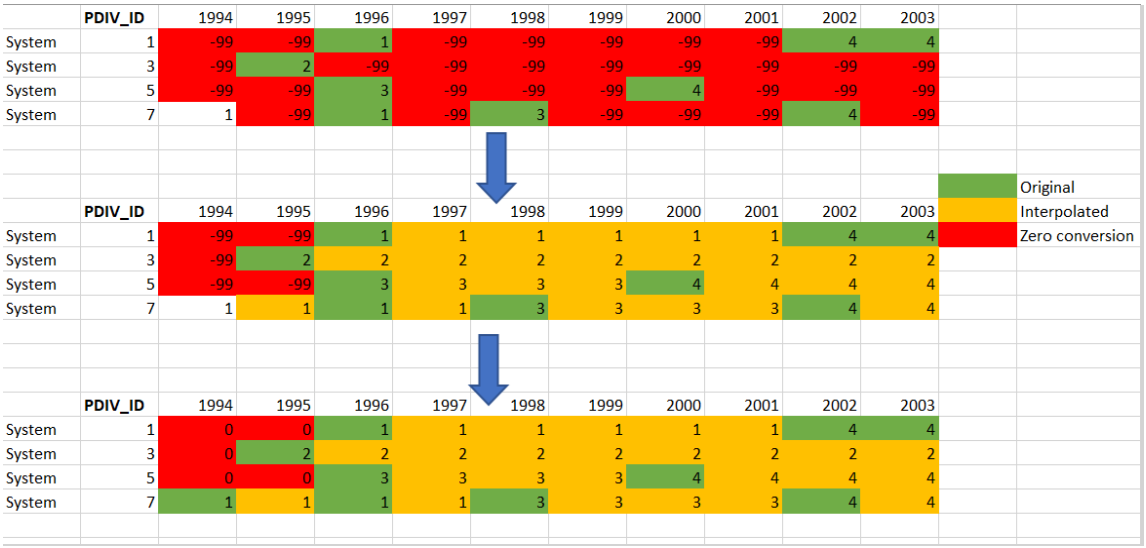

	PDIV_ID	1994	1995	1996	1997	1998	1999	2000	2001	2002	2003
System	1	-99	-99	1	-99	-99	-99	-99	-99	4	4
System	3	-99	2	-99	-99	-99	-99	-99	-99	-99	-99
System	5	-99	-99	3	-99	-99	-99	4	-99	-99	-99
System	7	1	-99	1	-99	3	-99	-99	-99	4	-99

	PDIV_ID	1994	1995	1996	1997	1998	1999	2000	2001	2002	2003
System	1	-99	-99	1	1	1	1	1	1	4	4
System	3	-99	2	2	2	2	2	2	2	2	2
System	5	-99	-99	3	3	3	3	4	4	4	4
System	7	1	1	1	1	3	3	3	3	4	4

	PDIV_ID	1994	1995	1996	1997	1998	1999	2000	2001	2002	2003
System	1	0	0	1	1	1	1	1	1	4	4
System	3	0	2	2	2	2	2	2	2	2	2
System	5	0	0	3	3	3	3	4	4	4	4
System	7	1	1	1	1	3	3	3	3	4	4

Figure A1.2 Forward Fill Method Example. Example of the ffill() method used in the analysis 1. A pivot function organized the wells by FPDIV_KEY and Irrigation system, leaving the years in the columns 2. The ffill() function in python was used to fill in the first number in every row until a new number was reached, then that number would start filling in 3. If there was no number before (like the red ones), they were converted it to 0 meaning no system.

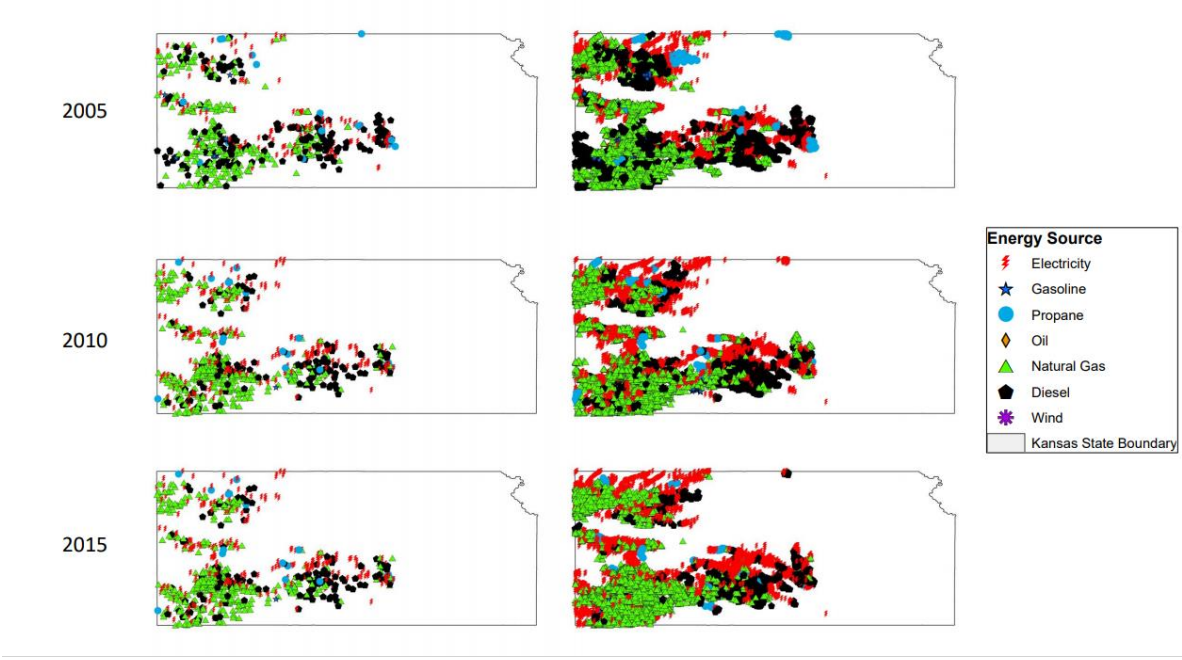

Figure A1.3 Distribution Of Irrigation Wells By Energy Source Spatial distribution of irrigation wells by energy type: (1) WIMAS energy type data (left column); and, (2) after extrapolation to all FPDIV_KEYs using 'nearest neighbor' method of ArcGIS *Spatial Join* tool (right column).

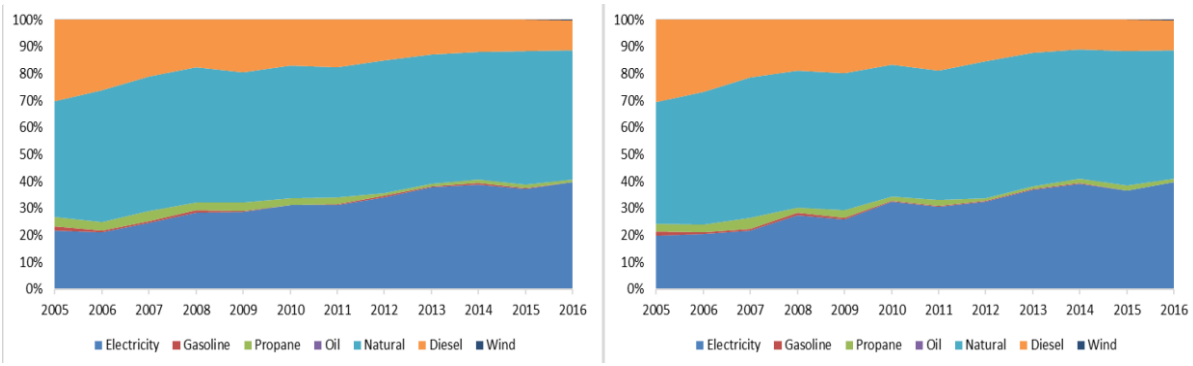

Figure A1.4 Comparison Between Observed and Extrapolated Energy Sources Proportion of FPDIV_KEYs using each energy type: as observed (left) and, after nearest neighbor extrapolation (right).

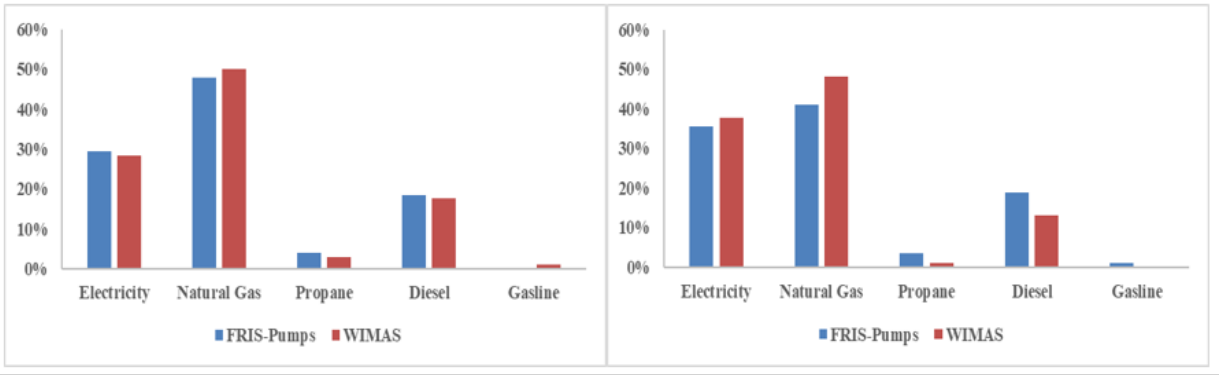

Figure A1.5 Energy Source Comparisons (WIMAS vs FRIS) Comparison of energy source percentages in WIMAS data (HPA_KS) and FRIS data (pumps) in 2008 (left) and 2013 (right) to justify the FRIS data use when energy source investigations in WIMAS were unavailable before 2005. Years when FRIS data were used are 1994, 1998, and 2003. Energy source percentages in interim year (1995-1997, 1999-2002, 2004) were linearly interpolated based on known percentages in FRIS or WIMAS.

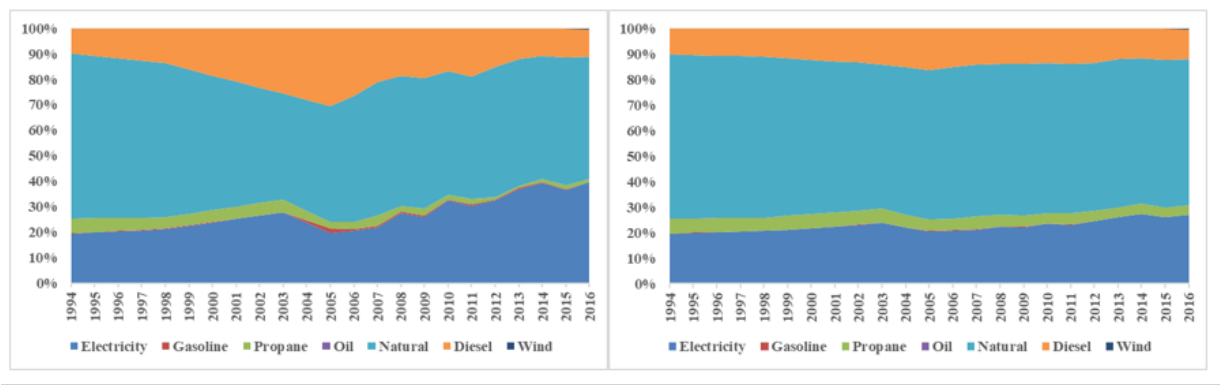

Figure A1.6 Energy Source from 1994 to 2016 for HPA Calculation of energy source percentages in 1994-2016 for HPA Kansas with actual energy source counts (left) and virtual energy source counts (right). For virtual energy source scenario, energy source was kept the same as in 1994 for FPDIV_KEY that appeared again in later years, and energy source was kept as actual for FPDIV_KEY that newly appeared in later years.

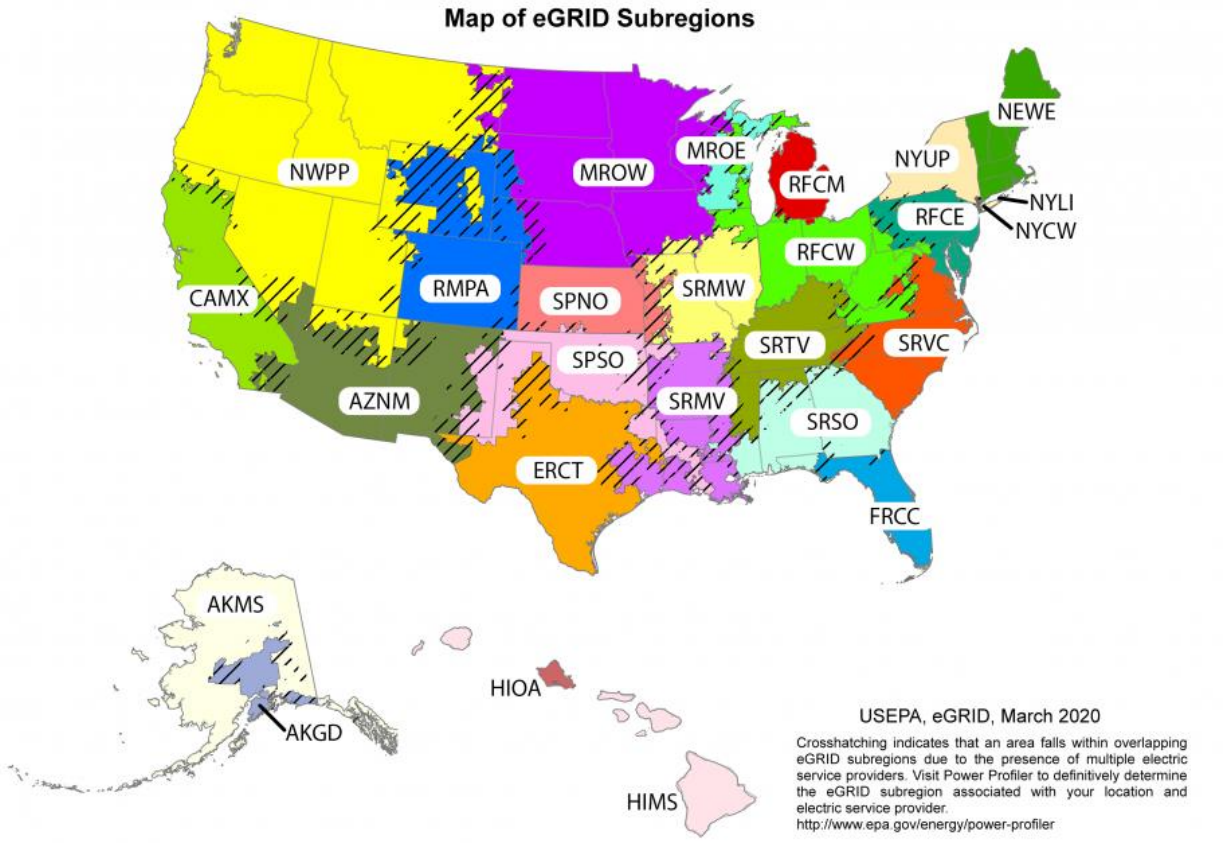

Figure A1.7 Electric Grid Definitions eGRID2014 regions definition(*LTS. DATASMART LCI Package n.d.*, n.d.)

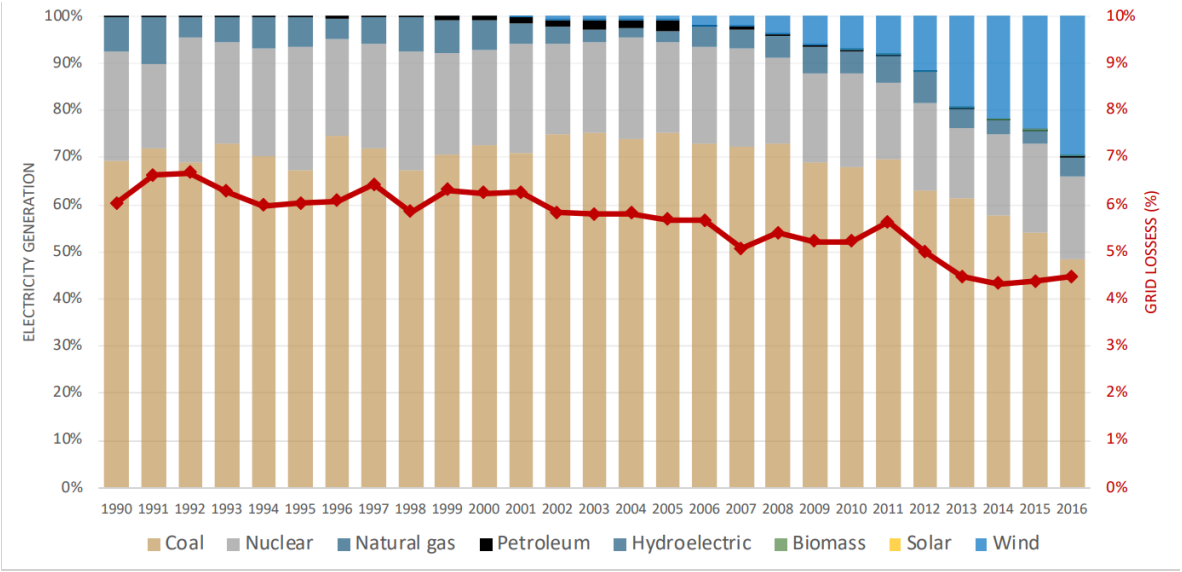

Figure A1.8 Electricity Generation Over Time Electricity generation and grid losses over time for Kansas

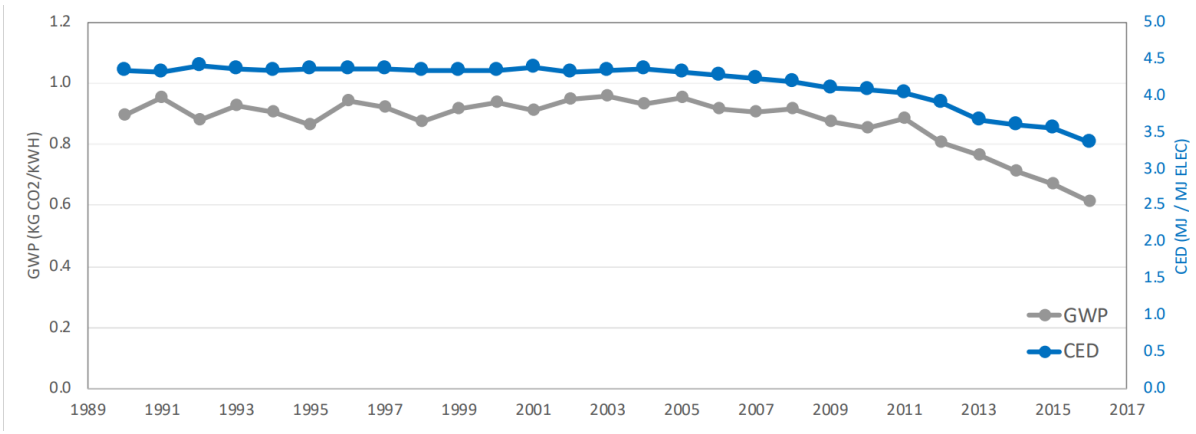

Figure A1.9 GWP & LCA of Electricity Production Life-cycle Global Warming Potential (GWP) and Cumulative Energy Demand (CED) of electricity production over time

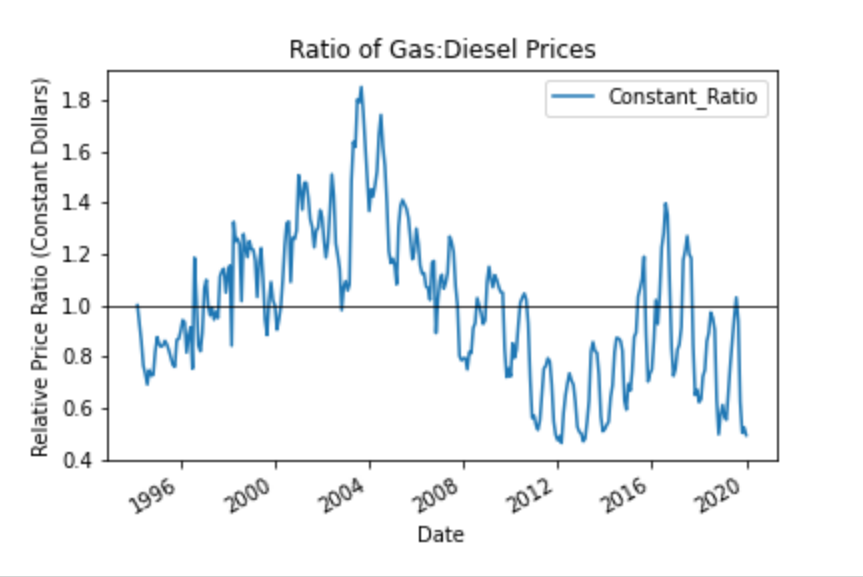

Figure A1.10 Ratio of Gas to Diesel Prices , from EIA databases.(U.S. Energy Information Administration, 2020a, 2020b)

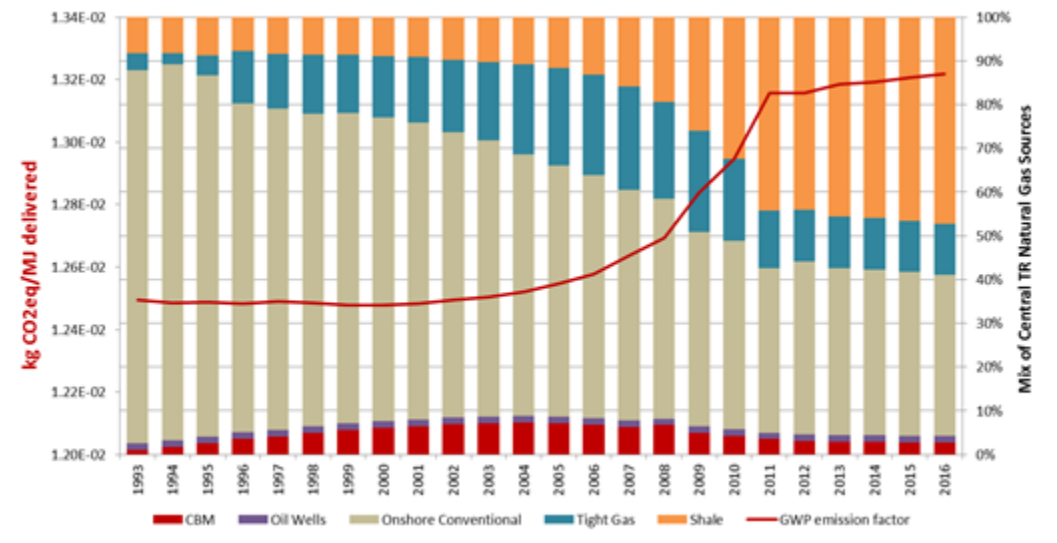

Figure A1.11 GWP of Natural Gas from Irrigation Life-cycle Global Warming Potential (GWP) of natural gas from well-to-irrigation. The life-cycle GWP (red line, left axis) increases as the share of natural gas from shale increases and onshore conventional decreases over time (right axis).

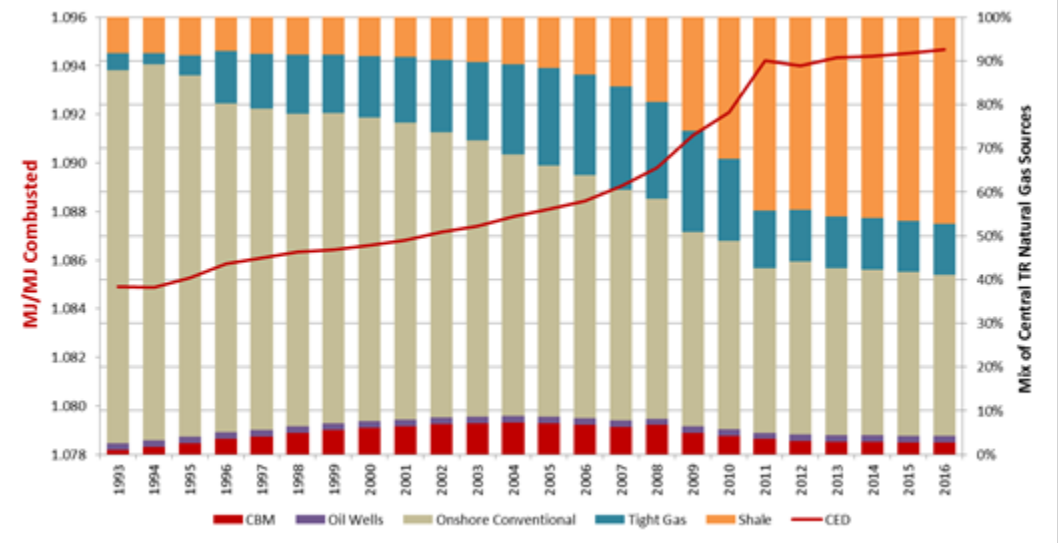

Figure A1.12 CED of Natural Gas from Irrigation Cumulative Energy Demand (CED) of natural gas from well-to-irrigation. The CED (red line, left axis) increases as the share of natural gas from shale increases and onshore conventional decreases over time (right axis).

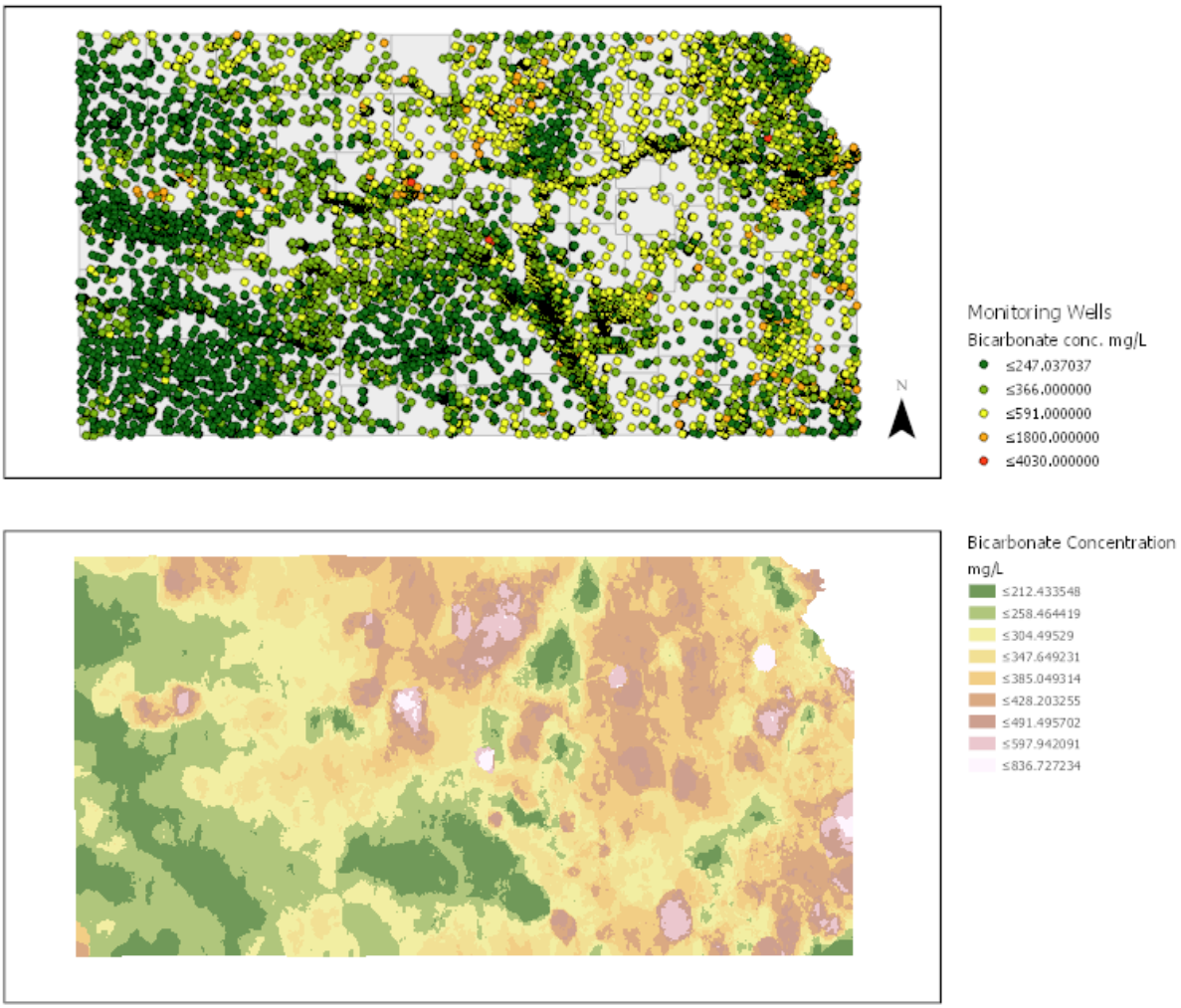

Figure A1.13 Bicarbonate Kiriging Results. shows the kriging interpolation of bicarbonate concentrations across Kansas. Universal Kriging was used to compensate for the topographic first order trend and large data set.

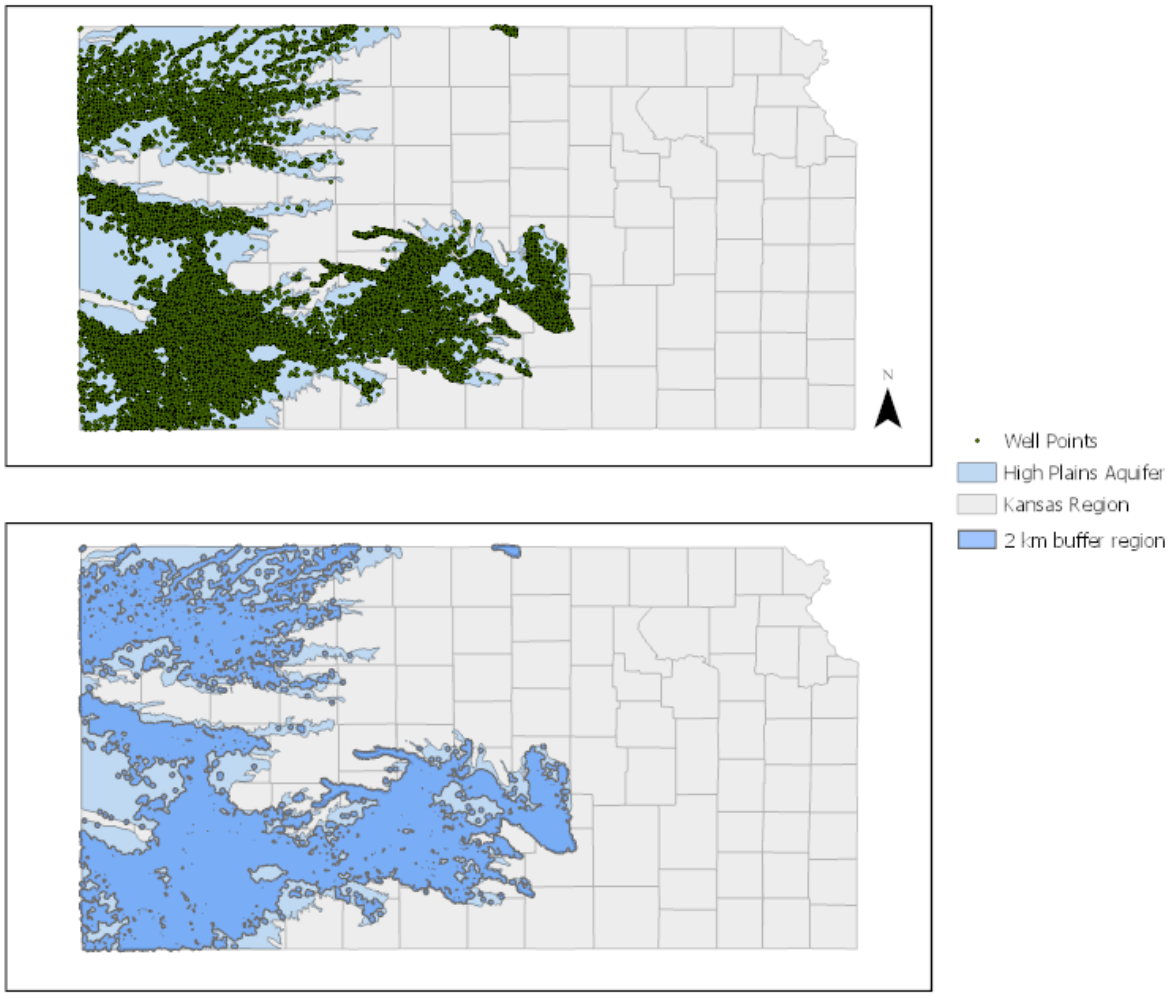

Figure A1.14 Proposed Pumping Buffer. shows the created buffer zones for "active" irrigation. 1 km buffers were created to get an accurate value for seasonal area of irrigation, where carbon release has it's largest impact.

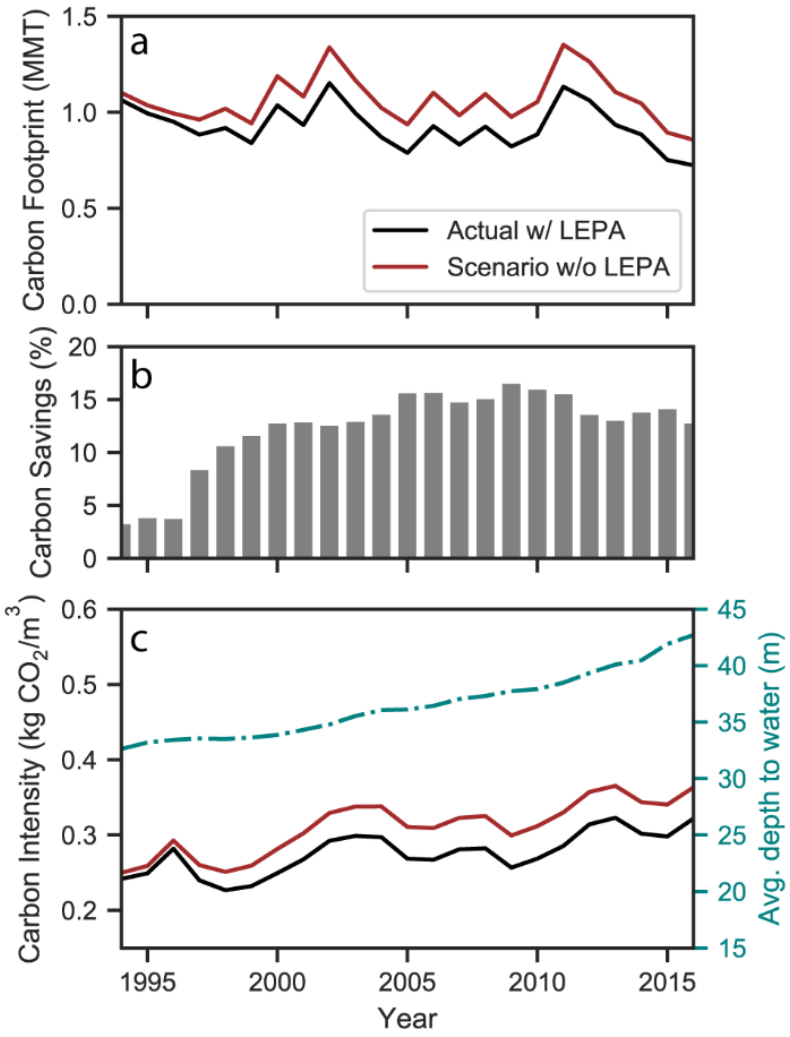

Figure A1.15 Scenarios on Carbon Footprint. shows the change in carbon emissions per cubic meter of water pumped. This is shown along with a change in water depth line to indicate the offset that LEPA integration has created. We graphed the total kg carbon emitted estimated from the static irrigation scenario and compared them in terms of percent difference relative to the observed "LEPA" scenario.

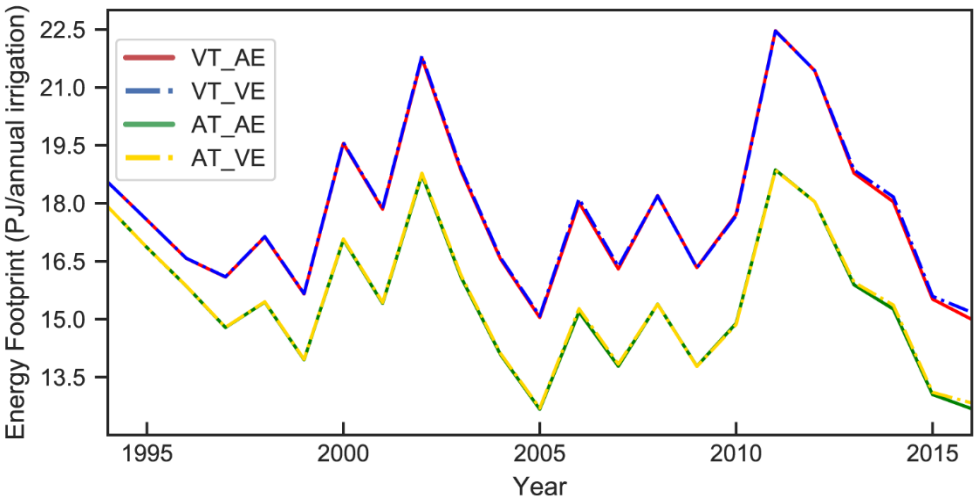

Figure A1.16 Energy Footprint on Various Scenarios Shows the energy footprint of all scenarios in our analysis. Here, we varied irrigation technology and energy source. VT_AE: Irrigation technology was held constant from 1994, and energy source is what was observed. VT_VE: both irrigation technolgy and energy source was held constant from 1994. AT_AE: this is the scenario where no variables were held constant, actual results. AT_VE: Irrigation technology is what was observed and energy source was held constant from 1994 until the end of our study period.

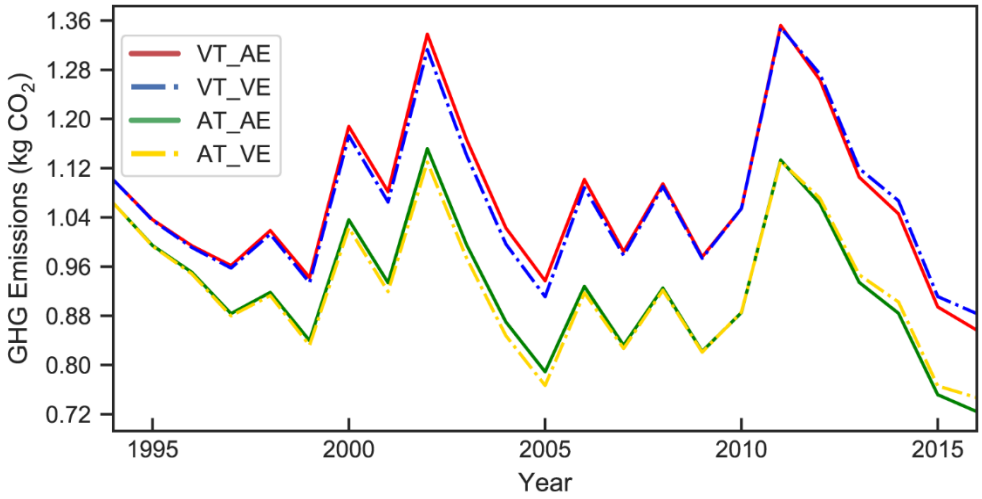

Figure A1.17 GHG on Various Scenarios Shows the carbon footprint of all scenarios in our analysis. Scenarios are the same as Figure A1.17. Here we see the influence of 2 large energy soure shifts in our study period, the diesel growth in 2005, and the electricity growth in the later 2010s.

Table A1.1 Percent Distribution of Systems. Percent distribution of irrigation systems in the HPA

Year	Flood	Trickle-Drip	Center Pivot	LEPA	Sprinkler other than cp	Center Pivot & Flood	Subsurface Drip with other	Other	Center Pivot w/ mobile drip
1994	36%	0.25%	47%	6.9%	1.8%	7.6%	0.00%	0.00%	0.00%
2001	16%	0.24%	20%	52%	1.3%	9.1%	0.05%	0.00%	0.00%
2016	3.6%	1.4%	8.6%	81%	1.2%	3.5%	0.42%	0.11%	0.11%

CHAPTER 2: CONUS ENERGY MODEL

1. Abstract

Agricultural intensification and freshwater availability both dominate energy production in the United States. Almost half of the water consumed in the United States is used for agricultural production. The increase in irrigated acreage at both the national and county levels have created new areas of interest in terms of energy consumption both spatially and temporarily. 70 % of water consumption can be directly attributed to irrigated acreage and agriculture. In this study, we use previously established Farm Resource Regions and county level aggregates to estimate direct energy from on-farm Irrigation. The purpose of this study is to estimate energy consumption from crop irrigation and explore the relationship between water use, energy consumption and crop type across counties and Farm Resource regions. Results indicate energy use per county ranged between 0 and 2.33 MWh/per acre irrigated for an irrigated season. Nebraska, California, Texas, Arkansas, Idaho, and Kansas account for 64% of all energy consumed for agricultural purposes in the continental United States. While farms across the country may source their water from aquifers or surface bodies, over 60% of states source their freshwater from shallow or deep aquifers. Among Farm Resource Regions, the Fruitful Rim, Mississippi Portal and Prairie Gateway were some of the highest energy consumers in the agricultural sector. Results indicate that energy use varies greatly spatially, with patterns of similarity within States and Farm Resource Regions.

2. Introduction

Freshwater availability and technology shapes production and energy consumption in the United States agricultural sector (Dimitri et al., 2005). In 2015, 42% of water consumption in the United States is from agricultural irrigation (Dieter et al., 2018). Water scarcity in recent decades has forced farmers and crop producers to rethink the way they manage their farms, introduce new technologies, and maintain their water use (Marshall et al., 2015). While these innovations have increased production, the practices are often unsustainable and thus result in the rapid water table declines (Famiglietti, 2014; Konikow, 2015; Konikow & Kendy, 2005; Scanlon et al., 2021), increased energy demand and greenhouse gas emissions. These factors play a critical role in agriculture, and they must be closely examined to understand their current and future impacts from local and regional dynamics.

Rapid expansion of irrigated acreage from 1935 to the 1970s in the United States led to many states being dependent on crop production as their main economic input. Since the 1970s, average farm size has remained steady at around 440 acres (USDA, 2021). States like Nebraska, California, Arkansas, Texas, Idaho, and Kansas account for over 55% of total irrigated acreage in the United States (USDA, 2021; Vilsack & Reilly, 2013). Early in the 1980s, most irrigation systems in agriculturally intensive western states were gravity fed systems that required little to no pressurization. In the coming decades, many of these states began adopting pressure sprinkler irrigation systems that increased water use efficiency and allowed farmers to continue or expand their crop production with less irrigation (Hrozencik & Aillery, 2021). This led to a shift in water resources, as pressurized systems require steady inputs, either from storage reservoirs, canals, shallow groundwater, or deep aquifers (Fan & McCann, 2020; Hrozencik et al., 2021; Pfeiffer, 2010). These states are often underlain by major aquifers that supply their freshwater demand.

Exploitation of these resources for commercial, residential, and agricultural uses has caused massive declines in water storage since predevelopment (Dieter et al., 2018; Famiglietti, 2014; Haacker et al., 2016; Wada et al., 2010). Regions that are too arid to rely on surface water sources find themselves drilling deeper wells and using more energy to pump from those depths. States that rely on groundwater use have found that, while switching lower-pressure sprinklers can offset some increased energy demand from deeper water tables, regions that introduce new technology should implement strict water management policies to truly decrease energy costs and help their ground water levels recover (Deines et al., 2019; McCarthy et al., 2020).

For farmers in the United States, the economics of irrigation and crop production are significant drivers of agricultural production (Innovation, Agricultural Productivity and Sustainability in the United States, 2016). Even then, market-driven agriculture trends can often interfere with sustainable practices if not properly integrated. Understanding the complex system of production, energy cost and water use from local to regional scales can help stakeholders and policymakers reduce the overexploitation of water resources in the agricultural sector. Understanding how local energy use for irrigation is affected by regional conditions can aid in making informed decisions and increase crop yield while mitigating costs (Deines et al., 2019).

Many studies have estimated the total energy use by the agricultural sector in the United States (Beckman et al., 2013; Camargo et al., 2013; EPA, 2014; Hitaj & Suttles, 2016a; Miranowski & Miranowski, 2006; Shahbaz et al., 2018). These studies often involve nationally aggregated energy estimates based on the operating costs of production and crop yield of given regions. One of the complications that arise with scale is the lack of spatial variability when the estimates are published. Valuable information is lost when the distribution of energy consumption is limited to national or state values.

Here, we upscale a previous method to estimate direct energy use (McCarthy et al., 2020). We define direct energy use as the product of total required lift, water use and the gravitational constant. This does not consider pumping efficiency, prime mover efficiency, or energy sources. Our method involves using county-level water use data along with state-level information on farm operations to estimate energy use across the CONUS. We then validate our results with available energy estimates from Kansas. Our final product will be a dataset containing energy estimates for 3,006 counties across the CONUS. We believe that spatially explicit county level estimates of direct energy use will significantly contribute to the complex agricultural sector in the United States.

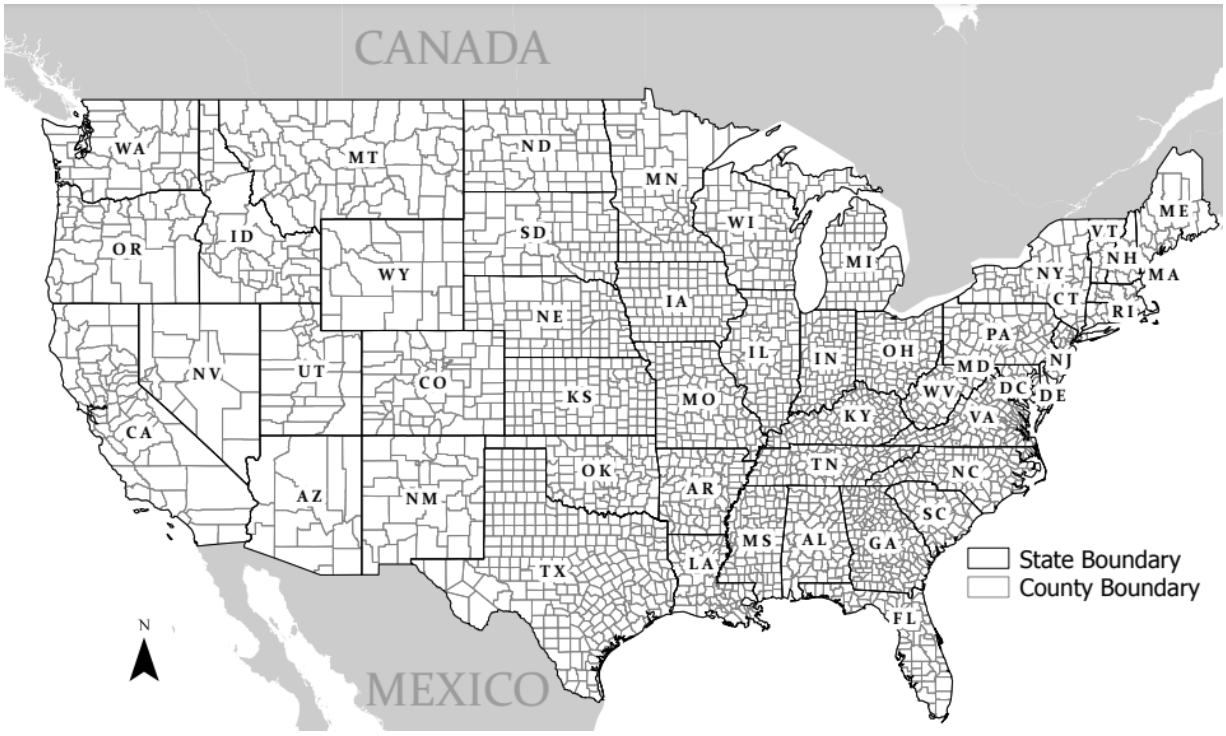

Figure 2.1 Map of Continental United States Counties. The United States contains over 3,000 counties. Here, we estimate energy consumption across the continental United States on a county level.

3. Materials and Methods

3.1 Study Region:

This study focuses on the continental United States of America. Here, we leverage county and state level information to provide accurate county level estimates of irrigation direct energy use for all 3,143 counties in the CONUS. In the early 2000s, the USDA published a report detailing resource regions based on: county farm characteristic clusters, land resource regions, farm production regions, and crop reporting districts. This study led to the establishment of 9 designated resource regions: the Heartland, Northern Crescent, Northern Great Plains, Prairie Gateway, Eastern Uplands, Southern Seaboard, Fruitful Rim, Basin and Range and the Mississippi Portal (Figure2.2) (Heimlich, 2000). The Heartland is commonly known as the corn belt, where the largest share of farms per county are found, along with the highest value of production and the most cropland. The Northern Crescent has the highest general populations and agricultural production in this region involves dairy, general crops, and cash grains. The Northern Great Plains is characterized by having largest acreage farms and lowest population with wheat, cattle, and sheep farms being more predominant. The Prairie Gateway region the second largest wheat, sorghum, cotton and rice production. The Eastern Uplands have the smallest farms out the regions with 15% of farms and 6% of national cropland. The Southern Seaboard has 11% of farms and 6% of cropland, known for having a combination of small and large farms. The fruitful rim has the highest share of fruits vegetables and cotton, this region also consists of large farms. Basin and Range has the smallest share of US cropland at 4%, wheat and sorghum are common crops. The Mississippi Portal has higher proportions of farms in their counties concentrating along the Mississippi basin. Each of these regions provides essential growth and agricultural production for the entire United States. Therefore, it is important to

understand how these individual regions source their water needs and manage their irrigation technologies.

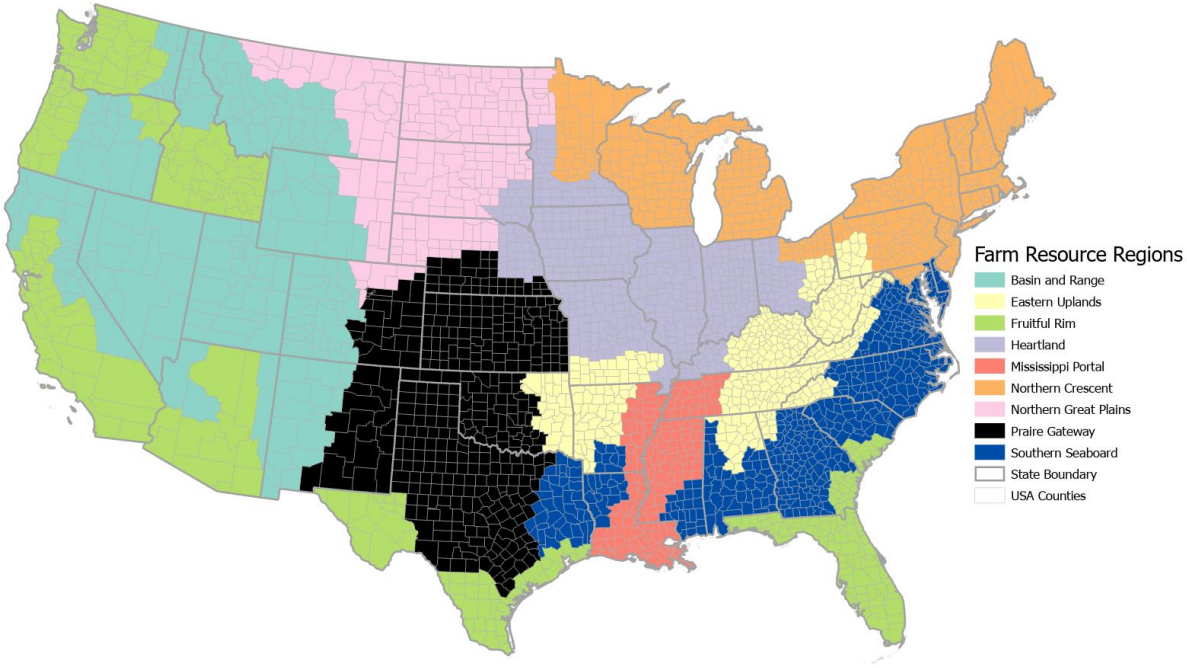

Figure 2.2 Farm Resource Regions. This map illustrates the spatial distribution of the Farm Resource Regions defined in 2000 by the USDA.

3.2 Data Sources:

The work presented in this study was compiled by county using ArcGIS (U.S. Department of Commerce, 2021). NASS county farm statistics were used to determine the number of farms in each county (*2017 Census of Agriculture*, 2019). Water use was derived from the 2015 USGS water use report by county, which reported water use in terms of surface water or groundwater fed irrigation (Dieter et al., 2018). In some counties, surface water or groundwater fed irrigation was not specified, so the 2013 FRIS dataset was used to estimate irrigation water source by state and downscaled to counties that were missing this information (Vilsack & Reilly, 2013). Irrigation efficiency by state was also estimated from FRIS and

downscaled to counties (Vilsack & Reilly, 2013). CONUS -wide depth to water and transmissivity estimates were obtained from (Zell & Sanford (, 2020). Specific yield was derived from SSURGO (Soil Survey Staff, 2021). Estimates of irrigated acreage were obtained from MiRAD dataset, and an augmentation method was applied using USGS irrigated acreage estimates (J. F. Brown & Pervez, 2014; Dieter et al., 2018; Pervez & Brown, 2010). NLDAS 2A Yearly Forcing data was used to obtain county level estimates of precipitation, temperature, and potential evapotranspiration nationwide ((Xia et al., 2012)). USDA was used to derive maturity dates for corn, cotton, wheat, soy, rice in 2017 (*2017 Census of Agriculture*, 2019). For validation purposes, energy results from a previous estimate of energy consumption in Kansas was aggregated by county and compared with our national results (McCarthy et al., 2020).

3.3 Farms and Irrigated acreage:

This study takes an approximation to the energy estimate approach detailed in our previous study (McCarthy et al., 2020). However, the previous approach dealt with point data directly collected from farmer surveys. This was possible through the Kansas program that supports a high detail farm data acquisition infrastructure. For a national context, generalizations must be made from various sources. In this study, a broader approach was taken to estimate individual farm resource expenditures, farm use, and irrigated acreage.

Farm resources were either downscaled or upscaled to county-level statistics. In the case of farm numbers, the 2017 NASS Agricultural Census dataset was used to obtain county level reported number of farms. The number of farms was used to estimate average farm acreage and pumping rate for each county. Irrigated acreage estimates from the USGS for 2015 were originally used for this model (Dieter et al., 2018). However, the USGS dataset method began to exhibit state bias when irrigated acreage was factored into energy estimates. This may be due to

USGS reports for national estimated being sourced by individual states reporting methods for farm statistics. To remedy this, irrigated area estimates from the MiRAD dataset were summarized within each county of interest (J. F. Brown & Pervez, 2014). The summarized values were then compared with the USGS irrigated acreage estimates on a county-by-county basis. While the MiRAD dataset had a higher spatial resolution in terms of irrigated acreage; some counties showed no irrigated acreage when aggregated. For counties that had previously reported active farms and had no MiRAD irrigated acreage, the USGS estimate was used as a proxy for irrigated acreage. Each county in the CONUS has a unique identifier attribute called the Federal Information Processing Standards (FIPS). A shapefile was created with number of farms, irrigated acreage and FIPS code for each county.

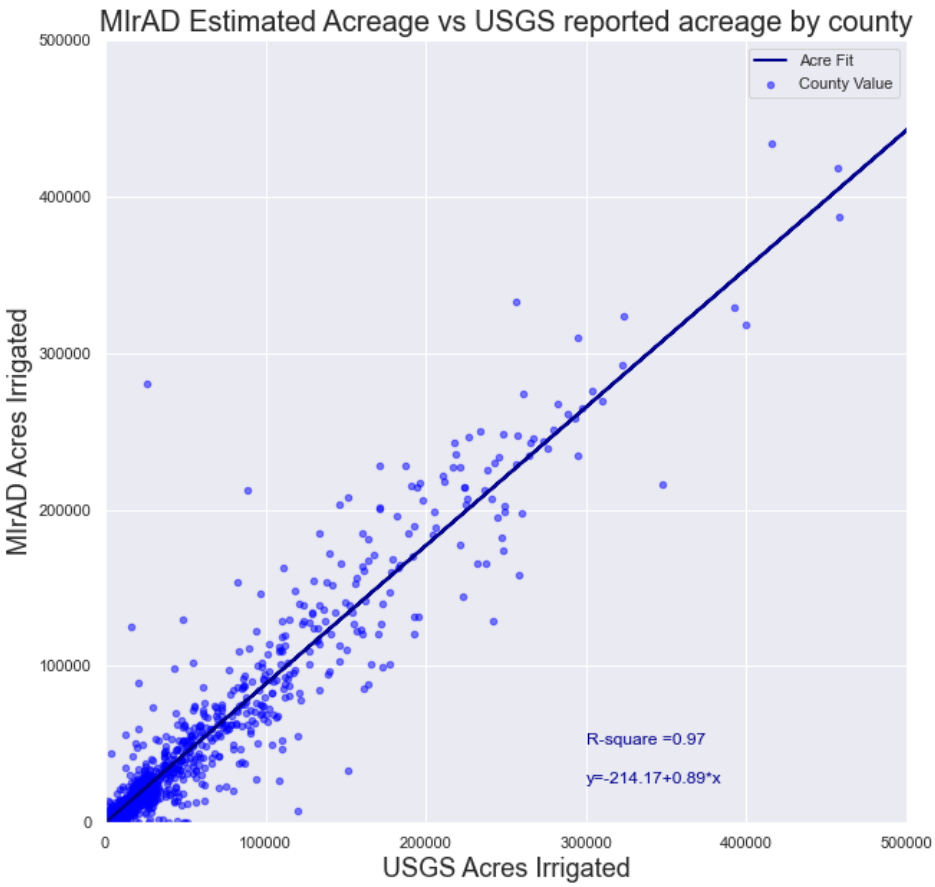

Figure 2.3 MiRAD Estimated Acreage vs USGS reported acreage by county. Scatterplot depicting the relationship between two irrigated acreage estimates. The MiRAD dataset is spatially distributed in 250 km resolution grids, while the USGS dataset is distributed on a county basis. For the sake of comparison, the MiRAD estimated acreage was summarized within US counties using a summation function. Comparison depicts total estimated Irrigated acreage per county from MiRAD vs. reported acreage per county from the USGS 2015 dataset.

3.4 Irrigation Requirements:

Our energy estimate method requires a series of parameters, including pressurization requirements and pumping durations. State-level reported efficiencies from the 2013 FRIS survey were compiled for our pressurization estimates (Vilsack & Reilly, 2013). The dataset includes information relating to irrigated acreage per state, and subdivides the number of farms per state according to the irrigation technology it uses. For our study, we used estimates of lower pressure systems, medium pressure and high pressure irrigation systems. The divisions in reported tables describe irrigation technologies ambiguously. However, they do make

distinctions for sprinkler systems, flood, or gravity fed. Using this information, a reasonable pressurization value was set for each subdivision and an average pressurization value was estimated using the proportion of each technology by state.

$$P_{avg} = \frac{(n_l * P_l + n_m * P_m + n_h * P_h)}{n_{Total}} \qquad \text{Equation 2.1}$$

Where:

P_{avg} is the average pressurization in a given State.

n_i is the number of systems (l is low pressurization, m is medium pressurization, h is high pressurization)

P_i is the assigned pressurization value for each system type

Irrigation pumping schedules are not consistent across the United States. Pumping requirements may vary according to geographic, crop, and weather conditions. To estimate the drawdown resulting from irrigation, we incorporate the length of the pumping season for each county. We used a regression based on NLDASS historical precipitation data along with SSURGO plant available water information and available water capacity (AWC). NASS keeps a record of historical maturity dates for various crops. Here, we evaluated the maturity dates of corn, cotton, hay, soy, spring wheat, and winter wheat for each state. In our pumping date model, we defined the onset of the irrigation season to be an excess of 60% AWC. Once our start date was defined for each state, we estimated the maximum maturity date for all crops in each state. Our resulting value provided the length of the pumping season for our irrigation systems. We then downscaled these estimated into county level information using two regression models of the pumping season length; M5p and Random forest regression models. Overall, the random forest regression model performed better than the M5P model, so that result was chosen for our

estimates of pump dates (A2.4). A time series of pumping dates from 1991 to 2020 was created, from which the 2015 county level pumping estimates were extracted and used for this study.

3.5 Water Use and Source:

The USGS 2015 water use report was used to obtain county-level water use and water source information augmented by the 2013 Farm & Ranch Irrigation survey (Dieter et al., 2018; Vilsack & Reilly, 2013). The USGS reports total water use and irrigation water use. In some counties, total water use was not provided where active farms are known to occur. In these cases, the 2013 Farm and Ranch irrigation Survey was used to estimate water use. The FRIS dataset reports water use in terms of average acre-foot of water used per state. For counties that were missing data, the average acre-foot per acre value was multiplied by the known or estimated acreage for the given county to yield a rough estimate of water use. After this method was applied, total water use for each state was aggregated compared to reported total water use by state from the USGS and accepted as reasonable estimates. From this aggregation of datasets, we obtained a county level result for water use in the CONUS.

3.6 Direct Energy Estimates by County:

Here, we estimate the direct energy used in farms, without accounting for pump or prime mover efficiency, nor are we including the indirect energy resulting from varying energy sources, pesticides and fertilizers. The fundamental energy estimate that is used for this study is a multiplication of mass, gravity, and height. Direct energy is described as follows:

$$E_D = \rho g V L_T \qquad \text{Equation 2.2}$$

where:

ρ is the density of water, assumed to be 1000 kg/m^3,

g is the gravitational constant, 9.8016 m/s^2,

V is the annual volume of water pumped per county provided by USGS reports and augmented by 2013 FRIS data , and

L_T is the total effective lift (m), given by:

$$L_T = L_{WT} + L_{CD} + L_{WD} + L_{PR} \quad \text{Equation 2.3}$$

where:

L_{WT}(m) is the lift from the water table to the ground surface at the start of the pumping season (this is set to 0 for surface water irrigation sources),

L_{CD}(m) is the additional lift due to the cone of depression that forms in the well during the pumping season,

L_{WD} (m) is the additional lift due to drawdown within the well because of frictional losses in and within the immediate vicinity of the well and screen factor,

L_{PR} (m) is the effective lift due to pressurization and of water and pipe losses necessary for each irrigation system type.

Once most of the lift components were estimated or sourced, we estimate drawdown depth using the Cooper-Jacobs method (Kranz et al., 2007a, 2007b, 2008). The pump rate (Q) was estimated as the quotient of our known water use and our estimated irrigation pumping dates. Transmissivity was obtained from the national shallow groundwater model (Zell & Sanford, 2020). All equations and methods for energy estimates are described in (McCarthy et al., (2020), except for carbon estimates and prime mover or pumping efficiencies factored into the updated equation presented here. For ease of computation, and due to the complex nature of pumping efficiencies, we are only estimating direct energy, with no efficiencies factors incorporated into the equation.

3.7 Kansas Validation:

We validated our results based on a detailed database available in the state of Kansas, which included all necessary farm operation components to estimate our energy consumption. The final product from our previous work (McCarthy et al., 2020) was a series of point features with energy use in the High Plains Aquifer portion of Kansas. For our new CONUS scale energy estimates, the Kansas results, from the WIMAS database, allowed for validation. For ease of comparison, the WIMAS results were aggregated by county. Only counties whose area was underlain by 80% of the High Plains Aquifer or more were selected for validation. This resulted in 24 counties being used to validate our results.

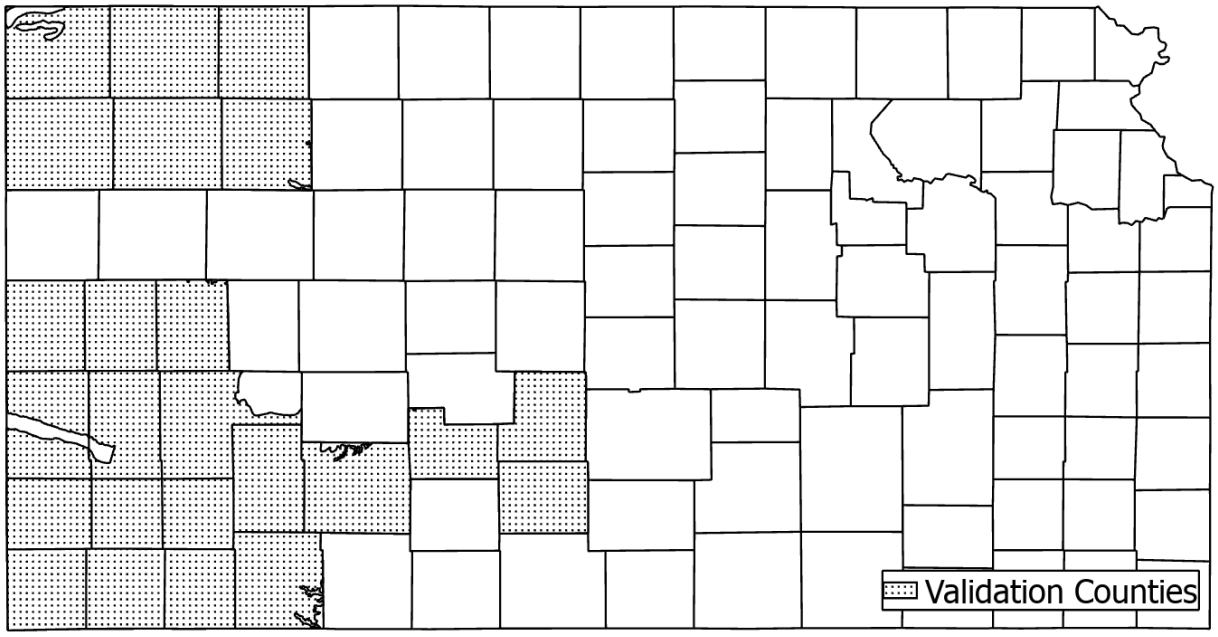

Figure 2.4 Selected Counties for Validation. 24 Counties from the Kansas dataset fit the parameters of our validation process. The area underlaying these counties is encompassed by at least 85% of central HPA. The results from (McCarthy et al. (, 2020) for these counties are compared with those from the up-scaled CONUS method developed here.

Previous work with energy estimates suggested that the water table depth is one of the most influential components of energy use in agricultural irrigation. Therefore, we recreated the energy estimate to study the relationship between our WIMAS and CONUS based on a variable

water table. The depth to water from the WIMAS results was sourced from a High Plains Aquifer water table estimates (Haacker et al., 2016), while the CONUS estimate used water table results from a shallow groundwater table model (Zell & Sanford, 2020).

4. Results & Discussion

4.1 Kansas Validation Results:

We analyzed the relationship between the WIMAS results from our previous study and the new results from our CONUS study. Since our previous study had a smaller scope and higher data availability, the final energy result considered the full Life Cycle Assessment of its energy consumption, along with prime mover and pump efficiencies. Therefore, we decided to compare only the direct energy result from the previous study and this new method. Figure 2.5 shows the percent difference between these two results, relative to the Kansas results. From this, we can see the distribution of differences between the counties. Around the edges of the central HPA, there is a tendency to overestimate the energy, where the CONUS results tend to be 1-60% higher than the WIMAS result. Closer to the central HPA, the opposite effect is apparent. Here, the CONUS result is 30 to 60% less than the WIMAS result.

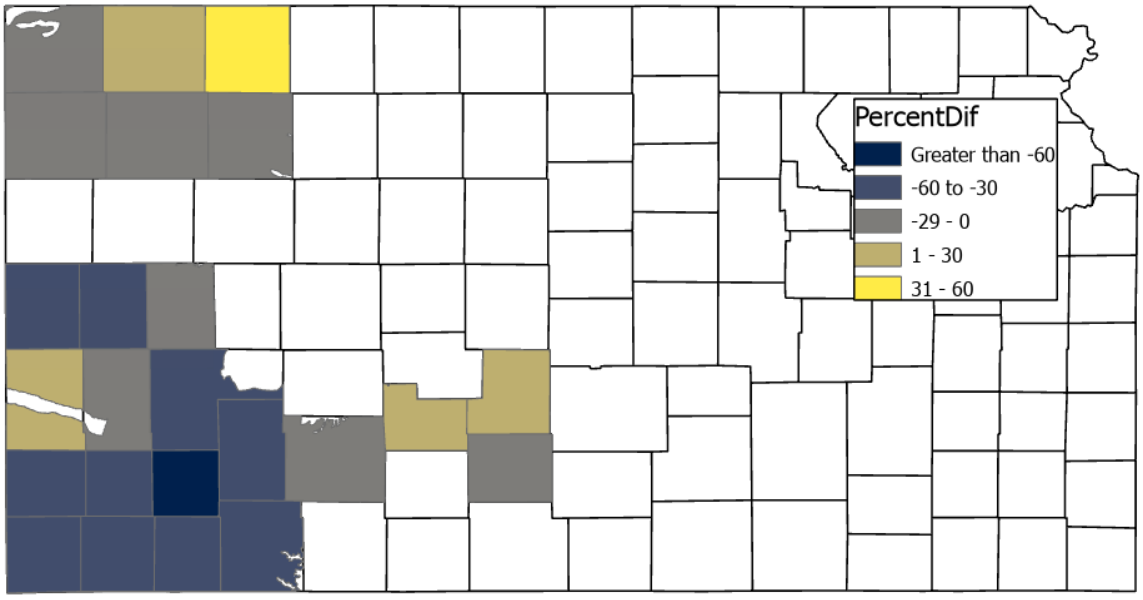

Figure 2.5 Percent difference in energy consumption WIMAS vs CONUS. 24 Counties from the Kansas dataset fit the parameters of our validation process. The area underlaying these counties is encompassed by at least 85% of central HPA. The results from (McCarthy et al., 2020) for these counties is compared with the results from the up-scaled CONUS method.

From the previous study, a key factor that contributed to the spatial estimates of energy was the depth to water (McCarthy et al., 2020). In this comparison and along the central HPA, over-exploitation and heavy agricultural intensification of the aquifer is more prominent in the center of the aquifer, where farmland and wells have been developed for decades. To understand the impact of the water table on the relative difference between the two results, the CONUS method was augmented with the water table dataset from the WIMAS (Haacker et al., 2016). The original CONUS result was then plotted against the WIMAS result and the augmented CONUS result was plotted against the WIMAS result, as shown on figure 2.6. Results from both linear analyses showed statistical significance and a strong relationship. For the original CONUS results, where the depth to water was sourced from Zell & Stanford, the linear relationship exhibited a Pearson R-squared value of 0.91 ($p<<0.05$). In the case of the adjusted CONUS result, where the depth to water was replaced with the Haacker water levels, the relationship

between CONUS and WIMAS became even more correlated, with a Pearson R-squared value of 0.99 ($p<<0.05$). Results clearly indicate a strong relationship between both methods and their results.

(Zell & Sanford, 2020)The depth to water used in this study combined 75 shallow subsurface models to create a long-term shallow water table depth along the CONUS (Zell & Sanford, 2020). While this provided reliable nationwide source for water table depths, it is a spatially smoothed estimate that does not represent water levels in areas that are heavily pumped. The water table in areas where agricultural intensification is prominent tend to fluctuate, with declining water tables over extended periods of extraction (Konikow, 2013, 2015; Konikow & Kendy, 2005). The validation from our model shows that, in general, our CONUS estimate underestimates direct energy requirements in regions where aquifer exploitation and fluctuating water tables are present. In fringe regions of major aquifers, the depth to water estimate is more in line with current conditions. When more temporally explicit depth to water information is available for our CONUS model, energy results are more similar to the WIMAS model (Figure 2.6) in regions where seasonal irrigation significantly affects the water table.

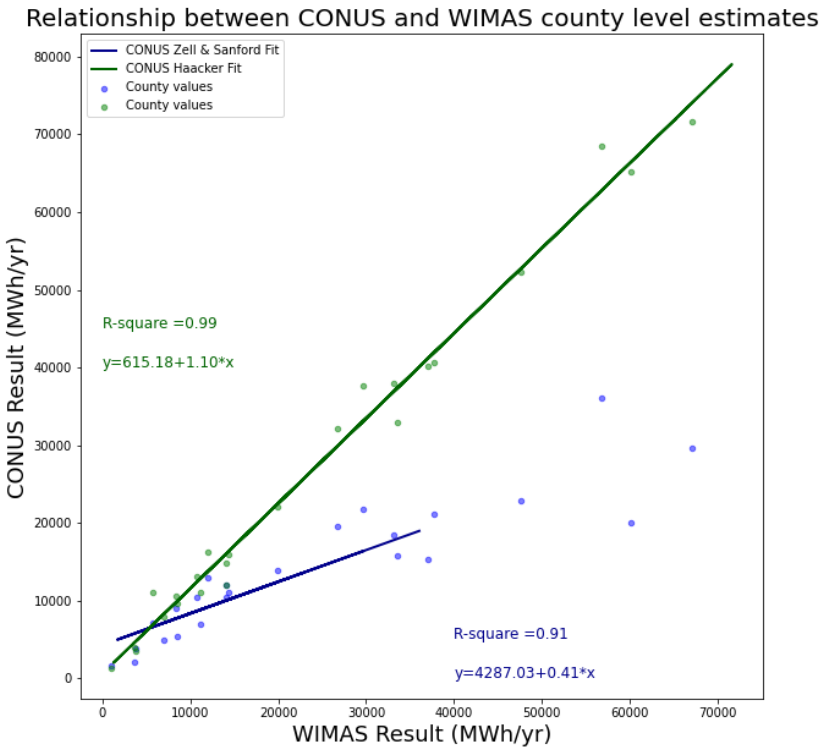

Figure 2.6 Linear relationship between WIMAS vs CONUS results. (Zell & Sanford, 2020) Here, the 24 counties are plotted on a scatterplot depicting their linear relationship. The blue points and line of best fit represent a relationship between the WIMAS results and the CONUS results. The green group represents the same relationship; however, the CONUS estimate is using depth to water values from the Kansas dataset (Haacker et al., 2016)as opposed to the CONUS predevelopment depth to water dataset (Zell & Sanford, 2020).

4.2 Direct Energy Use:

Direct energy consumption in the CONUS varies greatly with geography. Energy consumption per county ranged between 0 and 2.33 MWh/per acre irrigated for an irrigated season. The states with the largest irrigated areas (in million acres) are: Nebraska (9.5), California (9.3), Texas (5.7), Arkansas (4.5), Idaho (3.8) and Kansas (3.0), representing ~64% of total direct energy consumption across the CONUS. As is illustrated in figure 2.7, energy consumption from agricultural irrigation is dominated by regions of agricultural intensification, generally found in the Central and Western CONUS, with higher use in Southern counties. Energy use sourced from groundwater has the highest consumption rate in California, where

roughly 3000 Gigawatt-hours are required just for the direct energy at the farms. The largest consumer for Surface water sourced irrigation in terms of direct energy consumption is Idaho, with roughly 1500 Gigawatt-hours in a typical irrigated season. In terms of total energy consumption, the five highest direct energy consuming states in the CONUS are California with > 3200 GWh, Idaho (>2000 GWh), Arkansas (1700 GWh), Nebraska (1100 GWh) and Colorado (810 GWh).

In 2012, the U.S. Energy Information Administration estimated that the U.S. agriculture sector consumed around 800 trillion Btu of energy (Annual Energy Outlook, 2014). Of that, almost 500 trillion is associated with crop production. In 2015, the USDA estimated that the direct energy used on farms to be ~1,000 trillion Btu (Hitaj & Suttles, 2016b). In both studies, direct energy included all direct energy needs at the farm including pump efficiency, prime mover efficiency, fertilizer application, and pesticide application. In contrast, our model estimates only considers depth to water and volume pumped, without factoring in the components of energy consumption. We estimated that the direct energy use in the US to be 49.7 trillion Btu for the CONUS.

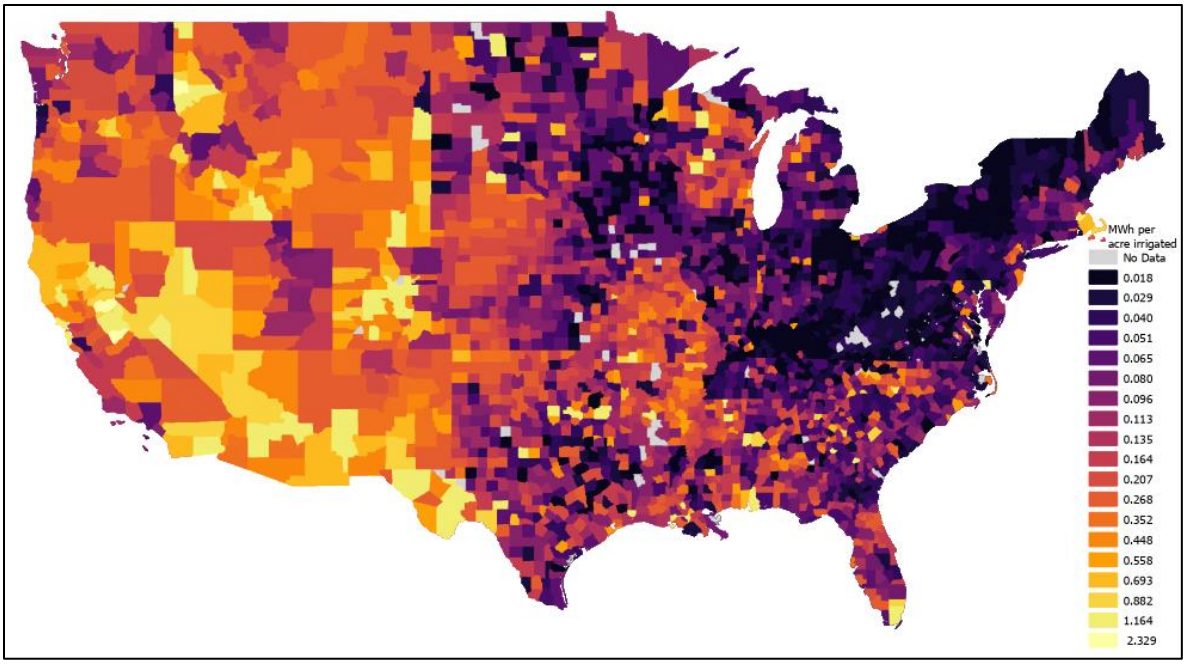

Figure 2.7 County-level Energy Results. This map depicts the county-level energy results from the CONUS-wide estimate in MWh/year, counties shown in grey contain no data.

4.3 Water Sources:

The general distribution of water sources across the CONUS is highly variable. Topography, geography, weather, and water use regulations all affect how water is sourced and distributed. Groundwater extraction is very common in arid regions that do not have sufficient precipitation for rainfed agriculture, such as the Great Plains region in central United States and the Central Valley region in California. Areas closer to the Mississippi or other large bodies of water, such as Northern Wisconsin have relatively even proportions of groundwater to surface water sources. Figure 2.8 shows the proportion of groundwater to surface water usefor irrigation; Kansas has the lowest and Montana has the highest proportion of surface water use. In terms of water consumption, California has the highest total groundwater consumption at over 19 km^3 and Idaho has the largest surface water consumption rate of roughly 14 km^3 every year. In the High Plains Aquifer, a total of 21 km^3 of groundwater and surface water combined are used every year.

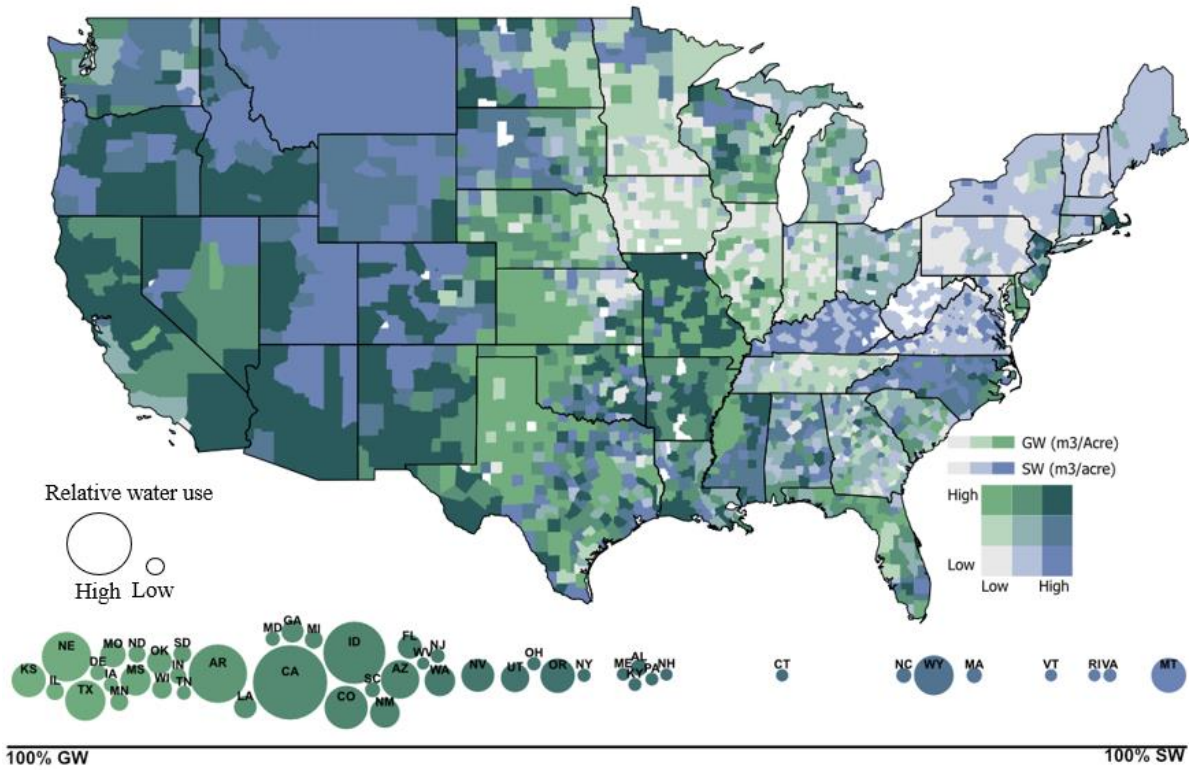

Figure 2.8 Water source distribution throughout CONUS. Here, we see a map detailing the distribution of groundwater and surface water along counties. In terms of cubic meter of water used per irrigated acre. The bee swarm plot at the bottom shows the distribution of total groundwater resources per state, where a positive increase along the x-axis relates to a higher distribution of surface water sourced irrigation.

4.4 Energy Use by Farm Resource Region and Major Crop:

As expected, major crop distribution and energy consumption varied greatly across resource regions. Figure 2.9 depicts the distribution of counties grouped by crop with the highest reported allocated acreage.

In the Heartland, over 400,000 farms and almost 6 million irrigated acres were reported. 43% of counties in this region reported corn as the highest acreage crop, while the other 57% reported soybeans. Direct energy consumption for this region is estimated to be around 490 GWh with an average total lift of 30 meters and 90% of irrigation sourced by groundwater. The Heartland has the highest share of farms amongst the resource regions, and the 4th largest share of irrigated acreage, meaning a higher rate of small to medium farms than other regions.

However, profitability in this region has remained relatively steady for smaller farms. The USDA Economic Research Service estimated that profitability in this region increased by 64% between 1982 and 2012 only for larger crop farms (Key, 2018). The farms in this region have shifted towards larger farms, with improved technology adoption and efficient farm practices (Hitaj & Suttles, 2016b; Key, 2018; Saavoss et al., 2021).

In the Northern Crescent, over 260,000 active farms and 1.8 million irrigated acres were reported. 68% of counties reported corn as their major crop, followed by soybeans (29%) and wheat (3%). Direct energy consumption for the Northern Crescent is 100 GWh. Average total lift of 25 meters and 70% of irrigation water was sourced from groundwater. Lower water tables and high dependance on groundwater in this region can be beneficial to lower energy requirements. However, poor water management practices can lower the water table and lead to increased energy consumption. Studies in this region have shown that increased efficiency in irrigation technologies can result in higher yields and lower risk of losses in long term farming practices (Kim & Chavas, 2003; Koundouri et al., 2006).

The Northern Great Plains reported 85,000 farms and 3.3 million acres of irrigated land. 50% of counties reported wheat as crop with the highest allocated acreage, followed by soybeans (32%) and corn (18%). Direct energy in the Northern Great Plains is estimated at 680 GWh, with an average total lift of 39 meters and 77% of irrigation sourced from groundwater extraction. Wheat production in this region is a main driver of agriculture. In this region, climate change is expected to increase growing season availability, although crop yields are expected to decline (Conant et al., 2018).

In the Prairie Gateway around 300,000 farms and 12.6 million acres were reported. 43% of counties reported wheat as the highest acreage crop, followed by corn (25%), cotton (16%),

soybeans (15%) and rice (<1%). Direct energy use in the Prairie Gateway is estimated at 2100 GWh, average lift of 34 meters over 95% of water sourced for irrigation being extracted from groundwater. In this region, groundwater is sourced mainly from the High Plains Aquifer. This aquifer has experienced abundant agricultural development and over-exploitation in the last century (Dennehy et al., 2002; Haacker et al., 2016; Perry, 2006; Scanlon et al., 2012). Various programs in the region have been implemented to improve water management practices, reduce energy consumption, and increase efficient technology adaptation (Butler et al., 2018; Cotterman et al., 2018; Deines et al., 2019).

In the Eastern Uplands, 257,000 farms and around 267,000 irrigated acres were reported. Soy was the highest reported acreage crop across the region (51%), followed by corn (47%), cotton (>1%) and wheat (>1%). The direct energy estimated for this region is 29 GWh with and average total lift of 26 meters and 66% of irrigation water being sourced from groundwater. This region is not heavily dominated by agriculture, due in part to the low relative irrigated agriculture and number of farms. This region is generally considered to be in a low water stress classification, where some of the smallest farms in the US are found (Morris & Persons, 2019; Spangler et al., 2020).

The Southern Seaboard reported 187,000 farms with around 1.6 million irrigated acres. Soybeans were allocated the highest acreage among 47% of counties, followed by cotton (25%), corn (24%), wheat (3%) and Rice (<1%). Direct energy estimated for this region is 141 GWh, average total lift of 22 meters and 57% of irrigation being sourced from groundwater. Agricultural production and energy use in this region is generally lower than its counterparts.

The Fruitful Rim reports 187,000 farms and over 16.7 million irrigated acres. In this region, 39% of counties report wheat as the highest allotted acreage crop, followed by corn

(30%), cotton (24%), rice (5%) and soybeans (>1%). Direct energy consumption for this region is the highest, with over 6,000 GWh used during the irrigated season. Average total lift for this region is 43 meters and 77% of irrigation is sourced from groundwater. This region accounts for the highest energy use out of all the regions, even greater than the Prairie Gateway, Mississippi Portal and Basin and Range regions combined. Many states in this region experience intense water extraction and recent policies have attempted to incentivize low-energy technology adoption (Sears et al., 2018).

In the Basin and Range region, counties report 70,000 farms and 4.8 million acres irrigated. 78% of counties report wheat as their highest acreage crop, followed by corn (18%), cotton (1.9%) and rive (1.9%). The direct energy estimated for this region is 1650 GWh, while average total lift is the highest at 59 meters. 53% of irrigation in this region is sourced from groundwater.

The Mississippi Portal contains 71,000 farms and 7.7 million irrigated acres. 84% of counties report soybeans as their highest allocated acreage crop, followed by rice (6%), corn (6%) and cotton (3%). Direct energy estimated for this region is 2100 GWh and average total lift is 29 meters. In this region, over 88% of irrigation is sourced from groundwater. Irrigated cropland in this region.

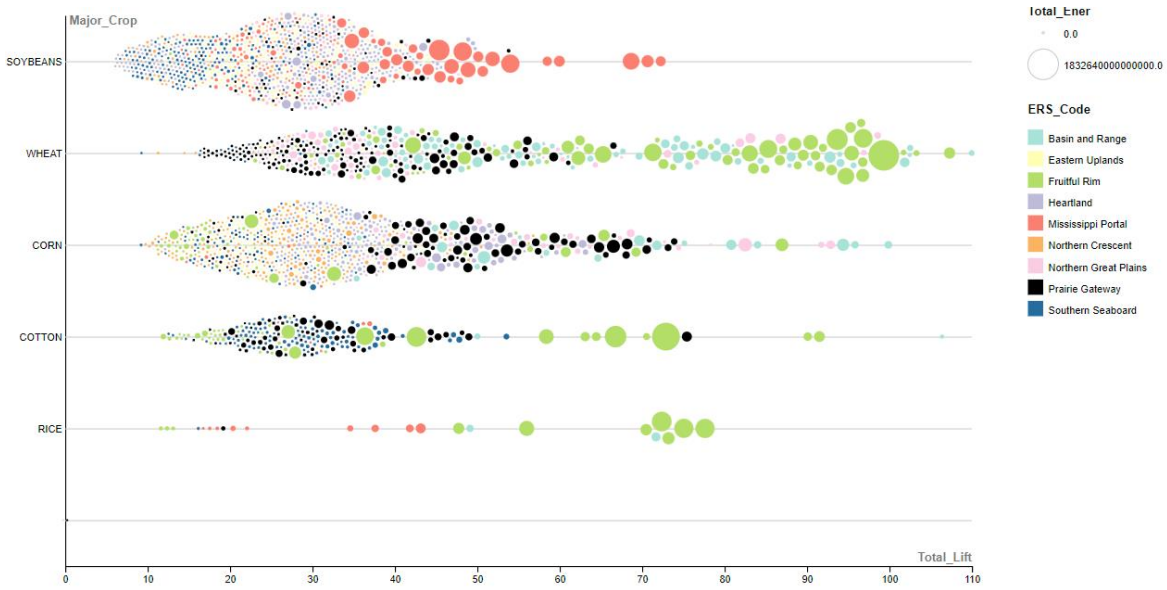

Figure 2.9 Distribution of Crops and Total Lift along Farm Resource Regions. This figure is a multifaceted bee swarm plot. Each bubble in the plot represents a county. The counties are then grouped by most abundant crop (in acres used) and colored according to their Farm Resource Region. The size of each bubble also represents total energy used. Total lift is as defined in section 2.6.

4.5 Limitations and Future Work:

This model provides a simple method to estimate direct energy use across large scales. Through our validation process we determined that our model is comparable to more locally explicit models (Fig 2.6), yet accurate estimates of direct energy better information about recent water table depths in areas where there have been significant. While our model can estimate Direct Energy for each County in the continental United States, it does not fully encompass all the energy components associated with farming. Sources of energy consumption such as fertilizer application, pesticide application, efficiency losses through pump type, efficiency losses through prime mover and fuel type would affect the final estimate of direct energy at the farm (A. D. Schneider & L. L. New, 1986; Anani & Adetunji, 2021; Curran, 2018; Gellings & Parmenter, 2004; Schneider & New, 1988). Further investigation into the indirect energy consumption, such as the energy that goes into sourcing various fuel types or the energy source would provide another expanded resource for policymakers and farmers deciding on investment in the agricultural sector and their respective location (Aguilera et al., 2017; Salmoral & Yan, 2018b; Vora et al., 2017b). Finally, future assessments with such a model could estimate the temporal trend in energy use, if adequate data become available.

5. Conclusions

This simple model provides an estimate of the direct energy consumption across space from irrigation across the CONUS. The Fruitful Rim, Mississippi Portal and Prairie Gateway regions are the highest energy consumers, with a combined direct energy use of over 10,000 GWh yearly.

While irrigated acreage in the Prairie Gateway is comparable to the Fruitful Rim, direct energy consumption in the first is 35% of the energy consumed in the latter. Energy consumption

in the Fruitful Rim is equivalent to the energy use of Prairie Gateway, Mississippi Portal and Basin and Range combined, even though the latter has nearly twice the irrigated acreage as the former. This indicates a need for increased intervention on groundwater management practices for areas with high groundwater extraction rates, as is proposed in other studies (Pfeiffer, 2010; Pfeiffer & Lin, 2014; Sorensen & Daukas, 2010; Spangler et al., 2020). While proposed water management practices have been implemented in the past, the rebound effect, which is the phenomenon that occurs when improved technologies lead to increased use of more efficient technology, might prevent water policy from being effective (Polimeni et al., 2012; Sears et al., 2018). The spatially explicit model presented here, allows for improved understanding of county-scale dynamics of energy use that are tied into a complex national system. National climate patterns can be evaluated at a county level and future climate and agricultural assessments can be downscaled and fed into local water management policy with more ease. This information can benefit county, state and national policymakers to base their water management practices more specifically among such a complex agricultural sector (Beckman et al., 2013; Uddameri & Reible, 2018).

Efficient crop rotation practices and diversification can improve yields and decrease the need for tillage and excessive fertilization, especially in regions that have low crop diversity. This is especially important as climate change affects precipitation, growing season length, and temperatures (Conant et al., 2018; Davis et al., 2017; Zhao et al., 2020).

6. Acknowledgments

This work is supported by INFEWS grant 2018-67003-27406 (accession no. 1013707) from the USDA National Institute of Food and Agriculture, “Developing Pathways Toward Sustainable Irrigation across the United States Using Process-based Systems Models (SIRUS)”.

Any opinions, findings, and conclusions or recommendations expressed in this publication are those of the author and do not necessarily reflect the views of the USDA.

APPENDIX

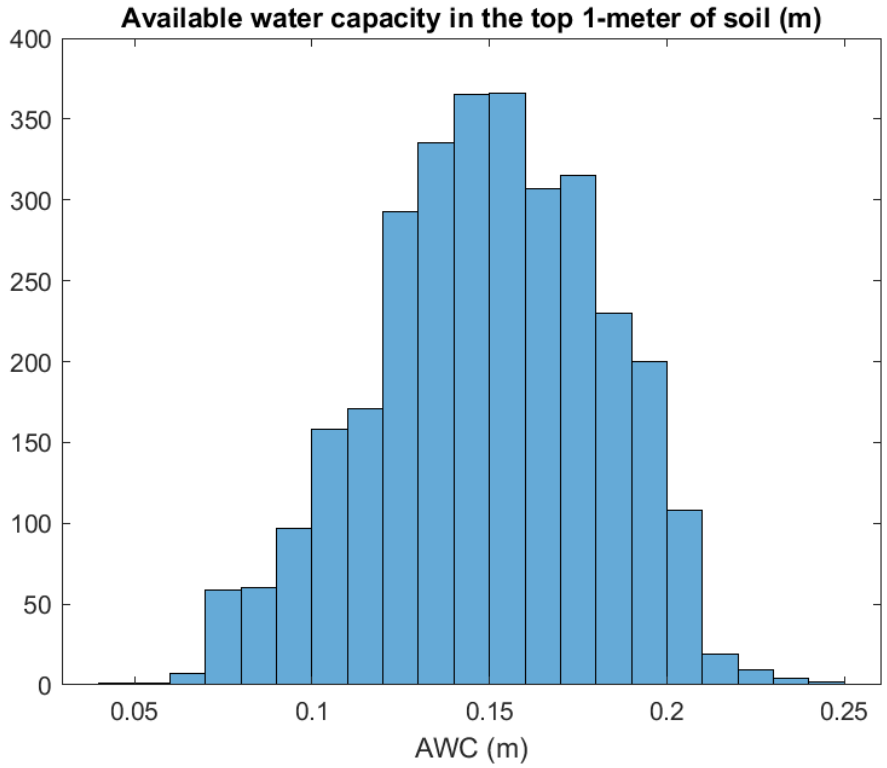

Figure A2.1 AWC in Top Meter of Soil Available water capacity measured in the top 1-meter of soil. This is a normal distribution of the top 1 meter of soil and its available water capacity.

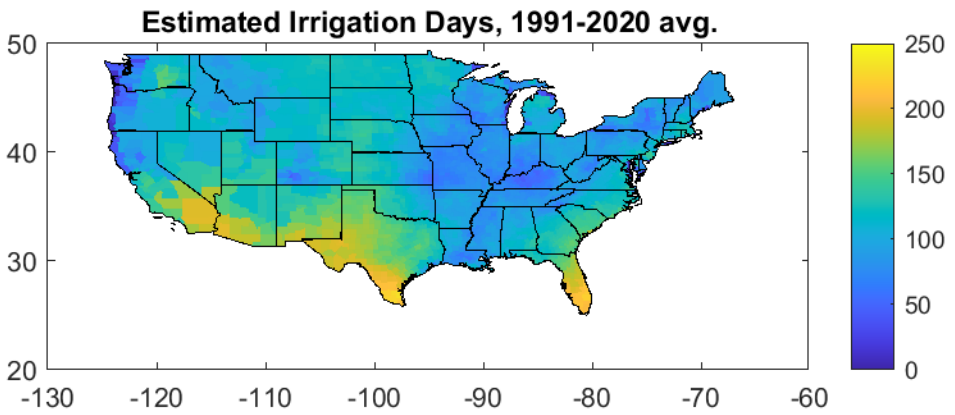

Figure A2.2 Estimated Irrigation Days from 1991 to 2020 This result is from the regression model used. Values are estimated using known maturity dates and estimated irrigation start dates based on AWC. Long term average estimate is shown here.

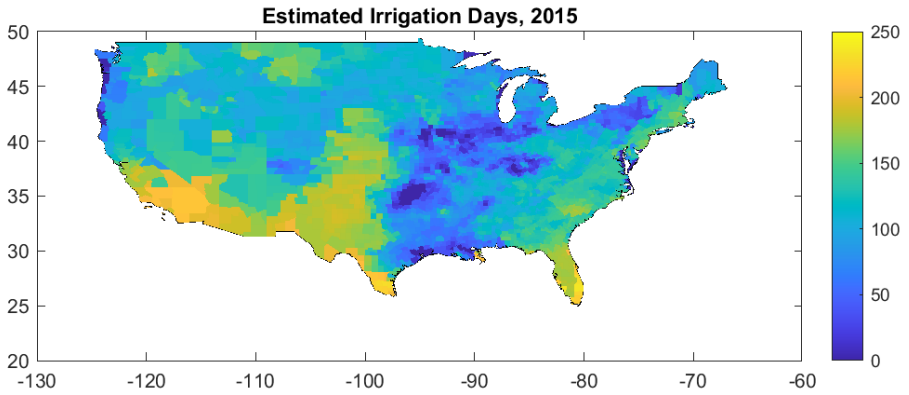

Figure A2.3 Estimated Irrigation Days for 2015 This result is from the regression model used. Values are estimated using known maturity dates and estimated irrigation start dates based on AWC for the year of 2015, where our water use data is obtained.

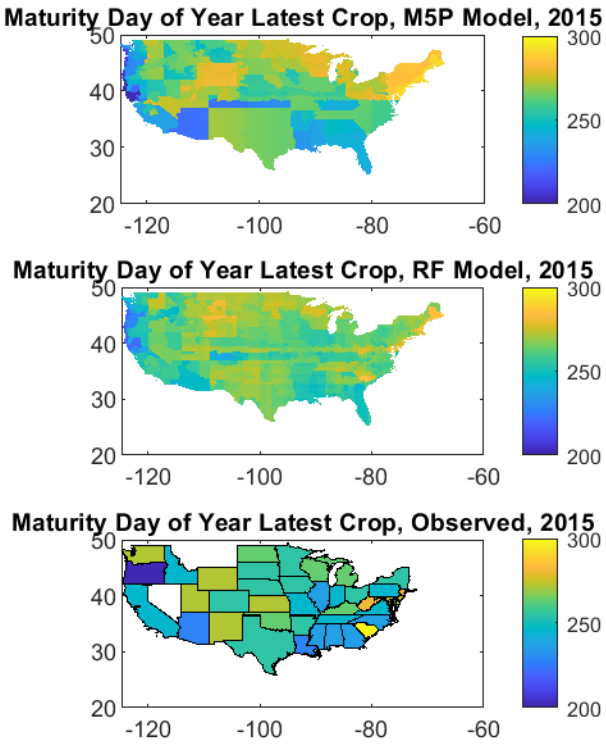

Figure A2.4 Maturity Date Regression Models Maturity dates were obtained from common crops: corn, cotton, soy and soy. Two models were used to downscale the maturity dates; M5P regression and RandomFrst regression tools. Bottom panel shows data availability, top two panels depict downscaled results on county basis.

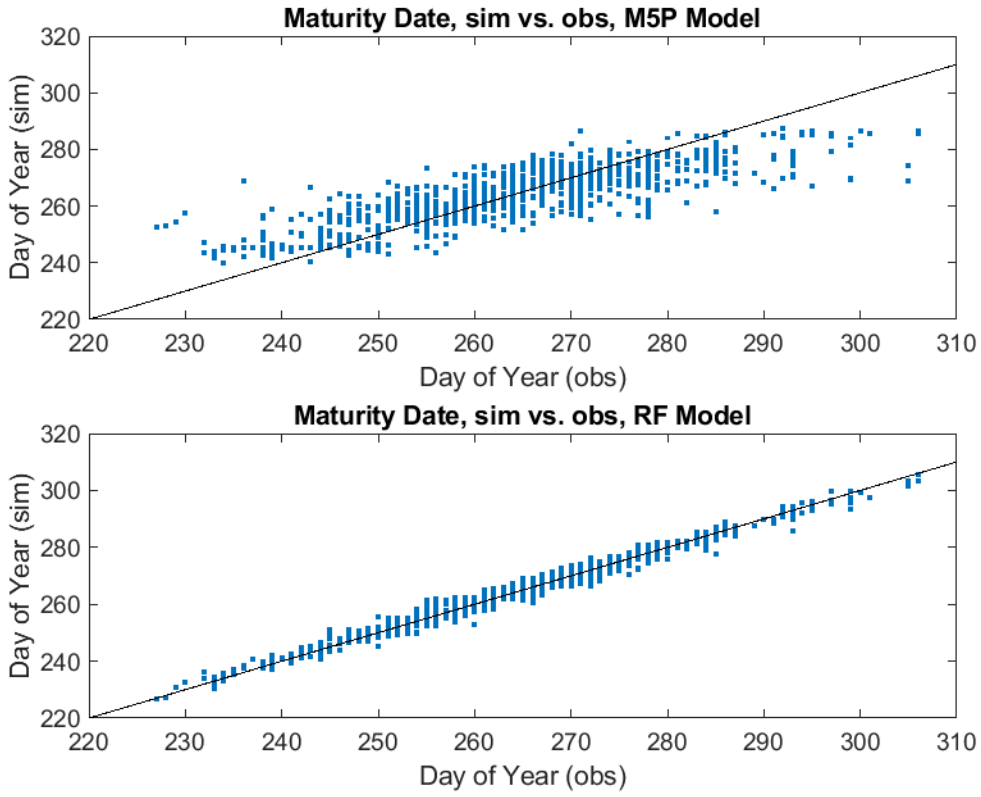

Figure A2.5 Maturity Date Regression Validation Regression results from the model runs on maturity dates. Based on the regression of obs. Vs simulated, the RF model creates a better proxy for maturity date behavior for our downscaled pumping date estimate.

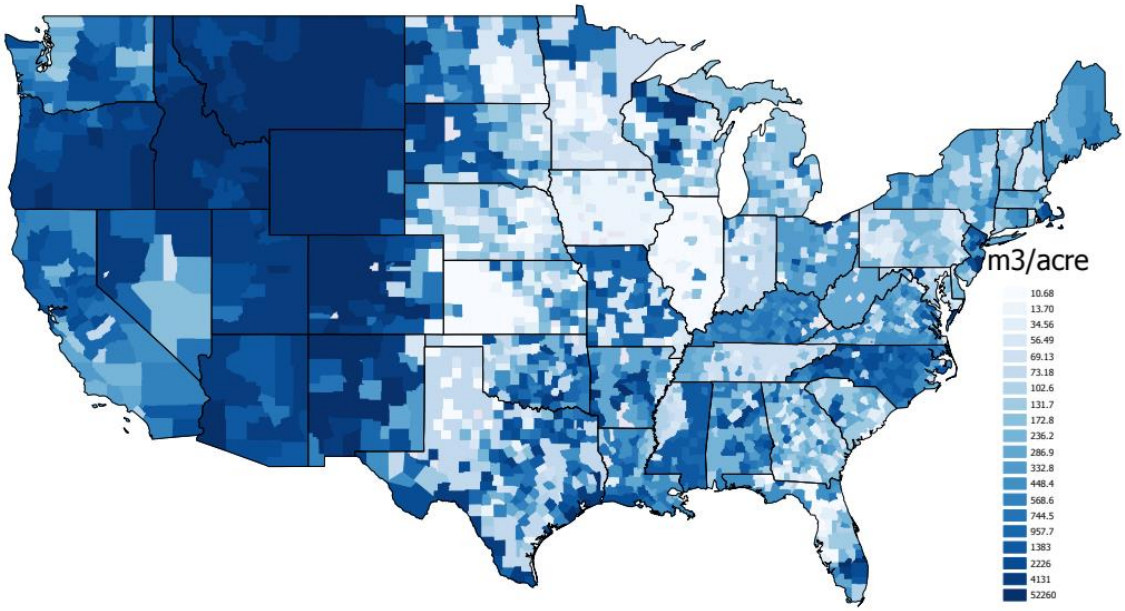

Figure A2.6 County-level Surface Water Use total water use reported from USGS in 2015 for each county sourced from surface water in meters cubed per acre irrigated. Most common surface water use is shown in the western CONUS.

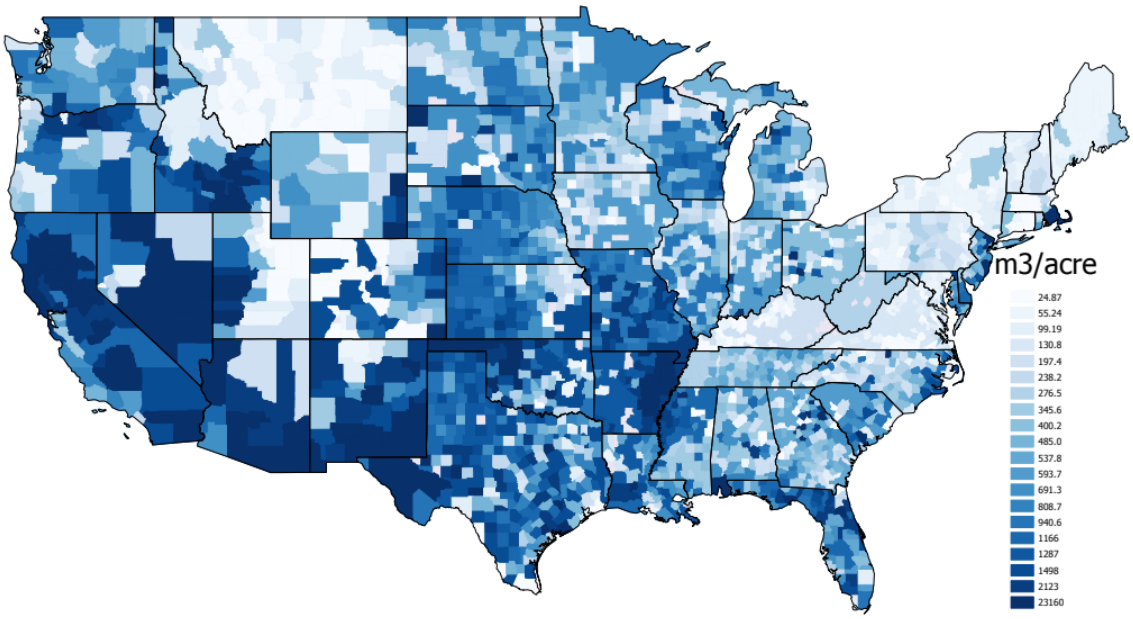

Figure A2.7 County-level Groundwater Use Groundwater use distribution across the CONUS. Data is sources from 2015 USGS report on water use. Higher water use tends to correlate with locations of known and major aquifers.

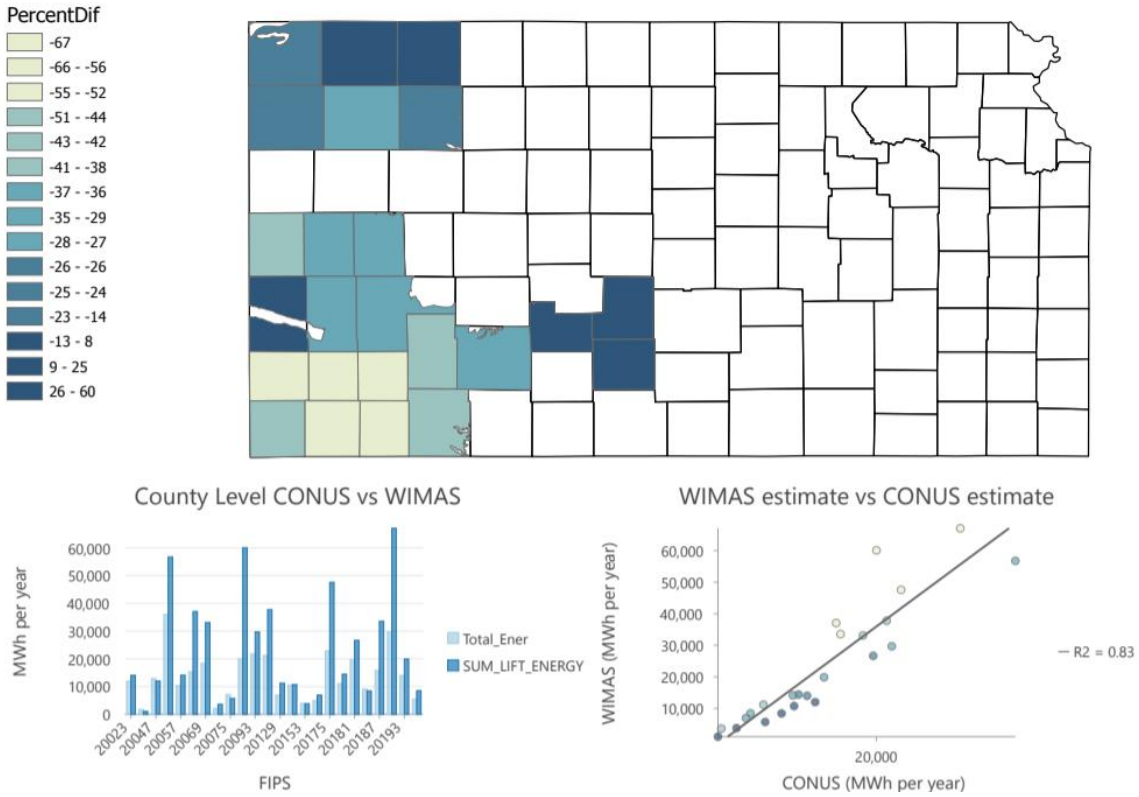

Figure A2.8 Kansas Validation Results Detailed results on comparison between WIMAS estimate of energy consumption and CONUS estimate. Top map shows the percent difference in direct energy consumption between two estimates, relative to WIMAS. MWh per year in direct energy is shown in the left bar graph for each county. Direct linear plot of WIMAS vs CONUS is shown in right graph, shows positive relationship between both estimates.

REFERENCES

REFERENCES

2017 Census of Agriculture. (2019). https://www.nass.usda.gov/AgCensus/

A. D. Schneider, & L. L. New. (1986). Engine Efficiencies in Irrigation Pumping from Wells. *Transactions of the ASAE*, *29*(4), 1043–1046. https://doi.org/10.13031/2013.30267

Aguilera, E., Guzman, G. I., Infante-Amate, J., Soto, D., Garcia-Ruiz, R., Errera, A., Villa, I., Torremocha, E., Carranza, G., & Gonzales de Molina, M. (2017). *The input side . Calculating the embodied energy of agricultural inputs* (Issue January).

Anani, O. A., & Adetunji, C. O. (2021). Role of Pesticide Applications in Sustainable Agriculture. In *Applied Soil Chemistry* (pp. 235–256). John Wiley & Sons, Ltd. https://doi.org/https://doi.org/10.1002/9781119711520.ch13

Annual Energy Outlook 2014. (2014). www.eia.gov/analysis/model-documentation.cfm

ArcGIS Pro Python reference. (n.d.). esri.

Ashworth, W. (2006). *Ogallala Blue*. The Countryman Press.

Beckman, J., Borchers, A., & Jones, C. A. (2013). *Agriculture's Supply and Demand for Energy and Energy Products United States Department of Agriculture*. https://ssrn.com/abstract=2267323

Brown, G. O. (2002a). The history of the Darcy-Weisbach equation for pipe flow resistance. *Proceedings of the Environmental and Water Resources History*, *40650*(January), 34–43. https://doi.org/10.1061/40650(2003)4

Brown, G. O. (2002b). The history of the Darcy-Weisbach equation for pipe flow resistance. *Proceedings of the Environmental and Water Resources History*, *40650*(January), 34–43. https://doi.org/10.1061/40650(2003)4

Brown, J. F., & Pervez, M. S. (2014). Merging remote sensing data and national agricultural statistics to model change in irrigated agriculture. *Agricultural Systems*, *127*, 28–40. https://doi.org/10.1016/j.agsy.2014.01.004

Butler, J. J., Bohling, G. C., Whittemore, D. O., & Wilson, B. B. (2020). A roadblock on the path to aquifer sustainability: underestimating the impact of pumping reductions. *Environmental Research Letters*, *15*(1), 014003. https://doi.org/10.1088/1748-9326/ab6002

Butler, J. J., Whittemore, D. O., Wilson, B. B., & Bohling, G. C. (2018). Sustainability of aquifers supporting irrigated agriculture: a case study of the High Plains aquifer in Kansas. *Water International*, *43*(6), 815–828. https://doi.org/10.1080/02508060.2018.1515566

Camargo, G. G. T., Ryan, M. R., & Richard, T. L. (2013). Energy use and greenhouse gas emissions from crop production using the farm energy analysis tool. *BioScience*, *63*(4), 263–273. https://doi.org/10.1525/bio.2013.63.4.6

Cederstrand, J., & Becker, M. (1998). *Digital map of hydraulic conductivity for High Plains aquifer in parts of Colorado, Kansas, Nebraska, New Mexico, Oklahoma, South Dakota, Texas, and Wyoming*. https://doi.org/10.3133/ofr98548

Conant, R. T., Kluck, D., Anderson, M. T., Badger, A., Boustead, B. M., Derner, J. D., Farris, L., Hayes, M., Livneh, B., McNeeley, S., Peck, D., Shulski, M., Small, V., & Program, U. S. G. C. R. (2018). *Northern Great Plains* (D. Reidmiller, C. W. Avery, D. R. Easterling, K. E. Kunkel, K. L. M. Lewis, T. K. Maycock, & B. C. Stewart, Eds.). https://doi.org/10.7930/NCA4.2018.CH22

Cotterman, K. A., Kendall, A. D., Basso, B., & Hyndman, D. W. (2018). Groundwater depletion and climate change: future prospects of crop production in the Central High Plains Aquifer. *Climatic Change*, *146*(1–2), 187–200. https://doi.org/10.1007/s10584-017-1947-7

Curran, J. (2018). *Irrigation pump efficiency. Presentation given by James Curran, water resource consultant.*

Curtis, L. M. (Auburn U., & Tyson, T. W. U. (1988). Energy Requirements: The Center Pivot Irrigation System. *Circular Anr-507*.

Daccache, A., Ciurana, J. S., Rodriguez Diaz, J. A., & Knox, J. W. (2014). Water and energy footprint of irrigated agriculture in the Mediterranean region. *Environmental Research Letters*, *9*(12). https://doi.org/10.1088/1748-9326/9/12/124014

Daher, B., Lee, S. H., Kaushik, V., Blake, J., Askariyeh, M. H., Shafiezadeh, H., Zamaripa, S., & Mohtar, R. H. (2019). Towards bridging the water gap in Texas: A water-energy-food nexus approach. *Science of the Total Environment*, *647*, 449–463. https://doi.org/10.1016/j.scitotenv.2018.07.398

Davis, K. F., Seveso, A., Rulli, M. C., & D'Odorico, P. (2017). Water savings of crop redistribution in the United States. *Water (Switzerland)*, *9*(2). https://doi.org/10.3390/w9020083

DeBoer, D. W., Lundstrom, D. R., & Wright, J. A. (1983). Efficiency analysis of electric irrigation pumping plants in the upper midwest, U.S.A. *Energy in Agriculture*, *2*, 51–59. https://doi.org/10.1016/0167-5826(83)90006-2

Deines, J. M., Kendall, A. D., Butler, J. J., & Hyndman, D. W. (2019). Quantifying irrigation adaptation strategies in response to stakeholder-driven groundwater management in the US High Plains Aquifer. *Environmental Research Letters*, *14*(4). https://doi.org/10.1088/1748-9326/aafe39

Dennehy, K. F., Litke, D. W., & McMahon, P. B. (2002). The High Plains Aquifer, USA: groundwater development and sustainability. *Geological Society, London, Special Publications*, *193*(1), 99–119. https://doi.org/10.1144/GSL.SP.2002.193.01.09

Dieter, C. A., Maupin, M. A., Caldwell, R. R., Harris, M. A., Ivahnenko, T. I., Lovelace, J. K., Barber, N. L., & Linsey, K. S. (2018). Water Availability and Use Science Program Estimated Use of Water in the United States in 2015. In *Water Availability and Use Science Program*. https://doi.org/10.3133/cir1441

Dimitri, C., Effland, A., Conklin, N., & States, U. (2005). *The 20th Century Transformation of U.S. Agriculture and Farm Policy The 20th Century Transformation of U.S. Agriculture and Farm Policy*. www.ers.usda.gov

EIA. (2020a). *Electricity Data Browser*.

EIA. (2020b). *Overview of energy markets*.

EPA. (2008). Direct Emissions from Stationary Combustion Sources. *Energy Economics*, *34*(5), 1580–1588. https://doi.org/10.1016/j.eneco.2011.11.013

EPA. (2014). Annual energy outlook 2014. *U.S. Energy Information Addministration*, 1–269. www.eia.gov/forecasts/aeo

Famiglietti, J. S. (2014). The global groundwater crisis. *Nature Climate Change*, *4*(11), 945–948. https://doi.org/10.1038/nclimate2425

Famiglietti, J. S., & Rodell, M. (2013). Water in the balance. *Science*, *340*(6138), 1300–1301. https://doi.org/10.1126/science.1236460

Fan, Y., & McCann, L. (2020). Adoption of pressure irrigation systems and scientific irrigation scheduling practices by U.S. farmers: An application of multilevel models. *Journal of Agricultural and Resource Economics*, *45*(2), 352–375. https://doi.org/10.22004/ag.econ.302459

Farm and Ranch Irrigation Survey. (n.d.). United States Department of Agriculture. Retrieved March 9, 2020, from https://www.nass.usda.gov/Surveys/Guide_to_NASS_Surveys/Farm_and_Ranch_Irrigation/index.php

Foster, T., Brozović, N., & Butler, A. P. (2015). Why well yield matters for managing agricultural drought risk. *Weather and Climate Extremes*, *10*, 11–19. https://doi.org/10.1016/j.wace.2015.07.003

Foster, T., Brozović, N., & Speir, C. (2017). The buffer value of groundwater when well yield is limited. *Journal of Hydrology*, *547*, 638–649. https://doi.org/10.1016/j.jhydrol.2017.02.034

Fraizer, R. S. (2004). *Comparative Energy Costs for Irrigation Pumping*. 4.

Furrow Irrigation. (2011). 321–321. https://doi.org/10.1007/978-90-481-3585-1_653

Gellings, C., & Parmenter, K. (2004). Energy efficiency in fertilizer production and use. *Efficient Use and Conservation of Energy. Encyclopedia of Life Support Systems (EOLSS)*.

Greenhouse gases, regulated emissions, and energy use in transportation (GREET) GREET.net Computer Model. (2017a). In *Argonne National Laboratory* (1.3.0.13239 database 13239).

Greenhouse gases, regulated emissions, and energy use in transportation (GREET) GREET.net Computer Model. (2017b). In *Argonne National Laboratory* (1.3.0.13239 database 13239).

Gutentag, E. D., Heimes, F. J., Krothe, N. C., Luckey, R. R., & Weeks, J. B. (1984). Geohydrology of the High Plains aquifer in parts of Colorado, Kansas, Nebraska, New Mexico, Oklahoma, South Dakota, Texas, and Wyoming (USGS, USA, groundwater). *US Geological Survey Professional Paper*, *1400 B*. https://doi.org/10.3133/pp1400B

Haacker, E. M. K., Kendall, A. D., & Hyndman, D. W. (2016). Water Level Declines in the High Plains Aquifer: Predevelopment to Resource Senescence. *Groundwater*, *54*(2), 231–242. https://doi.org/10.1111/gwat.12350

Handa, D., Frazier, R. S., Taghvaeian, S., & Warren, J. G. (2019). The efficiencies, environmental impacts and economics of energy consumption for groundwater-based irrigation in Oklahoma. *Agriculture (Switzerland)*, *9*(2). https://doi.org/10.3390/agriculture9020027

Hanson, B., & Putnam, D. (2004). *Flood Irrigation of Alfalfa: How Does it Behave?* 13–15.

Hecox, G. R., Macfarlane, P. a, & Wilson, B. B. (2002). Calculation of Yield for High Plains Wells: Relationship between saturated thickness and well yield. *Kansas Geological Survey, 2002-25C*(785), 1–22.

Heimlich, R. E. (2000). *Farm Resource Regions*. https://www.ers.usda.gov/publications/pub-details/?pubid=42299

Henggeler, J. C., & Vories, E. D. (2009). Evaluating center pivot distribution uniformity from catch can tests. *American Society of Agricultural and Biological Engineers Annual International Meeting 2009, ASABE 2009*, *4*(09), 2416–2429. https://doi.org/10.7150/thno.18816

Hitaj, C., & Suttles, S. (2016a). *United States Department of Agriculture Trends in U.S. Agriculture's Consumption and Production of Energy: Renewable Power, Shale Energy, and Cellulosic Biomass*. www.ers.usda.gov/publications/eib-economic-information-bulletin/eib159

Hitaj, C., & Suttles, S. (2016b). *United States Department of Agriculture Trends in U.S. Agriculture's Consumption and Production of Energy: Renewable Power, Shale Energy, and Cellulosic Biomass*. www.ers.usda.gov/publications/eib-economic-information-bulletin/eib159

Holman, J. D., & Foster, A. J. (2017). *Kansas State University Agricultural Experiment Station and Cooperative Extension Service*.

Hrozencik, R. A., & Aillery, M. (2021). *Trends in U.S. Irrigated Agriculture: Increasing Resilience Under Water Supply Scarcity*. www.ers.usda.gov

Hrozencik, R. A., Wallander, S., & Aillery, M. (2021). *Irrigation Organizations: Water Storage and Delivery Infrastructure*.

Innovation, Agricultural Productivity and Sustainability in the United States. (2016). OECD. https://doi.org/10.1787/9789264264120-en

Ireland, P., & Clausen, D. (2019). Local action that changes the world: Fresh perspectives on climate change mitigation and adaptation from Australia. In *Managing Global Warming* (pp. 769–782). https://doi.org/10.1016/b978-0-12-814104-5.00027-2

Kansas Electricity Profile 2018. Table 10. Supply and disposition of electricity. (2018).

Keller, A. B. (2012). *NGL 101 – The Basics. Presentation given by Anne B. Keller at EIA*. EIA.

Kenny, J. F., & Juracek, K. E. (2013). Irrigation Trends in Kansas, 1991-2011. *U.S. Geological Survey Fact Sheet 2013–3094*, *October*, 4.

Key, N. (2018). *USDA ERS-Productivity Increases With Farm Size in the Heartland Region Productivity Increases With Farm Size in the Heartland Region Feature: Farm Economy Productivity Increases With Farm Size in the Heartland Region*. https://www.ers.usda.gov/amber-waves/2018/december/productivity-increases-with-farm-size-in-the-heartland-region/[4/3/202011:07:12AM]

Kim, K., & Chavas, J. P. (2003). Technological change and risk management: An application to the economics of corn production. *Agricultural Economics*, *29*(2), 125–142. https://doi.org/10.1016/S0169-5150(03)00081-1

Konikow, L. F. (2013). *Groundwater Depletion in the United States (1900-2008)*. https://pubs.usgs.gov/sir/2013/5079/

Konikow, L. F. (2015). Long-Term Groundwater Depletion in the United States. *Groundwater*. https://doi.org/10.1111/gwat.12306

Konikow, L. F., & Kendy, E. (2005). Groundwater depletion: A global problem. *Hydrogeology Journal*. https://doi.org/10.1007/s10040-004-0411-8

Koundouri, P., Nauges, C., & Tzouvelekas, V. (2006). Technology adoption under production uncertainty: Theory and application to irrigation technology. *American Journal of Agricultural Economics*, *88*(3), 657–670. https://doi.org/10.1111/j.1467-8276.2006.00886.x

Kranz, W. L., Irmak, S., Martin, D. L., Yonts, C. D., & Specialists, E. I. (2007a). *Converting Center Pivot Sprinkler Packages : System Considerations*. *1124*(February).

Kranz, W. L., Irmak, S., Martin, D. L., Yonts, C. D., & Specialists, E. I. (2007b). *Flow Control Devices for Center Pivot Irrigation Systems*. *888*(February), 1–3.

Kranz, W. L., Martin, D. L., Irmak, S., van Donk, S. J., & Yonts, C. D. (2008). *Minimum Center Pivot Design Capacities in Nebraska #1851*. 4.

Li, H., & Zhao, J. (2018). Rebound Effects of New Irrigation Technologies: The Role of Water Rights. *American Journal of Agricultural Economics*, *100*(3), 786–808. https://doi.org/10.1093/ajae/aay001

LTS. DATASMART LCI Package n.d. (n.d.).

Marshall, E., Aillery, M., Malcolm, S., & Williams, R. (2015). *Climate Change, Water Scarcity, and Adaptation in the U.S. Fieldcrop Sector*. www.ers.usda.gov

Martin, D. L., Dorn, T. W., Melvin, S. R., Corr, A. J., & Kranz, W. L. (2011). *Available from CPIA, 760 N*. 104–116.

McCarthy, B., Anex, R., Wang, Y., Kendall, A. D., Anctil, A., Haacker, E. M. K., & Hyndman, D. W. (2020). Trends in Water Use, Energy Consumption, and Carbon Emissions from Irrigation: Role of Shifting Technologies and Energy Sources. *Environmental Science and Technology*. https://doi.org/10.1021/acs.est.0c02897

McClaskey, J., & Colyer, J. (2018). *Department of 2018 Annual Report*.

McGill, B. M., Hamilton, S. K., Millar, N., & Robertson, G. P. (2018). The greenhouse gas cost of agricultural intensification with groundwater irrigation in a Midwest U.S. row cropping system. *Global Change Biology*, *24*(12), 5948–5960. https://doi.org/10.1111/gcb.14472

McGuire, V. L., Lund, K. D., & Densmore, B. K. (2012). *Specific yield, High Plains aquifer*.

Miranowski, J., & Miranowski, J. A. (2006). *Energy Consumption in US Agriculture*. https://www.researchgate.net/publication/5132863

Morris, S., & Persons, T. M. (2019). *Irrigated Agriculture: Technologies, Practices, and Implications for Water Scarcity*. https://www.gao.gov/products/gao-20-128sp

National Elevation Dataset - NAVD88 Meters - 1/3rd-Arc-Second (Approx. 10m). (2012).

National Oceanic and Atmospheric Administration. (2020). *Climate at a Glance*. https://www.ncdc.noaa.gov/cag/statewide/time-series

National Water Information System data available on the World Wide Web (USGS Water Data for the Nation). (2016). https://doi.org/http://dx.doi.org/10.5066/F7P55KJN

Nejadhashemi, A. P., Wardynski, B. J., & Munoz, J. D. (2012). Large-scale hydrologic modeling of the michigan and wisconsin agricultural regions to study impacts of land use changes. *Transactions of the ASABE*, *55*(3), 821–838.

New Applications and Permits. (n.d.). Retrieved February 4, 2020, from https://agriculture.ks.gov/divisions-programs/dwr/water-appropriation/new-applications-and-permits

New, L. (1988). *Pumping Plant and Irrigation Costs*.

Perry, C. A. (2006). *Effects of Irrigation Practices on Water Use in the Groundwater Management Districts Within the Kansas High Plains, 1991–2003*. https://pubs.usgs.gov/sir/2006/5069/pdf/SIR20065069.pdf

Pervez, M. S., & Brown, J. F. (2010). Mapping irrigated lands at 250-m scale by merging MODIS data and National Agricultural Statistics. *Remote Sensing*, *2*(10), 2388–2412. https://doi.org/10.3390/rs2102388

Pfeiffer, L. (2010). The effect of irrigation technology on groundwater use. *Choices*, *25*(3).

Pfeiffer, L., & Lin, C. Y. C. (2014). Does efficient irrigation technology lead to reduced groundwater extraction? Empirical evidence. *Journal of Environmental Economics and Management*, *67*(2), 189–208. https://doi.org/10.1016/j.jeem.2013.12.002

Pfister, S., Vionnet, S., Levova, T., & Humbert, S. (2016). Ecoinvent 3: assessing water use in LCA and facilitating water footprinting. *International Journal of Life Cycle Assessment*, *21*(9), 1349–1360. https://doi.org/10.1007/s11367-015-0937-0

Polimeni, J. M., Mayumi, K., Giampietro, M., & Alcott, B. (2012). The jevons paradox and the myth of resource efficiency improvements. In *The Jevons Paradox and the Myth of Resource Efficiency Improvements*. https://doi.org/10.4324/9781849773102

Qi, S. L. (2010). *Digital map of the aquifer boundary of the High Plains aquifer in parts of Colorado, Kansas, Nebraska, New Mexico, Oklahoma, South Dakota, Texas, and Wyoming: U.S. Geological Survey Data Series 543.*

Revised Management Program Southwest Kansas Groundwater Management (Vol. 3, Issue 3). (2020).

Rodell, M., Famiglietti, J. S., Wiese, D. N., Reager, J. T., Beaudoing, H. K., Landerer, F. W., & Lo, M. H. (2018). Emerging trends in global freshwater availability. *Nature*, *557*(7707), 651–659. https://doi.org/10.1038/s41586-018-0123-1

Rogers, D. H., Lamm, F. R., & Aguilar, J. (2018). *Subsurface Drip Irrigation (SDI) Components : Minimum Requirements*.

Rothausen, S. G. S. A., & Conway, D. (2011). Greenhouse-gas emissions from energy use in the water sector. *Nature Climate Change*, *1*(4), 210–219. https://doi.org/10.1038/nclimate1147

Saavoss, M., Capehart, T., Mcbride, W., & Effland, A. (2021). *Trends in Production Practices and Costs of the U.S. Corn Sector*. www.ers.usda.gov

Salmoral, G., & Yan, X. (2018a). Food-energy-water nexus: A life cycle analysis on virtual water and embodied energy in food consumption in the Tamar catchment, UK. *Resources, Conservation and Recycling*, *133*(January), 320–330. https://doi.org/10.1016/j.resconrec.2018.01.018

Salmoral, G., & Yan, X. (2018b). Food-energy-water nexus: A life cycle analysis on virtual water and embodied energy in food consumption in the Tamar catchment, UK. *Resources, Conservation and Recycling*, *133*(September 2017), 320–330. https://doi.org/10.1016/j.resconrec.2018.01.018

Scanlon, B. R., Faunt, C. C., Longuevergne, L., Reedy, R. C., Alley, W. M., McGuire, V. L., & McMahon, P. B. (2012). Groundwater depletion and sustainability of irrigation in the US High Plains and Central Valley. *Proceedings of the National Academy of Sciences*. https://doi.org/10.1073/pnas.1200311109

Scanlon, B. R., Rateb, A., Pool, D. R., Sanford, W., Save, H., Sun, A., Long, D., & Fuchs, B. (2021). Effects of climate and irrigation on GRACE-based estimates of water storage changes in major US aquifers. *Environmental Research Letters*, *16*(9), 094009. https://doi.org/10.1088/1748-9326/ac16ff

Schneider, A., & New, L. (1988). *Irrigation pumping plant efficiencies – High Plains and Trans-Pecos areas of Texa*. The Texas A&M University System. https://doi.org/MP-1643

Sears, L., Caparelli, J., Lee, C., Pan, D., Strandberg, G., Vuu, L., & Lawell, C. Y. C. L. (2018). Jevons' Paradox and efficient irrigation technology. *Sustainability (Switzerland)*, *10*(5), 1–12. https://doi.org/10.3390/su10051590

Service, C. E. (n.d.). *Drip Irrigation Basics*. 1–8.

Shahbaz, M., Zakaria, M., Shahzad, S. J. H., & Mahalik, M. K. (2018). The energy consumption and economic growth nexus in top ten energy-consuming countries: Fresh evidence from using the quantile-on-quantile approach. *Energy Economics*, *71*, 282–301. https://doi.org/10.1016/j.eneco.2018.02.023

Skone, T. J., Jamieson, M., Shih, C., Cooney, G., & Schivley, G. (2015). *NETL Upstream Dashboard Tool Documentation*. https://doi.org/10.2172/1513244

Skone, T. J., Littlefield, J., Marriott, J., Cooney, G., Jamieson, M., Jones, C., Demetrion, L., Mutchek, M., Shih, C., Curtright, A. E., Schivley, G., Yost, A., & Krynock, M. (2016). *Life Cycle Analysis of Natural Gas Extraction and Power Generation*. https://doi.org/10.2172/1480993

Smajstrla, A. G., & Zazueta, F. S. (2003). *Loading Effects on Irrigation Power Unit Performance 1*.

Smidt, S. J., Kendall, A. D., & Hyndman, D. W. (2019). Increased dependence on irrigated crop production across the CONUS (1945-2015). *Water (Switzerland)*, *11*(7). https://doi.org/10.3390/w11071458

Soil Survey Staff. (2021). *Soil Survey Geographic (SSURGO) Database*. https://sdmdataaccess.sc.egov.usda.gov/?referrer=Citation.htm-SSURGOLink

Sorensen, A., & Daukas, J. (2010). Policy approaches to energy and resource use in US agriculture. In *Renewable Agriculture and Food Systems* (Vol. 25, Issue 2, pp. 109–117). https://doi.org/10.1017/S1742170510000086

Spangler, K., Burchfield, E. K., & Schumacher, B. (2020). Past and Current Dynamics of U.S. Agricultural Land Use and Policy. *Frontiers in Sustainable Food Systems*, *4*. https://doi.org/10.3389/fsufs.2020.00098

Stocker, T. F., Qin, D., Plattner, G. K., Tignor, M. M. B., Allen, S. K., Boschung, J., Nauels, A., Xia, Y., Bex, V., & Midgley, P. M. (2013). Climate change 2013 the physical science basis: Working Group I contribution to the fifth assessment report of the intergovernmental panel on climate change. *Climate Change 2013 the Physical Science Basis: Working Group I Contribution to the Fifth Assessment Report of the Intergovernmental Panel on Climate Change*, *9781107057*, 1–1535. https://doi.org/10.1017/CBO9781107415324

Uddameri, V., & Reible, D. (2018). Food-energy-water nexus to mitigate sustainability challenges in a groundwater reliant agriculturally dominant environment (GRADE). *Environmental Progress and Sustainable Energy*, *37*(1), 21–36. https://doi.org/10.1002/ep.12726

U.S. Department of Commerce, U. S. C. B. (2021, September 13). *USA Counties (Generalized)*. Esri.

U.S. Energy Information Administration. (2020a). *Natural Gas Prices*.

U.S. Energy Information Administration. (2020b). *Weekly U.S. No 2 Diesel Retail Prices*.

USDA. (2021). *Farms and Land in Farms 2020 Summary*. https://www.ers.usda.gov/webdocs/publications/44197/13566_eib3_1_.pdf

Velasco-Muñoz, J. F., Aznar-Sánchez, J. A., Belmonte-Ureña, L. J., & Román-Sánchez, I. M. (2018). Sustainable water use in agriculture: A review of worldwide research. *Sustainability (Switzerland)*, *10*(4), 1–18. https://doi.org/10.3390/su10041084

Vilsack, T., & Reilly, J. T. (2013). *Farm and Ranch Irrigation Survey*. https://www.nass.usda.gov/Publications/AgCensus/2012/Online_Resources/Farm_and_Ranch_Irrigation_Survey/

Vora, N., Shah, A., Bilec, M. M., & Khanna, V. (2017a). Food-Energy-Water Nexus: Quantifying Embodied Energy and GHG Emissions from Irrigation through Virtual Water Transfers in Food Trade. *ACS Sustainable Chemistry and Engineering*, *5*(3), 2119–2128. https://doi.org/10.1021/acssuschemeng.6b02122

Vora, N., Shah, A., Bilec, M. M., & Khanna, V. (2017b). Food-Energy-Water Nexus: Quantifying Embodied Energy and GHG Emissions from Irrigation through Virtual Water

Transfers in Food Trade. *ACS Sustainable Chemistry and Engineering*, *5*(3), 2119–2128. https://doi.org/10.1021/acssuschemeng.6b02122

Wada, Y., van Beek, L. P. H., van Kempen, C. M., Reckman, J. W. T. M., Vasak, S., & Bierkens, M. F. P. (2010). Global depletion of groundwater resources. *Geophysical Research Letters*, *37*(20), 1–5. https://doi.org/10.1029/2010GL044571

Whittemore, D. O., Townsend, M. A., Sorensen, B. S., Yound, D. P., & Schloss, J. A. (2000). *Regional Groundwater Quality Provinces*.

Wilson, B., Bartley, J., Emmons, K., Bagley, J., Wason, J., & Stankiewicz, S. (2005). Water Information Management and Analysis System, Version 5, for the Web. User Manual. *Kansas Geological Survey Open File Report 2005-30.*, 37.

Wood, W. W., & Hyndman, D. W. (2017). Groundwater Depletion: A Significant Unreported Source of Atmospheric Carbon Dioxide. *Earth's Future*, *5*(11), 1133–1135. https://doi.org/10.1002/2017EF000586

WORLD GEODETIC SYSTEM 1984 (WGS 84). (n.d.). Retrieved February 4, 2020, from https://www.nga.mil/ProductsServices/GeodesyandGeophysics/Pages/WorldGeodeticSystem.aspx

Xia, Y., Mitchell, K., Ek, M., Sheffield, J., Cosgrove, B., Wood, E., Luo, L., Alonge, C., Wei, H., Meng, J., Livneh, B., Lettenmaier, D., Koren, V., Duan, Q., Mo, K., Fan, Y., & Mocko, D. (2012). Continental-scale water and energy flux analysis and validation for the North American Land Data Assimilation System project phase 2 (NLDAS-2): 1. Intercomparison and application of model products. *Journal of Geophysical Research: Atmospheres*, *117*(D3), n/a-n/a. https://doi.org/10.1029/2011JD016048

Zell, W. O., & Sanford, W. E. (2020). Calibrated Simulation of the Long-Term Average Surficial Groundwater System and Derived Spatial Distributions of its Characteristics for the Contiguous United States. *Water Resources Research*, *56*(8). https://doi.org/10.1029/2019WR026724

Zhao, Y., Wang, Q., Jiang, S., Zhai, J., Wang, J., He, G., Li, H., Zhang, Y., Wang, L., & Zhu, Y. (2020). Irrigation water and energy saving in well irrigation district from a water-energy nexus perspective. *Journal of Cleaner Production*, *267*. https://doi.org/10.1016/j.jclepro.2020.122058